CGER-REPORT

ISSN 1341-4356

CGER-D041-2009

Carbon Sink Archives

An integrated system for storing, retrieving and analyzing 2-dimensional data related to the problem of terrestrial carbon sink

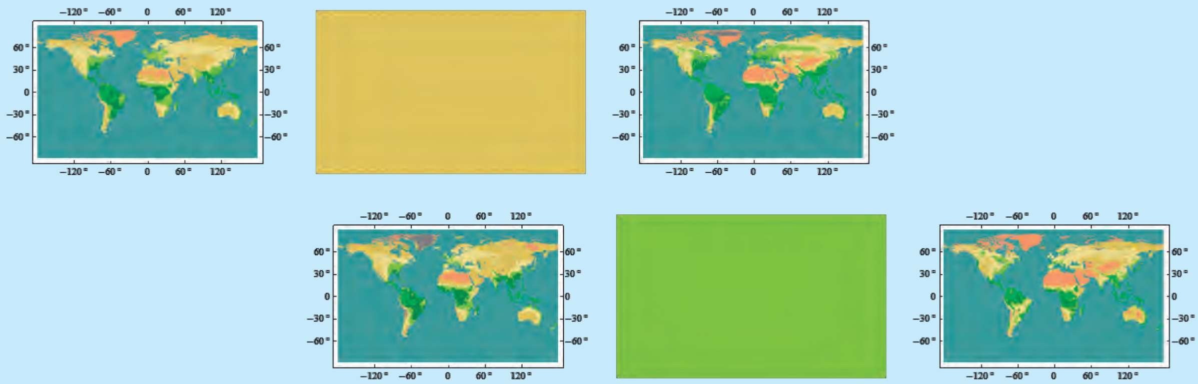

Georgii A. Alexandrov and Tsuneo Matsunaga

Center for Global Environmental Research

National Institute for Environmental Studies, Japan

CGER-REPORT

ISSN 1341-4356

CGER-D041-2009

Carbon Sink Archives

An integrated system for storing, retrieving and analyzing 2-dimensional data related to the problem of terrestrial carbon sink

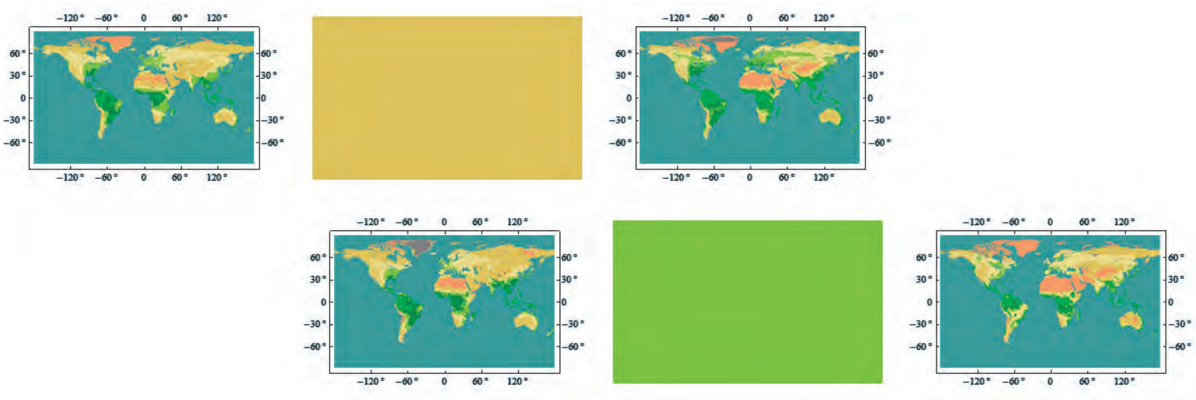

Georgii A. Alexandrov and Tsuneo Matsunaga

Center for Global Environmental Research

National Institute for Environmental Studies, Japan

Onogawa 16-2, Tsukuba, Ibaraki 305-8506, Japan

National Phone: 029-850-2349; FAX: 029-858-2645

International Phone: (+81)-29-850-2349; FAX: (+81)-29-858-2645

E-mail: www-cger@nies.go.jp

Visit our Home Page on http://www-cger.nies.go.jp

This publication is printed on paper manufactured entirely from recycled material (Rank A), in accordance with the Law Concerning the Promotion of Procurement of Eco-Friendly Goods and Services by the State and Other Entities.

Foreword

The Center for Global Environmental Research (CGER) at the National Institute for Environmental Studies (NIES) was established in October 1990. CGER's main objectives are to contribute to the scientific understanding of global environmental change and to identify solutions for pressing environmental problems. CGER conducts research from interdisciplinary, multi-agency and international perspectives, provides an intellectual infrastructure for research activities in the form of databases and a supercomputer system, and makes the data from its long-term global environmental monitoring available to the public.

In April 2006, CGER launched its new climate change program as one of the four priority initiatives forming the crux of the current five-year research plan at NIES. This program includes the development of a global environmental database related to climate change to provide fundamental data for global environmental research and policy making.

As a part of the global environmental database, a system for storing and analyzing geospatial data related to the studies of terrestrial carbon sink has been developed. This report explains the general structure of the system, named *Carbon Sink Archives*, introduces web-based tools available for data analysis, and highlights the current state of knowledge on the baseline annual productivity of the global terrestrial vegetation.

Coupled carbon cycle – climate model simulations show that climate feedbacks may amplify global warming over the next hundred years. Possible positive climate feedbacks imply a need for stronger emission reductions to stabilize carbon dioxide concentration in the future. *Carbon Sink Archives* is intended to reduce the uncertainty in climate feedbacks by providing a platform for comparative studies of carbon cycle models.

We hope this publication will stimulate regular evaluation of carbon cycle models and the development of consensual knowledge on carbon sequestration rate provided by the global terrestrial vegetation.

August 2009

Yasuhiro Sasano
Director
Center for Global Environmental Research
National Institute for Environmental Studies

Preface

Carbon Sink Archives is the world's first integrated web-based service for comparative studies of biosphere models, namely models of terrestrial carbon cycle and its components. These models are essential for a better understanding of terrestrial carbon sink -- the well-known phenomenon, that is not completely attributed to known biophysical mechanisms. Since models are not completely perfect, any result obtained with a single model should be compared with other models. *Carbon Sink Archives* provides all the means for such comparison: data, references, and software tools.

The first section of this report explains the general structure of the *Carbon Sink Archives* and its use for increasing research efficiency, for facilitating the formation of a research network and for producing usable information for policy making. The second section explains the process of getting results. Finally, the third section describes data that are available for model-intercomparison studies and for integration into policy relevant products.

The current version, *Carbon Sink Archives* 1.0, focuses on the baseline annual productivity of the global vegetation, that is, terrestrial Net Primary Production (NPP). The baseline annual NPP is a starting point of the carbon sink studies. It shows limits to further growth of human appropriation of naturally produced organic matter and limits to the usage of human-induced carbon sinks for controlling the atmospheric concentration of CO_2.

June 2009

Georgii Alexandrov

Tsuneo Matsunaga

National Institute for Environmental Studies

List of Figures

1. Introduction

This part provides an explanation of the general structure of the system and its contribution to increasing research efficiency, to facilitating the formation of a research network and to producing usable information for policy making. It offers a general review of what is happening in the world of data archiving and suggests some key objectives that should be taken into account to form a convenient infrastructure for storing, re-using, systematizing and integrating 2-dimensional (2D) data sets as related to the carbon sink problem.

1. 1. System objectives

One of the objectives of the integrated system for storing, retrieving and analyzing 2D data is to increase efficiency of researches carried out to attribute the terrestrial carbon sink to certain biophysical and socio-economical mechanisms. These research results affect significantly the strategy of carbon sequestration and emission reduction. Therefore another objective of the system is to produce policy relevant information [1] by means of data integration.

1.1.1 The problem of terrestrial carbon sink

On a the global scale the net CO_2 flux between land and atmosphere can be derived from the observed atmospheric CO_2 concentration by using an ocean model. This technique is referred to as deconvolution, and is used to verify the estimates of net flux from land-use change. The first use of deconvolution for this purpose revealed flaws in the global carbon budget. The difference between deconvoluted terrestrial flux and net flux from land-use was named "missing sink", suggesting that both estimates were correct, whereas the budget was not complete. The "missing sink" is also known under the name "residual terrestrial uptake", and is a major focus of interest for climate change scientists [2-14].

1.1.2 Thematic scope

The term 2-dimensional data is used here to denote geographically referenced data representing a continuous distribution of a geographical feature (such as temperature field) in raster form. This type of data is often referred to as "grid" -- that is, the entire assemblage of raster/cell/pixel values. It may be also referred to as 'digital map' for data of this type are often used as sources for producing digital cartographic files. The grids are produced from other grids by using a process-based model or from a discrete geographic distribution (such as station data) using appropriate interpolation methods.

The system focuses on 2D data and the information products derived from the 2D data related to the following themes:

- Productivity of the global vegetation (quantifying the mechanism of atmospheric CO_2 sequestration through organic matter synthesis)
- Net Ecosystem Exchange (quantifying the balance between organic matter synthesis and decomposition)
- Net Biome Exchange (quantifying the balance between increase in organic carbon at re-forested land and decrease of organic carbon at deforested land
- The drivers of terrestrial carbon sink and sources (climate, land cover, land use and so on)

- Auxiliary data needed for producing policy relevant information products (e.g., regional divisions: political, administrative, economical; and so on)

1.1.3 Relevance to CGER/NIES mission

In the five-year research plan that commenced in 2006, NIES identified four priority programs [15]. One of them is "Climate Change". CGER is responsible for promoting research related to this program. The missions of the Office for Global Environmental Database (OGED) include

> Development of a global environmental database related to climate change to provide fundamental data for global environmental research and policy making.

For the general public and policy makers, it is critical to understand the current status of scientific research and the confidence level of future projections based on these research results. As for terrestrial carbon balance studies, differences of estimated carbon sequestrations by terrestrial vegetation among models are especially of importance because estimates from these models are scientific bases of current discussion on the implementation of the Kyoto Protocol.

The current version of *Carbon Sink Archives* serves to this OGED's mission by providing global productivity data from various models and methods to analyze and compare these data.

1.2 Modern doctrine of data archiving

Modern scientific technologies have caused an explosion of research data, forming a large potential source of data for re-analysis and integrative studies. More than often research data, in digital form, have much longer life than the original project for which they were created. Since re-using of the research data increases the returns from public investment in research, the demand for developing procedures, policies and infrastructures for storing and sharing final research data is widely recognized [16-19].

Researchers normally store their final research data (factual material supporting research findings) in personal archives. However, they make open for public use only a very small portion of the data they generated in the course of research. Information and communication technologies open up new perspectives for massive re-using of research data. Data, stored in digital form, can be easily re-used for creation of new datasets when data from multiple sources are combined, for the exploration of topics not envisioned by the initial investigators, for testing of new or alternative hypotheses and methods of analysis.

Providing public access to research data, that are normally stored in private archives, encourages diversity of analysis and helps in creating usable information for policy making. This is, especially, important for enhancing concentrated efforts on implementation of the UN Framework Convention on Climate Change. "If we do not share common reliable data on global warming effects, we cannot establish effective remedies against these 'Inconvenient Truths' [20] .

1.3 Public archives related to the problem of terrestrial carbon sink

There are a number of public archives related to the problem of terrestrial carbon sink. Some of them are briefly reviewed below.

1.3.1 CDIAC

The Carbon Dioxide Information Analysis Center [21] is the primary global-change data and information analysis center of the U.S. Department of Energy (DOE). It focuses on the data and information products such as the landmark record of rising atmospheric CO_2 at Mauna Loa, long-term U.S. and global climate data, and global, regional, and national CO_2 emissions from fossil-fuel combustion.

1.3.2 ORNL DAAC

The Oak Ridge National Laboratory Distributed Active Archive Center [22], sponsored by NASA, maintains biogeochemical and ecological data and models useful in environmental research.

1.3.3 IPCC DDC

The Environmental Data Section of the Data Distribution Centre of the Intergovernmental Panel on Climate Change [23] provides access to baseline and scenario data for a range of non-climate conditions in the atmospheric, aquatic and terrestrial environments. These include data on atmospheric carbon dioxide concentrations, land use and land cover.

1.3.4 GEO data portal

GEO data portal [24] provides access to the archive of data sets used by UNEP and its partners in the Global Environmental Outlook (GEO) report and other integrated environment assessments. The archive contains national, subregional, regional and global statistics and 2-dimensional data (maps), related to such topics as Freshwater, Population, Forests, Emissions, Climate and GDP.

1.4 Innovative features of the *Carbon Sink Archives*

Carbon Sink Archives differs conceptually from the archives reviewed above. It is focusing on the dynamism of data it helps to manage and employs the Web 2.0 “shiso” [25] that “aims to transform a society into an aggregated intelligence acting like a huge cyborg, by connecting people’s individual intelligence (assumed as CPUs) through information and communications technology”. This conceptual basis manifests itself in the system design as follows.

1.4.1 Participatory design

The system is designed as an integrated collection of personal data archives regularly updated by archive holders and software tools constantly upgraded by system designers to meet the needs of archive holders.

1.4.2 Self-correction principle

The progress in data quality is stimulated through providing various tools for routine checks of data consistency.

1.4.3 Inference tool

Data collection on a specific subject is viewed as a knowledge base for deriving normative knowledge on this subject -- that is, consensual policy relevant estimates of biosphere characteristics. Every addition to data collection launches a computer program that update normative knowledge.

1.5 Stakeholders

Since terrestrial carbon sink is an important issue of Global Environmental Research, *Carbon Sink Archives* are targeted at various categories of organizations and individuals.

The major institutional stakeholders of *Carbon Sink Archives* are organizations that are formed, or evolved, to fulfill the following missions:

- to integrate and disseminate the data of Global Environmental Research;
- to promote international partnership for global environmental conservation through organizing seminars and training courses;
- to provide scientific support for policymaking.

The following categories of data producers may have a strong interest in services that facilitate data archiving and complementing the personal archives with the shared and re-used grids related to the problem of terrestrial carbon sink:

- Ecosystem modelers
- Remote sensing scientists
- Atmospheric transport modelers
- Climate modelers
- Modelers of socio-economic processes

The collection of maps associated with the data stored in *Carbon Sink Archives* may find its use in teaching as a source of visual aids for the courses on biosphere science, vegetation science, climatology, environmental/ecological economics and so on.

2. System manual

The version 1.0 of the *Carbon Sink Archives* is intended primarily to facilitate networks activities that would result in forming a set of global grids characterizing model projections of

- Baseline productivity of terrestrial ecosystems and its annual and decadal variations;
- Annual and decadal anomalies in net terrestrial uptake;
- Baseline carbon sequestration in afforestation and reforestation projects;
- Baseline carbon emissions associated with deforestation;

The baseline value is the average value of the variable under concern during a relatively large period of time, inter-annual variations are expressed as departures from the baseline value.

The system consists of the following components:

- Web-portal for introducing research data available for sharing and re-using by subscribers
- File server for storing and downloading the data
- Database server for registering data submitted for sharing, retrieving available data, and posting demands for data needed to integrate someone personal archive
- Application server for data visualization, summarization, analysis, verification, validation, inter-comparison, and knowledge engineering
- Data set
- Toolkit of web-based applications

2.1 Web portal

The *Carbon Sink Archives* web portal (Figure 1.1) is a gateway to the system for data storing, retrieving and analyzing. Therefore it integrates web directories rather than the links to subscriber websites.

A website offering access to a categorized listing of other websites is called a web directory. Although a directory may be considered as a database of hyperlinks, it differs from a conventional database in that it is optimized for lookup and browsing. The *Carbon Sink Archives* web-portal integrates the

- Directory of subscribers
- Directory of research subjects
- Directory of web applications

The directory of subscribers (Figure 1.4) contains information about *Carbon Sink Archives* subscribers: name, e-mail address, phone number and hyperlink to the personal web page on the *Carbon Sink Archives* server. Subscribers are those of registered users, who keep a part of their personal archives on the *Carbon Sink Archives* server. They are named as subscribers (to OGED service), because *Carbon Sink Archives* may be also considered as a web-based service for sharing data. The personal web page provides hyperlinks to the data files, manuals, maps, charts, and slides that the subscriber uploaded on the *Carbon Sink Archives* server.

The directory of research subjects (Figure 1.3) lists research subjects and provides hyperlinks to their web pages. The web page of a subject provides hyperlinks to relevant data files, manuals, maps, charts, and slides that are stored on the *Carbon Sink Archives* server.

The directory of web applications (Figure 1.2) lists and annotates web-based services provided by *Carbon Sink Archives*, including hyperlinks to their web pages (for further details) and direct hyperlink to web-applications.

2.2 Database of file references / search tools

The data stored in *Carbon Sink Archives* are registered in the online database of file references.

The current version of *Carbon Sink Archives* employs RefWorks web-based software for running the online database of file references. A reference to a grid includes the following fields:

1. Author;
2. Title;
3. Year of uploading to *Carbon Sink Archives*;
4. Descriptors (keywords);
5. Recommended citation;
6. Implementation notes;
7. Registered name (i.e., the name that *Carbon Sink Archives* web tools described below can recognize);
8. URL of the website for downloading the file.

The references can be viewed (Figure 2.1) in built-in RefWorks format (Standard View, One line/Cite View, Full View) and custom formats (CarbonSinkArchives, CarbonSinkArchivesNotes, Carbon Balance and Management).

They can be sorted by Author, Title, or Year, and searched using 'Quick Search' or 'Advanced Search'. The 'Quick Search' searches all fields, and search terms are connected by "OR". 'Advanced Search' allows specifying fields and connecting search items by Boolean operators. The browsable indexes of authors and keywords can be accessed using 'Look up' options (Figure 2.2).

2.3 Web tools

The version 1.0 of *Carbon Sink Archives* includes a toolkit of web applications (Figure 3.1) for testing the validity of uploaded grids. The grid is the data file that contains the values of a geographical variable at the nodes of a geographical grid.

2.3.1 Technology

The software tools are written in Mathematica language [Wolfram, 1999] and arranged into a Mathematica package. Since the software tools are written in Mathematica language, they can be used via the web interface [Wickham-Jones, 2006] to the Mathematica kernel. This interface, webMathematica, allows a web site to deliver JavaServer pages that call Mathematica commands. When the commands are evaluated, the computed result is placed in the page.

2.3.2 Visualization of the global pattern

Show Grid (Figure 3.2) is the tool for visualizing the global pattern of a geographical variable represented by a grid. Enter to the box below the path to the grid location on the *Carbon Sink Archives* server (e.g. "UploadedGrids\4838305.grd") and press "GENERATE". The image of the grid displays the global pattern of the geographical variable using 6 colors that correspond to the following 6 ranges: 1) below 0.05-quantile; 2) between 0.05-quantile and first quartile; 3) between first quartile and median; 4) between median and third quartile; 5) between third quartile and 0.95-quantile; 6) above 0.95-quantile. The legend to the map can be displayed using *Show Legend* tool.

2.3.3 Descriptive statistics of the variable distribution

Show Grid (Figure 3.3) is the tool for calculating statistics of the variable distribution and for displaying a legend to the map created by the *Show Grid* tool. Enter to the box below the path to the grid location on the *Carbon Sink Archives* server (e.g. "UploadedGrids\4838305.grd") and press "GENERATE". The image of the legend display the following statistics of variable distribution: minimum, 0.05-quantile, first quartile, median, third quartile; 0.95-quantile, maximum. The global pattern of the variable can be displayed using *Show Grid* tool.

2.3.4 Comparison of global patterns originated by different models

Compare Grids (Figure 3.4) is the tool for comparing the global patterns of the variable calculated by using different models. The result of comparison is saved in the file that can be displayed using *Show Grid* tool. Enter to each box below the path to the relevant grid location on the *Carbon Sink Archives* server (e.g. "UploadedGrids\4838305.grd") and press "GENERATE"

2.3.5 Summarizing the global pattern by pie diagram

Show Pie Chart is the tool is for summarizing the global pattern of the variable as a pie diagram displaying the contribution of (1) the boreal belt, (2) northern mid-latitudes, (3) low latitudes, and (4) southern mid-latitudes. Enter to the box below the path to the grid location on the *Carbon Sink Archives* server (e.g. "UploadedGrids\4838305.grd") and press "GENERATE".

2.3.6 Summarizing the global pattern by bar diagram

Show Bar Chart is the tool is for summarizing the global pattern of the variable as a bar diagram displaying the contribution of (1) the boreal belt, (2) northern mid-latitudes, (3) low latitudes, and (4) southern mid-latitudes. Enter to the box below the path to the grid location on the *Carbon Sink Archives* server (e.g. "UploadedGrids\4838305.grd") and press "GENERATE".

2.3.7 Comparing global patterns region by region

Compare Bar Charts is the tool for comparing the global patterns of the variable calculated by using different models. The results of comparison are shown as a bar diagram displaying the contribution of (1) the boreal belt, (2) northern mid-latitudes, (3) low latitudes, and (4) southern mid-latitudes as bars placed side by side. Enter to the boxes below the paths to the grid locations on the *Carbon Sink Archives* server and press "GENERATE". (Version 1.0 does not support other regional divisions of the land, but the future versions of the system will do.)

2.3.8 Web-tools for "one-to-many" comparison

Consistency Test (Figure 3.5; 5.1-5.8) shows how far the estimate (y) from the average ($\bar{x}$) in comparison with the lowest (x_{min}) , or highest (x_{max}) estimate:

$$(1) \qquad z = \begin{cases} 100\dfrac{y-\bar{x}}{x_{\min}-\bar{x}}, & y < \bar{x} \\ 100\dfrac{y-\bar{x}}{x_{\max}-\bar{x}}, & y \ge \bar{x} \end{cases}$$

The (z) is positive when the estimate falls within the bounds defined by the normative data ($x_{min} \le y \le x_{max}$), and negative when it falls outside those bounds. The estimate is said to be 100% consistent with the normative data if it coincides with the average estimate.

The *Novelty Test* (Figure 3.6; 6.1-6.8) value is positive if inclusion of the estimate into the normative data shifts the average estimate. It returns the relative value of the shift with respect to the width of the confidence interval for the average estimate:

$$(2) \qquad z = 100\frac{y-x}{u}$$

where x is the original mean value, y is the mean value changed due to inclusion of the estimate into the normative data, u is the half-width of the original confidence interval.

The *Progressivity Test* (Figure 3.7; 7.1-7.8) value is positive if inclusion of the estimate into the normative data narrows the confidence interval of the average estimate. It returns the relative decrease in the width of the confidence interval:

$$(3) \qquad z = 100\frac{x-y}{x}$$

where x is the original width of the confidence interval, y is the width of confidence interval changed due to inclusion of the estimate into the normative data.

2.4 System versions

Since *Carbon Sink Archives* is a community-oriented system, it is upgraded and updated on a frequent basis, responding to community requests.

The version number corresponding to a new development of the system has the pattern: 'VersionNumber.RevisionNumber.BuildNumber', where 'VersionNumber' is increased when functionality of the system is changed significantly, 'RevisionNumber' is increased when a new web tool is added, and 'BuildNumber' is increased when a new data file is added. Every addition of data is considered as new developments of the system.

The system manual may not cover completely all the functions of versions higher than 1.0.

2.5 Getting results with *Carbon Sink Archives 1.0*

2.5.1 Getting access to *Carbon Sink Archives*

The *Carbon Sink Archives* is a web-based service provided by OGED on free basis for registered users. For getting access to *Carbon Sink Archives*, you need to send an informal e-mail to the Head of the Office asking for registration. The passwords for accessing *Carbon Sink Archives* components will be sent you by e-mail and you will get access to

- Web Portal at URL: https://project.nies.go.jp/csa/
- Database of file references at URL: http://www.refworks.com/refworks
- Application server at URL: http://db.cger.nies.go.jp/csa/

2.5.2 Getting the list of model outputs on a specific subject

All files stored in the *Carbon Sink Archives* are listed in the database of file references. To get the list of model outputs on specific subject

1. go to URL: http://www.refworks.com/refworks
2. choose Individual Log-in
3. enter user name and password (you will see the full list of file references)
4. select Lookup by Descriptor in Search pop-up menu (you will see the list of subjects)
5. select a subject (you will see the list of file references related to this subject)

2.5.3 Analyzing outputs of a given model

To analyze outputs of a given model

1. find the reference to the model outputs in the database of file references (see section 2.5.2)
2. Write down its registration name or copy it to the clipboard (the content of the field “Registered as”)
3. go to URL: http://db.cger.nies.go.jp/csa/
4. select ShowBarChart
5. enter or paste the registration name of the grid into the field “The grid location”
6. press the button “GENERATE”
7. you will see a bar diagram displaying the totals of a geographical variable under concern for (1) the boreal belt, (2) northern mid-latitudes, (3) low latitudes, and (4) southern mid-latitudes
8. on the left-side menu press “ShowGrid”
9. enter or paste the registration name of the grid into the field “The grid location”
10. press the button “GENERATE”
11. you will see a map displaying regions of high and low values of the geographical variable; the regions are colored using six colors; the regions of very high values (above 95th percentile) are colored emerald green, the regions of high values (between 75tn and 95th percentile) are colored green, the regions where the geographical variable has values above average (between 50th and 75th percentile) are colored yellow green, the regions where the geographical variable has values below average (between 50th and 25th percentile) are colored green yellow, the regions of low values (between 25th and 5th percentile) are colored ‘banana yellow’, the regions of very low values (below 5th percentile) are colored ‘sandy brown’.

12. on the left-side menu press “ShowLegend”
13. enter or paste the registration name of the grid into the field “The grid location”
14. press button “GENERATE”
15. you will see the ranges of values categorized by the 5^{th}, 25^{th}, 50^{th}, 75^{th} and 95^{th} percentiles and corresponding to the map colors.

2.5.4 Comparing two model outputs (peer-to-peer comparison)

To compare model outputs

1. find the references to the model outputs in the database of file references (see section 2.5.2)
2. write down their registration names or copy them to the clipboard (the content of the field “Registered as”)
3. go to URL: http://db.cger.nies.go.jp/csa/
4. select CompareBarCharts
5. enter or paste the registration name of the first grid into the field “First grid location”
6. enter or paste the registration name of the second grid into the field “Second grid location”
7. press the button “GENERATE”
8. you will see a bar diagram displaying the totals of a geographical variable under concern for (1) the boreal belt, (2) northern mid-latitudes, (3) low latitudes, and (4) southern mid-latitudes; the outputs of the first model are colored red.
9. on the left-side menu press “Evaluate regional differences”
10. enter the registration names of the grids in the corresponding fields and press “GENERATE”
11. you will see the table displaying regional totals for each model and their differences
12. on the left side menu press “Compare cell values”
13. enter the registration names of the grids in the corresponding fields and press “GENERATE”
14. write down or copy the temporal registration name of the generated grid
15. on the left side menu press “Show regional values”
16. enter the temporal registration of the generated grid in the field “The grid location”, add quotation marks, and press “GENERATE”
17. you will see a bar diagram displaying the differences in totals of a geographical variable under concern for (1) the boreal belt, (2) northern mid-latitudes, (3) low latitudes, and (4) southern mid-latitudes
18. on the left-side menu press “ShowGrid”
19. enter or paste the registration name of the grid into the field “The grid location”
20. press the button “GENERATE”

21. you will see a map displaying regions where the difference between the second model estimate and the first model estimate falls within six ranges; the regions of very high values (above 95th percentile) are colored emerald green, the regions of high values (between 75th and 95th percentile) are colored green, the regions where this geographical variable has values above average (between 50th and 75th percentile) are colored yellow green, the regions where this geographical variable has values below average (between 50th and 25th percentile) are colored green yellow, the regions of low values (between 25th and 5th percentile) are colored ‘banana yellow’, the regions of very low values (below 5th percentile) are colored ‘sandy brown’.
22. on the left-side menu press “ShowLegend”
23. enter or paste the registration name of the grid into the field “The grid location”
24. press the button “GENERATE”
25. you will see the ranges of values categorized by the 5th, 25th, 50th, 75th and 95th percentiles and corresponding to the map colors.

2.5.5 Comparing model outputs to an ensemble of model outputs (one-to-many comparison)

To compare model outputs to an ensemble of model outputs

1. find the reference to the model outputs in the database of file references (see section 2.5.2)
2. write down its registration names or copy them to the clipboard (the content of the field “Registered as”)
3. go to URL: http://db.cger.nies.go.jp/csa/
4. press “ConsistencyTest”
5. enter or paste the registration name of the grid into the field “Enter grid location”
6. press the button “GENERATE”
7. you will see a horizontal bar diagram displaying the results of the consistency test (section 3.2.4) -- that is, for which regions estimates of the model under concern fall within the range of estimates produced with a given model ensemble.
8. return to main menu and press “ProgressivityTest”
9. enter or paste the registration name of the grid into the field “Enter grid location” and press “GENERATE”
10. you will see a horizontal bar diagram displaying the results of progressivity test (section 3.2.4) -- that is, for which regions estimates of the model under concern reduce uncertainty in the mean value of the geographical variable.
11. return to main menu and press “NoveltyTest”
12. enter or paste the registration name of the grid into the field “Enter grid location” and press “GENERATE”

13. you will see a horizontal bar diagram displaying the results of the novelty test (section 3.2.4) -- that is, or which regions estimates of the model under concern suggest a dramatic shift in the mean value of the geographical variable.

3. Data set description

The current version of *Carbon Sink Archives* includes a set of global grids closely related to carbon sequestration. The collection of grids characterizing baseline terrestrial productivity (i.e., productivity of natural vegetation corresponding to typical climate conditions) is the largest one.

3.1 Baseline productivity of the global vegetation (single model outputs)

The amount of plant organic matter produced on an annual basis, so called net primary production or NPP, is the basic characteristic of the biosphere. It shows biosphere potential to supply primary food energy source for non-autotrophic species including humans. Human appropriation of terrestrial net primary production stems not only from the demand for food but also for fuel, construction materials, and paper. It is estimated to be from 8 to 15 PgC y^{-1} in total (including 3-6 PgC y^{-1} associated with food supply) [26].

NPP also shows biosphere potential to steer the Earth system by absorbing CO_2, a gas whose atmospheric concentration affects global climate. NPP characterizes the “gross” terrestrial carbon sink -- the amount of CO_2 annually sequestered by vegetation. The net terrestrial uptake is much smaller, because the “gross” sink is compensated for by various carbon sources. The coupled carbon-cycle-climate models show a wide range of projections for the magnitude of the terrestrial uptake in the middle of this century: from 0 to 8 PgC y^{-1} [27].

Appropriation (or re-direction) of NPP is also one method of climate change mitigation. Protecting non-living organic matter from decomposition and burning [28], reducing deforestation rates [29-31] and increasing the age of wood harvest [32] will “re-direct” NPP to the carbon pools with longer turnover times. Implementation of these measures may partly compensate for emissions from fossil fuel burning, which hopefully will not exceed 30% of the total terrestrial NPP by 2050.

The total terrestrial NPP is generally assumed to be about 60 PgC y^{-1} [33]. Biosphere models differ on this value (Figures 8.1-8.16, 9.1-9.17). In modelling terrestrial productivity we are facing the problem of structural uncertainty: there is no single true model for attributing NPP to environmental factors, we have to choose among competing conceptual frameworks. Field observations hardly allow us to make a reasonable choice between competing conceptual frameworks, to form an agreement on the best model structure, or to even discriminate between adequate descriptions of significant processes from inadequate ones [34]. Hence, any conclusion based on a single model can be accepted only as a justified hypothesis -- establishing its general validity requires testing against other models (Figures 5.1-5.9, 6.1-6.9, 7.1-7.9, 10.1-10.15, 11.1-11.15).

3.1.1 Miami NPP

The Miami model [35]-[36] relates NPP either to mean annual temperature (T_a) or to annual precipitation (P_a):

$$NPP(T_a, P_a) = min\{NPP_T(T_a),\ NPP_h(P_a)\};$$
(4) $$NPP_T(T_a) = \frac{1350}{1+\exp(1.315-0.119T_a)};$$
$$NPP_h(P_a) = 1350(1-\exp(-0.000664P_a))$$

where T_a and P_a are mean annual temperature and annual amount of precipitation, respectively.

Plotting NPP against T_a we can see (Figure 4.1) that the data fit well $NPP_T(T_a)$ in case of biomes of sufficient water supply. Moreover, in line with the underlying logic of the Miami model. NPP of the biomes of limited water supply is lower than predicted by $NPP_T(T_a)$. Plotting NPP against P_a we can see (Figure 4.1) that the curve of humidity dependence $NPP_h(P_a)$ runs across the typical NPP values of these biomes, whereas NPP of biomes of limited heat supply is lower than predicted by $NPP_h(P_a)$.

3.1.2 Montreal NPP

The Montreal model [37] assumes that NPP is controlled by actual evapotranspiration (AET):

(5) $$NPP(AET) = 1350(1-\exp(-0.0009695(AET-20)))$$

Plotting NPP against AET (Figure 4.2) we can see that the data fit well this model, excepting those representing the biome of shrublands.

3.1.3 TGER NPP

This model is based on the empirical relationship between annually NDVI and NPP [38]:

(6) $$NDVI = 0.4(1-\exp(-0.0055059NPP)$$

that was derived from the same data as the Miami NPP and Montreal NPP models. In contrast to these models, the TGER-NPP model was expected to produce estimates of "actual" NPP -- that is, NPP of "actual" vegetation that is supposedly less productive than "potential natural vegetation". Indeed, TGER-NPP gives lower estimates of tropical forest productivity. However, it gives higher estimates for productivity of boreal forests (Figure 9.12).

3.1.4 TsuBiMo NPP

TsuBiMo employs Oikawa's approach to scaling up Gross Primary Production (GPP) from a single leaf to canopy [39,40]. This approach is based on the assumption that the light dependence of photosynthesis at the single leaf is of the Michaelis-Menten type:

(7) $$P_{g,leaf} = p_{\max}\frac{K\cdot I_{can}(L)}{p_{\max}/\beta + K\cdot I_{can}(L)},$$

where β is light-use efficiency, K is light extinction coefficient, L is cumulative leaf area index above the level of the leaf ($0 \le L \le LAI$), and $I_{can}(L)$ is the light intensity at this level which is supposed to be equal to $I_a exp(-K\cdot L)$, where I_a is the light intensity above the canopy.

Integration over all leaf layers and over the daily course of I_a, which is approximated by the formula $I_a(t)=I_o sin^2(\pi t/D)$, where D is day length, gives:

(8) $$GPP_{daily} = 2D\frac{p_{\max}}{K}Ln\left[\frac{1+\sqrt{1+\beta\, I_o/(p_{\max}/K)}}{1+\sqrt{1+\beta\, I_o\exp(-K\cdot LAI)/(p_{\max}/K)}}\right].$$

Light attenuation coefficient (K) depends not only on the leaf inclination angle, which is relatively constant for a given species, but also on the mode of foliage distribution [41]. Observations show that the mode of foliage distribution may be changing with LAI to keep an inverse relationship between K and LAI [42]. It was also found that the inverse relationship between K and LAI gives a maximum of GPP for a given LAI [43]. This relationship implies minor variations in FPAR (fraction of absorbed photosynthetically active radiation) of continuous vegetation cover, and allows for a reduction of the number of globally varying parameters:

(9) $$GPP = 2\cdot D_v\cdot G\cdot k\cdot p_K Ln\left\{\frac{1+\sqrt{1+\beta\cdot I_o/p_K}}{1+\sqrt{1+\varphi\cdot\beta\cdot I_o/p_K}}\right\}$$

where $\varphi=\exp(-K\cdot LAI)=0.1$, $p_K=p_{max}/K$, $\beta=$ (0.06 μmol CO_2)·(μmol photons)$^{-1}$, G is the length of the growing season, D_v is the average day length during the growing season, I_o is light intensity at noon, k is the constant for conversion assimilated CO_2 to synthesized dry matter.

Reduction in the number of model parameters generally leads to a less complicated model with more objective parameter values, and reduction to a single parameter makes its value to be completely determined by data. Since NPP is calculated using an empirical formula [37]:

(10) $$NPP = 3000\left(1-\exp\left(-GPP/4140\right)\right),$$

where NPP and GPP are given in (g $d.m.$) m^{-2} y^{-1}, TsuBiMo outputs depends only on settings of p_K - a single lumped parameter (SLP) that serve as a quantitative characteristic of vegetation.

Numerical inversion of the model restores SLP from NPP (and D, G, I_o) measured at numerous locations. Thus derived SLP values are used to formulate an empirical model linking SLP to some climatic variables (Figure 4.3):

(11) $$p_K = 32.3\exp\left[-\left(\frac{T_v-30}{11.2}\right)^2\right]\cdot\frac{\left(RFL_v/2.6\right)^{4.57}}{1+\left(RFL_v/2.6\right)^{4.57}},$$

where p_K is expressed in (μmol CO_2) m^{-2} s^{-1}, T_v and RFL_v are mean monthly temperature and monthly rain factor averaged over the vegetation period, $RFL_v=P_v/T_v$, where P_v is the monthly precipitation averaged over the vegetation period.

Since the geographical distribution of climatic variables is known, this empirical model is used to assigning SLP to each node of the geographical grid.

In the latest versions, the temperature dependence of SLP is modeled [44] by the Arrhenius function modified to describe the effect of temperature on enzyme activity (Figure 4.4) :

(12)
$$p_{K,T} = p_{K,opt} G_A(T_v;T_{opt}); \quad G_A(T) = \frac{2f(T)}{1+f^2(T)};$$
$$f(T) = \exp\left(\frac{E_a}{RT_{opt}} - \frac{E_a}{RT} \right)$$

where R is the universal gas constant, E_a is the activation energy, T_{opt} is the optimal temperature. In common with other functions used for modeling the temperature response of plant productivity, the curve of function G_A is almost symmetrical and bell-shaped. The special convenience of G_A is that it relates the width of the "bell" to thermodynamic concepts, such as the activation energy of chemical reactions converting carbon dioxide and water to carbohydrates.

It should be also mentioned that average monthly data over the vegetation period is based on monthly NDVI. For example, T_v is the weighted mean of monthly temperatures (higher than 0.1 ^oC) where weights are as follows

(13)
$$w_m = max\left\{ 0, \frac{NDVI_m - 0.05}{\sum_{m \in M}(NDVI_m - 0.05)} \right\},$$

M is the set of numbers denoting correspondence to the months with monthly temperature higher than 0.1^oC and NDVI higher than 0.05.

3.1.5 GLO-PEM NPP

GLO-PEM [45,46] is a production efficiency model (PEM). It relates NPP to APAR using a conversion coefficient, ε, referred to as light use efficiency:

(14)
$$NPP = \sum_t \varepsilon_t APAR_t$$

where

(15)
$$APAR = F_{PAR} PAR$$

and

(16)
$$\varepsilon_t = \varepsilon^* \sigma_t P_g P_m,$$

F_{PAR} is the fraction of PAR absorbed by the canopy, ε^* is unstressed photosynthetic potential in terms of gross production, σ_t is the reduction of ε^* caused by stressors, P_g is the reduction due to growth respiration (P_g=0.75), P_m is the reduction due to maintenance respiration.

For C3 photosynthesis ε^* is modeled as a function of air temperature, CO_2 compensation point and the O_2/CO_2 specificity ratio. For C4 photosynthesis it is invariant with temperature. F_{PAR} is modeled by a linear function of NDVI. P_m=1-R_m , where R_m is the fraction of GPP loss due to maintenance respiration. It is calculated using a semi-empirical relationship with aboveground biomass, W, which is calculated from the minimum annual visible channel reflectance.

3.1.6 Biome-BGC NPP

Biome-BGC (Biome BioGeochemical Cycles) [13] calculates NPP as a difference between GPP simulated with Farquhar approach and autotrophic respiration subdivided into growth respiration and maintenance respiration. The growth respiration is assumed to be a constant part of GPP, and the maintenance respiration is calculated as a function of tissue nitrogen concentration.

3.1.7 BEAMS NPP

Biosphere model integrating Eco-physiological And Mechanistic approaches using Satellite data (BEAMS) [47] is a production efficiency model (PEM). It relates GPP to APAR using a conversion coefficient, ε, referred to as light use efficiency:

(17) $$GPP = \varepsilon_t \, APAR_t$$

where

$$APAR = F_{PAR} \, PAR$$

and

$$\varepsilon_t = \varepsilon_{\max} s_t \ ,$$

F_{PAR} is the fraction of PAR absorbed by the canopy, ε_{max} is unstressed photosynthetic potential in terms of gross production, s_t is the reduction of ε_{max} caused by stressors.

The reduction of maximum light-use efficiency by environmental stress is calculated proceeding from a photosynthesis model and stomatal conductance:

(18) $$s_t = \frac{p_t}{p_{opt}}$$

The rate of photosynthesis is modeled using the Farquhar approach, where the maximum rate of carboxylation ($V_{c,\,max}$) is a function of temperature (T) and soil moisture factor (w_c):

(19) $$V_{c,\max} = V_{c,\max,25} \, Q_{10,V_{c,\max}}^{(T-298.15)/10} \, w_c$$

where w_c is calculated from volumetric soil moisture using the equation from SiB2. The soil moisture factor for stomatal conductance is calculated using the another equation.

The NPP is a difference between GPP and autotrophic respiration which is subdivided into growth and maintenance respiration of leaves ($R_{g,L}$ and $R_{m,L}$), roots ($R_{g,F}$ and $R_{m,F}$), and stems ($R_{g,W}$ and $R_{m,W}$). The maintenance respiration is proportional to the biomass (m_x) stored in a given pool:

(20) $$R_{m,x} = r_{m,x} m_x Q_{10}^{(T-10)/10}$$

The growth respiration is proportional to the difference between the portion of GPP translocated to a given pool and maintenance respiration:

(21) $$R_{g,x} = r_{g,x} (F_{GPP,x} - R_{m,x})$$

The mass of leaves (m_L) is calculated from leaf area index (LAI) and specific leaf area (SLA). The mass of stems (as wells as the mass of roots) is calculated proceeding from a balance equation where litterfall is proportional to the mass of stems.

3.1.8. MODIS-NPP

MODIS-NPP [48,49] is a production efficiency model (PEM). It relates GPP to APAR using a conversion coefficient, ε, referred to as light use efficiency:

$$GPP = \varepsilon_t \, APAR_t$$

where

$$APAR = F_{PAR} \, PAR$$

and

$$\varepsilon_t = \varepsilon_{\max} s_t \ ,$$

F_{PAR} is the fraction of PAR absorbed by the canopy, ε_{max} is unstressed photosynthetic potential in terms of gross production, s_t is the reduction of ε_{max} caused by stressors.

The stressors are daily temperature, T_d , and daylight average vapor pressure deficit, V_d :

(22) $$s = s_1(T_d)\, s_2(V_d)$$

(23) $$s_1(T_d) = \begin{cases} 0, T_d < T_{d,\min} \\ \dfrac{T_d - T_{d,\min}}{T_{d,\max} - T_{d,\min}}, T_{d,\min} \le T_d \le T_{d,\max} \\ 1, T_d > T_{d,\max} \end{cases}$$

where $T_{d,max}$ is the daily temperature above which light-use efficiency is not stressed by heat supply, and $T_{d,min}$ is the daily temperature below which assimilation of organic matter is negligible.

(24) $$s_2(V_d) = \begin{cases} 1, V_d < V_{d,\min} \\ \dfrac{V_{d,\max} - V_d}{V_{d,\max} - V_{d,\min}}, V_{d,\min} \le V_d \le V_{d,\max} \\ 0, V_d > V_{d,\max} \end{cases}$$

where $V_{d,min}$ is the daylight average vapor pressure deficit below which light-use efficiency is not stressed by water supply, and $V_{d,max}$ is the daylight average vapor pressure deficit above which assimilation of organic matter is negligible.

$T_{d,max}$, $T_{d,min}$, $V_{d,min}$, $V_{d,max}$, and ε_{max} are the functions of land-cover tabulated at 11 biome classes.

The annual NPP is the difference between annual GPP and autotrophic respiration which is subdivided into growth and maintenance respiration of leaves ($R_{g,L}$ and $R_{m,L}$), fine roots ($R_{g,F}$ and $R_{m,F}$), live wood ($R_{g,W}$ and $R_{m,W}$), and growth respiration of dead wood ($R_{g,D}$):

(25) $$R_{m,L} = r_{m,L} \sum_t m_L(t)\, Q_{10}^{(T_d(t)-20)/10}$$

where is the mass of leaves (m_L) is calculated from leaf area index (LAI) and specific leaf area (SLA):

(26) $$m_L = LAI / SLA$$

(27) $$R_{m,F} = r_{m,F} \sum_t m_F(t)\, Q_{10}^{(T_d(t)-20)/10}$$

where m_F is the mass of fine roots

(28) $$R_{m,W} = m_W\, r_{m,W} \sum_t Q_{10}^{(T_d(t)-20)/10}$$

where the mass of live wood (m_W) is proportional to the maximum mass of leaves ($m_{L,max}$) over the growing season

(29) $$m_W = \mu m_{L,\max}$$

(30) $$R_{g,L} = \lambda m_{L,\max} r_{g,L}$$

where λ is the annual proportion of leaf turnover.

The growth respiration is estimated to be 25% of annual NPP, that is

(31) $$NPP = \begin{cases} 0.8(GPP - R_m), GPP > R_m \\ 0, GPP \le R_m \end{cases}$$

The coefficients λ, μ, η_F, η_W, η_D, $r_{m,L}$, $r_{m,F}$, $r_{m,W}$, and SLA are the functions of land-cover tabulated at 11 biome classes. Q_{10}= 3.22 - 0.046T_d .

3.1.9 Madison NPP

This is an empirical model, that re-examines Miami NPP and Montreal NPP models proceeding from a larger reference data set of NPP field observations [50]. The model attributes the gradations in observed NPP to gradations in photosynthetically active radiation (PAR_v) available during the growing season (days with average temperature greater than zero) and takes into account a soil moisture stress index (WSI):

(32) $$NPP = 2720\, max \left\{ 0,\ 0.5 \frac{PAR_v}{PAR_{v,\max}} + 0.6\, WSI - 0.5 \right\}$$

The WSI measures water availability, and is defined as a ratio of the actual evapotranspiration (AET) to the potential evapotranspiration (PET). The highest value that this model may give (when PAR_v=$PAR_{v,max}$ and WSI=1) is 1632 gC m^{-2} y^{-1}. However, since either PAR_v < $PAR_{v,max}$ or WSI<1, NPP values did not exceed 1577 gC m^{-2} y^{-1}. $PAR_{v,max}$ is set at the value of annual photon flux density corresponding to 600 μmol PP m^{-2} s^{-1} multiplied by the number of days with daily temperature above 0^{o}C.

3.1.10 Sim-CYCLE NPP (rev)

The original version of Sim-CYCLE (Simulation of Carbon Cycle in Land Ecosystems) employed Oikawa's approach to scaling up Gross Primary Production (GPP) from a single leaf to canopy. The rate of light-saturated photosynthesis was modeled as the function of temperature (T) and foliar intercellular CO_2 concentration (C_i):

(33) $$p_{\max} = p_{opt} f_1(T) f_2(C_i)$$

(34) $$f_1(T) = \frac{(T - T_{\min})(T - T_{\max})}{(T - T_{\min})(T - T_{\max}) - (T - T_{opt})^2}$$

(35) $$f_2(C_i) = \frac{C_i}{K_{m,C_i} + C_i}$$

(36) $$C_i = \frac{g_s}{K_{m,g_s} + g_s} C_a$$

(37) $$g_s = \left(g_{s,\max} - g_{s,\min}\right)\frac{AET}{PET} + g_{s,\min}$$

where g_s is stomatal conductance, AET is actual evapotranspiration, PET is potential evapotranspiration, C_a is ambient CO_2 concentration.

NPP is calculated as the difference between GPP and autotrophic respiration which is subdivided into growth and maintenance respiration of leaves, stems and roots. Respiratory losses in each of the three compartments are modeled as follows:

(38) $$R_{m,k} = m_k\, r_{m,k} Q_{10}^{(T-T_0)/10}; k = 1,2,3$$

(39) $$R_{g,k} = \Delta m_k\, r_{m,k}; k = 1,2,3$$

where Δm is the specific growth.

In the revised version [51], the rate of photosynthesis is modeled using the Farquhar approach.

3.1.11 VEGAS NPP

The terrestrial carbon model VEgetation-Global-Atmosphere-Soil (VEGAS) is a Dynamic Global Vegetation Model [52,53]. It subdivides the global vegetation into four plant functional types (PFTs): broadleaf tree, needleleaf tree, cold grass, and warm grass. Photosynthesis is modeled as a function of light, temperature, soil moisture, and CO_2. NPP is calculated as a difference between GPP and respiratory losses from the three carbon pools: leaves, roots, and wood.

3.1.12 LPJ NPP

The Lund-Potsdam-Jena Dynamic Global Vegetation Model (LPJ) subdivides the global vegetation into ten plant functional types [54]: tropical broad-leaved evergreen, tropical broad-leaved raingreen, temperate needle-leaved evergreen, temperate broad-leaved evergreen, temperate broad-leaved summergreen, boreal needle-leaved evergreen, boreal needle-leaved summergreen, boreal broad-leaved summergreen, temperate herbaceous, tropical herbaceous. The net daily assimilation of carbohydrates is described by a production efficiency model (see also sections above):

(40) $$A_{nd} = \varepsilon_t\, APAR_t$$

where the light-use efficiency, ε_t, is a function of temperature, actual evapotranspiration, and ambient partial pressure of CO_2.

The annual NPP is calculated as a difference between the annual GPP and respiratory losses, R_m, from the three carbon pools: leaves, roots, and wood;

(41) $$NPP = 0.75(GPP - R_m)$$

assuming that the growth respiration comes to 25% of the annual NPP.

3.2 Baseline productivity of the global vegetation (blended model outputs)

The highly model-dependent results are not intended for offering policy relevant 'answers' or recommendations. Their usage is limited to demonstrating a quantitative framework for policy debates [55] and to delineating the field for political maneuvering [56]. Since the development of mitigation and adaptation policies requires objective information on the current state of knowledge, single model outputs should be combined to reduce model dependence.

There are several ways to blend model outputs. The most common one is simple averaging. The known deficiency of this approach is assigning equal weights to models that differ in their performance. Intuitively, it is reasonable to weigh the better models more. However, the crux lies in defining the metrics for model performance [57,58]. When model outputs can be compared with observations, the weights may be derived using Bayesian weighting scheme [59]. If this is not possible due to technical difficulties, then model outputs can be blended using an evolutionally stable scheme [60,61] that gives priority to earlier models.

3.2.1 Potsdam NPP

Comparison of global NPP models carried out more than a decade ago [62] resulted in releasing average estimates of NPP over a geographic grid with a half-degree resolution. These were the first normative data on global NPP created by summarizing modelling efforts. ("Normative data" means the data that result from a model ensemble, not from a single model, and therefore may be accepted as norms.) The released data set includes not only the mean values but also standard deviations that make it possible to assess an acceptable range of model estimates: Potsdam NPP (high) and Potsdam NPP (low).

3.2.2 Normative NPP

Terrestrial productivity has been the focus of biosphere studies over the last three decades. First, the global pattern of NPP was characterized by the data collected during the International Biological Program. Then, the data were turned into empirical models that related gradations in NPP to environmental factors of known geographic distribution. Later, a number of process-based models were developed in connection to the IGBP activities. This is definitely a field of science that hardly may be referred to as immature.

Nevertheless, the range of estimates remains roughly constant over this period. Earlier estimates of terrestrial NPP range from 10 to 100 PgC y^{-1} [63]. In the 1970s, they fell between 40 and 80 PgC y^{-1}. The estimates of empirical models [64] vary from 50 to 65 PgC y^{-1}, and the estimates of process-based models are expected to vary in the same range [62]. Re-analyses of the NPP measurements stored in the Osnabruck NPP database show that a 90% confidence interval suggested by available measurements is 50-70 PgC y^{-1} [65]. It seems that it may be difficult to reduce this 20% level of uncertainty in the commonly accepted estimate of terrestrial NPP while leaving research methods unchanged.

Therefore, we may speak only about the stability of normative estimates -- that is, the estimates representing the state of knowledge and, therefore, acceptable for use in policy relevant assessments.

The diversity of research results does not matter until a viable alternative to the commonly accepted norms emerges. The recent IPCC guidelines focused on objective reporting of uncertainty stemming from climate model pluralism [66]. However, epistemological pluralism [67,68] is no more a topical issue in "a world that is aware of its responsibility for planetary change and will demand globally concerted actions" [69,70]. One of the things that the world community is likely to expect from scientists is evaluating effectiveness of these actions in an objective and unambiguous manner [71]. Hence, it is a time to move the focus of attention to objective reporting of well-established beliefs.

Objective reporting of well-established beliefs suggests drawing distinction between normative knowledge (or text-book knowledge) and alternative knowledge (or frontier knowledge). The former is the solid knowledge that has stood the test of time and is well confirmed by a number of independent research studies. Frontier knowledge is something new, and something really new cannot be turned into solid knowledge immediately.

The evolution of scientific theories is often considered as a Darwinian process of natural selection that determines which theory survives and drifts them toward consensus [72]. There is nothing wrong with "natural selection" of models, with the exception of the risk of coming to an evolutionary deadlock. This risk can be significantly reduced through setting explicit criteria of "fitness" and detecting paradigm shifts in a timely fashion.

Since each model may be considered as normative for some regions and as alternative for others, it would be reasonable to draw distinction between pixel-based estimates, not between models. Then, the "fitness" of a new pixel-based estimate can be defined in an explicit form:

1. it must fall within the bounds defined by existing normative ensemble of estimates for a given pixel;
2. it must reduce the uncertainty on the normative estimate of NPP at the pixel under concern.

The uncertainty on the expected value can be quantified as the width of confidence interval: $\delta = 2\, c \cdot s \cdot n^{-1/2}$, where n is the number of estimates, s is standard deviation, c is the 95th percentile of Student's t distribution with n-1 degree of freedom.

Thus, the algorithm of the "artificial selection" may be formulated as follows:

1. Compare the new estimate for a given cell (x,y) of the geographic grid, u(x,y) with the normative ensemble of estimates for this cell, **w**(x,y).

2. If u(x,y)> w_{max}(x,y) or u(x,y)< w_{min}(x,y), normative NPP, v(x,y), remains unchanged; otherwise go to step 3.

3. Append u(x,y) to **w**(x,y), calculate the mean value, μ, of thus formed list of estimates and the width of its confidence interval, δ.

4. If δ is greater than the width of the confidence interval for the mean value of **w**(x,y), v(x,y) remains unchanged, otherwise v(x,y)= μ.

This algorithm filters out erroneous estimates as well as correct estimates when they dramatically contradict to the normative knowledge formed by the initial ensemble.

The latest version of the Normative NPP (Normative NPP 1.14.1) was constructed [61] from the outputs of the Miami NPP, Montreal NPP, TGER-NPP, Potsdam NPP (low), Potsdam NPP (high), TsuBiMo, GLO-PEM, Biome-BGC, BEAMS, Madison NPP, MODIS-NPP, Sim-CYCLE, VEGAS, LPJ. The initial model ensemble was formed from the outputs of the Miami NPP, Montreal NPP, TGER-NPP, Potsdam NPP (low), and Potsdam NPP (high).

3.2.3 Alternative NPP

Since no well-agreed-upon method exists at the moment for distinguishing between erroneous and correct estimates of NPP, every new estimate should be included either into the normative ensemble or into the alternative ensemble. The former represents the current state of the knowledge, whereas the latter represents emerging alternative to the current knowledge.

The alternative estimate is, thus, constructed as follows:

1. Compare the new estimate for a given cell (x,y) of the geographic grid, u(x,y) with the normative ensemble of estimates for this cell, **w**(x,y).

2. If w_{min}(x,y) < u(x,y)< w_{max}(x,y), alternative NPP, v(x,y), remains unchanged; otherwise go to step 3.

3. Append u(x,y) to **w**(x,y), calculate the mean value of thus formed list of estimates and the width of its confidence interval, δ.

4. If δ is less than the width of the confidence interval for the mean value of **w**(x,y), v(x,y) remains unchanged, otherwise go to step 5.

5. Append u(x,y) to the list of alternative estimates; calculate the mean value, μ, of thus formed list; set v(x,y)= μ.

The latest version of the Alternative NPP (Alternative NPP 1.14.1) was constructed [61] from the outputs of the Miami NPP, Montreal NPP, TGER-NPP, Potsdam NPP (low), Potsdam NPP (high), TsuBiMo, GLO-PEM, Biome-BGC, BEAMS, Madison NPP, MODIS-NPP, Sim-CYCLE, VEGAS, LPJ. The initial model ensemble was formed from the outputs of the Miami NPP, Montreal NPP, TGER-NPP, Potsdam NPP (low), and Potsdam NPP (high).

3.3 List of data files stored in *Carbon Sink Archives*

(1) Net Primary Production (TsuBiMo 1 NPP) - global grid of baseline annual estimates.

Grid produced by G. A. Alexandrov.

Related to: NPP; annual; global; TsuBiMo NPP; NPP-benchmarks

Registered as: "Benchmarks\\TsuBiMo1_NPP.grd"

Downloadable from: https://project.nies.go.jp/csa/AlexandrovArchive/Benchmarks/

Recommended citation:

Alexandrov G, Oikawa T: TsuBiMo: a biosphere model of the CO_2-fertilization effect. *Climate Research* 2002, 19: 265-270.

Alexandrov GA, Yamagata Y, Oikawa T: Towards a model for projecting Net Ecosystem Production of the world forests. *Ecological Modelling* 1999, 123: 183-191. Implementation notes: This is the grid of baseline annual NPP estmated with TsuBiMo model version 1.0.

(2) Gross Primary Production - global grids of annual estimates for 1982-2002

Grid produced by G. A. Alexandrov.

Related to: GPP; annual; global; TsuBiMo

Registered as: none

Downloadable from: https://project.nies.go.jp/csa/AlexandrovArchive/GPP/annual/global/grids/TsuBiMo6/

Recommended citation: Alexandrov, G.A., Oikawa, T. and Yamagata, Y., 2002. The scheme for globalization of a process-based model explaining gradations in terrestrial NPP and its application, Ecological Modelling, 148: 293-306.

Implementation notes: This is the folder containing the grids gpp1982.grd ... gpp2002.grd of annual NPP of potential natural vegetation.

(3) Net Ecosystem Production - global grids of annual estimates for 1982-2002

Grid produced by G. A. Alexandrov.

Related to: NEP; annual; global; TsuBiMo

Registered as: none

Downloadable from: https://project.nies.go.jp/csa/AlexandrovArchive/NEP/annual/global/grids/TsuBiMo6/

Recommended citation: Alexandrov G, Yamagata Y: Verification of carbon sink assessment: Can we exclude natural sinks? Climatic Change 2004, 67: 437-447.

Implementation notes: This is the folder containing the grids nep1982.grd ... nep2002.grd of climate driven departures of annual NEP.

(4) Net Ecosystem Production - global maps of annual estimates for 1982-2002

Map produced by G. A. Alexandrov.

Related to: NEP; annual; global; TsuBiMo

Registered as: none

Downloadable from: https://project.nies.go.jp/csa/AlexandrovArchive/NEP/annual/global/maps/TsuBiMo6/

Recommended citation: Alexandrov G, Yamagata Y: Verification of carbon sink assessment: Can we exclude natural sinks? Climatic Change 2004, 67: 437-447.

Implementation notes: This is the folder containing the maps nep1982.jpg ... nep2002.jpg of climate-driven departures of annual NEP.

(5) Net Primary Production - global grids of annual estimates for 1982-2002

Grid produced by G. A. Alexandrov.

Related to: NPP; annual; global; TsuBiMo

Registered as: none

Downloadable from: https://project.nies.go.jp/csa/AlexandrovArchive/NPP/annual/global/grids/TsuBiMo6/

Recommended citation: Alexandrov, G.A., Oikawa, T. and Yamagata, Y., 2002. The scheme for globalization of a process-based model explaining gradations in terrestrial NPP and its application, Ecological Modelling, 148: 293-306.

Implementation notes: This is the folder containing the grids npp1982.grd ... npp2002.grd of annual NPP of potential natural vegetation.

(6) Net Primary Production - global maps of annual estimates for 2000-2002

Map produced by G. A. Alexandrov.

Related to: NPP; annual; global; TsuBiMo

Registered as: none

Downloadable from: https://project.nies.go.jp/csa/AlexandrovArchive/NPP/annual/global/maps/TsuBiMo6/

Recommended citation: Alexandrov, G.A., Oikawa, T. and Yamagata, Y., 2002. The scheme for globalization of a process-based model explaining gradations in terrestrial NPP and its application, Ecological Modelling, 148: 293-306.

Implementation notes: This is the folder containing the grids npp2000.tif ... npp2002.tif of annual NPP of potential natural vegetation, and the legend in NPPLegend.bmp file.

(7) Net Primary Production (Miami NPP) - global grid of baseline annual estimates

Grid produced by E. O. Box.

Related to: NPP; annual; global; Miami NPP; NPP-benchmarks

Registered as: "Benchmarks\\MiamiNPP.grd"

Downloadable from: https://project.nies.go.jp/csa/AlexandrovArchive/Benchmarks/

Recommended citation: Box, E.O., Dye, D.G., Fujiwara, K., Tateishi, R. and Bai, X., 1994. Global environmental data sets from the Toyota Crown laboratory global engineering research project (1991-1994) on CD-ROM. University of Tokyo, Tokyo

Implementation notes: This is the grid of baseline annual NPP derived from mean annual temperature and annual amount of precipitation using an empirical model.

(8) Net Primary Production (Montreal NPP) - global grid of baseline annual estimates

Grid produced by E. O. Box.

Related to: NPP; annual; global; Montreal NPP; NPP-benchmarks

Registered as: "Benchmarks\\MontrealNPP.grd"

Downloadable from: https://project.nies.go.jp/csa/AlexandrovArchive/Benchmarks/

Recommended citation: Box, E.O., Dye, D.G., Fujiwara, K., Tateishi, R. and Bai, X., 1994. Global environmental data sets from the Toyota Crown laboratory global engineering research project (1991-1994) on CD-ROM. University of Tokyo, Tokyo

Implementation notes: This is the grid of baseline annual NPP derived from actual evapotranspiration using an empirical model.

(9) Net Primary Production (TGER-NPP) - global grid of baseline annual estimates

Grid produced by E. O. Box.

Related to: NPP; annual; global; TGER-NPP; NPP-benchmarks

Registered as: "Benchmarks\\TGER_NPP.grd"

Downloadable from: https://project.nies.go.jp/csa/AlexandrovArchive/Benchmarks/

Recommended citation: Box, E.O., Dye, D.G., Fujiwara, K., Tateishi, R. and Bai, X., 1994. Global environmental data sets from the Toyota Crown laboratory global engineering research project (1991-1994) on CD-ROM. University of Tokyo, Tokyo

Implementation notes: This is the grid of annual NPP derived from NDVI using an empirical model.

(10) Net Primary Production (Biome-BGC NPP) - global grid of baseline annual estimates

Grid produced by G. Churkina.

Related to: NPP; annual; global; Biome-BGC NPP; NPP-benchmarks

Registered as: "Benchmarks\\BiomeBGC_NPP.grd"

Downloadable from: https://project.nies.go.jp/csa/ChurkinaArchive/NPP/annual/global/grids/

Recommended citation:

Running SW, Hunt ERJ: Generalization of a forest ecosystem process model for other biomes, Biome-BGC, and an application for global-scale models. In Scaling Physiological Processes: Leaf to Globe. Edited by: Ehleringer JR and Field CB. San Diego, California, Academic Press; 1993:141-158. [Mooney Harold A (Series Editor): Physiological Ecology]

Churkina G, Trusilova K, Vetter M, Dentener F: Contributions of nitrogen deposition and forest regrowth to terrestrial carbon uptake. Carbon Balance and Management 2007, 2: 5. [www.cbmjournal.com/content/2/1/5]

Implementation notes: This is the grid of baseline annual NPP estmated with Biome-BGC version 4.1.1 (with carbon and nitrogen allocation routine from 4.1), which calculates water, carbon, and nitrogen pools dynamics as well as their fluxes on a daily basis.

(11) Net Primary Production (Biome-BGC NPP) - global grid of baseline annual estimates

Map produced by G. Churkina.

Related to: NPP; annual; global; Biome-BGC NPP; NPP-benchmarks

Registered as: none

Downloadable from: https://project.nies.go.jp/csa/ChurkinaArchive/NPP/annual/global/maps/

Recommended citation:

Running SW, Hunt ERJ: Generalization of a forest ecosystem process model for other biomes, Biome-BGC, and an application for global-scale models. In Scaling Physiological Processes: Leaf to Globe. Edited by: Ehleringer JR and Field CB. San Diego, California, Academic Press; 1993:141-158. [Mooney Harold A (Series Editor): Physiological Ecology]

Churkina G, Trusilova K, Vetter M, Dentener F: Contributions of nitrogen deposition and forest regrowth to terrestrial carbon uptake. Carbon Balance and Management 2007, 2: 5. [www.cbmjournal.com/content/2/1/5] Implementation notes: This is the map of baseline annual NPP estmated with Biome-BGC version 4.1.1 (with carbon and nitrogen allocation routine from 4.1), which calculates water, carbon, and nitrogen pools dynamics as well as their fluxes on a daily basis.

(12) Net Primary Production (Potsdam NPP) - global grid of baseline annual estimates

Grid produced by W. Cramer.

Related to: NPP; annual; global; Potsdam NPP; NPP-benchmarks

Registered as: "Benchmarks\\PotsdamNPP.grd"

Downloadable from: http://islscp2.sesda.com/ISLSCP2_1/html_pages/groups/carbon/model_npp_xdeg.html

Recommended citation: Cramer, W., D. W. Kicklighter, A. Bondeau, B. Moore III, G. Churkina, B. Nemry, A. Ruimy, A. L. Schloss and The Participants of the Potsdam NPP Model Intercomparison (1999). Comparing global models of terrestrial net primary productivity (NPP): overview and key results. Global Change Biology, Volume 5 Issue S1:1-15

Implementation notes: This is the grid of baseline annual NPP resulted from the Potsdam NPP inter-comparison study.

(13) Net Primary Production (SimCycle-NPP) - global grids of annual estimates for 1998-2000

Grid produced by A. Ito.

Related to: NPP; annual; global; SimCycle

Registered as: "Benchmarks\\SimCycleNPP2000.grd"

Downloadable from: https://project.nies.go.jp/csa/ItoArchive/NPP/annual/global/grids

Recommended citation:

Ito, A. and Oikawa, T. 2002. A simulation model of the carbon cycle in land ecosystems (Sim-CYCLE): A description based on dry-matter production theory and plot-scale validation. Ecological Modelling 151: 147-179.

Implementation notes: This is the folder containing the grids npp1998.grd ... npp2000.grd of annual NPP of potential natural vegetation.

(14) Net Primary Production (SimCycle-NPP) - global grids of annual estimates for 1998-2000

Map produced by A. Ito.

Related to: NPP; annual; global; SimCycle

Registered as: none

Downloadable from: https://project.nies.go.jp/csa/ItoArchive/NPP/annual/global/maps

Recommended citation: Ito, A. and Oikawa, T. 2002. A simulation model of the carbon cycle in land ecosystems (Sim-CYCLE): A description based on dry-matter production theory and plot-scale validation. Ecological Modelling 151: 147-179.

Implementation notes: This is the folder containing the maps npp1998.tif ... npp2000.tif of annual NPP of potential natural vegetation, and the legend in nppLegend.bmp file.

(15) NDVI - East Asia maps of monthly NDVI for 1997

Map produced by T. Matsunaga.

Related to: NDVI; monthly; East Asia

Registered as: none

Downloadable from: https://project.nies.go.jp/csa/MatsunagaArchive/NDVI/monthly/eastasia/maps/

Recommended citation: TBA

Implementation notes: TBA.

(16) Net Primary Production (GLO-PEM NPP) - global grid of baseline annual estimates
Grid produced by S. D. Prince.

Related to: NPP; annual; global; GLO-PEM NPP; NPP-benchmarks

Registered as: "Benchmarks\\GloPemNPP.grd"

Downloadable from: http://glcf.umiacs.umd.edu/data/glopem/

Recommended citation: Prince, S. D. and S. J. Goward. 1995. Global primary production: a remote sensing approach, Journal of Biogeography 22 : 316-336.

Implementation notes: This is the grid of baseline annual NPP resulted from the production efficiency model (GLO-PEM).

(17) Net Primary Production (BEAMS NPP) - global grid of baseline annual estimates
Grid produced by T. Sasai.

Related to: NPP; annual; global; BEAMS NPP; NPP-benchmarks

Registered as: "Benchmarks\\BeamsNPP.grd"

Downloadable from: https://project.nies.go.jp/csa/SasaiArchive/NPP/annual/global/grids/

Recommended citation: Sasai T, Ichii K, Yamaguchi Y, Nemani R: Simulating terrestrial carbon fluxes using the new biosphere model "biosphere model integrating eco-physiological and mechanistic approaches using satellite data" (BEAMS). Journal of Geophysical Research-Biogeosciences 2005, 110.

Implementation notes: This is the grid of baseline annual NPP estmated with BEAMS model.

(18) Net Primary Production (Madison NPP) - global grid of baseline annual estimates
Grid produced by D. Zaks.

Related to: NPP; annual; global; Madison NPP; NPP-benchmarks

Registered as: "Benchmarks\\MadisonNPP.grd"

Downloadable from: https://project.nies.go.jp/csa/ZaksArchive/NPP/annual/global/grids/

Recommended citation: Zaks DPM, Ramankutty N, Barford CC, Foley JA: From Miami to Madison: Investigating the relationship between climate and terrestrial net primary production. Global Biogeochemical Cycles 2007, 21: GB3004-doi:10.1029/2006GB002705.

Implementation notes: This is the grid of baseline annual NPP estmated with an empirical model.

(19) Net Primary Production (VEGAS NPP) - global grid of baseline annual estimates

Grid produced by N. Zeng.

Related to: NPP; annual; global; VEGAS NPP; NPP-benchmarks

Registered as: "Benchmarks\\VegasNPP.grd"

Downloadable from: https://project.nies.go.jp/csa/ZengArchive/NPP/annual/global/grids/

Recommended citation: Zeng N, Mariotti A, Wetzel P: Terrestrial mechanisms of interannual CO2 variability. Global Biogeochemical Cycles 2005, 19.

Zeng N: Glacial-interglacial atmospheric CO2 change - The glacial burial hypothesis. Advances in Atmospheric Sciences 2003, 20: 677-693.

Implementation notes: This is the grid of baseline annual NPP estmated with VEGAS model.

(20) Net Primary Production (MODIS NPP) - global grids of annual estimates for 2000-2006

Grid produced by M. Zhao.

Related to: NPP; annual; global; MODIS

Registered as: "Benchmarks\\MODIS_NPP_2000.grd"

Downloadable from: https://project.nies.go.jp/csa/ZhaoArchive/NPP/annual/global/grids/

Recommended citation: Zhao, M., S. W. Running, F. A. Heinsch, R. R. Nemani. (2008). Terrestrial Primary Production from MODIS. In Land Remote Sensing and Global Environmental Change: NASA's EOS and the Science of ASTER and MODIS.. Edited by C. Justice, M. Abrams, Springer, (in press).

Implementation notes: This is the folder containing the grids MODIS_NPP_2000.grd ... MODIS_NPP_2006.grd of annual NPP.

(21) Net Primary Production (MODIS NPP) - global maps of annual estimates for 2000-2006

Map produced by M. Zhao.

Related to: NPP; annual; global; MODIS

Registered as: none

Downloadable from: https://project.nies.go.jp/csa/ZhaoArchive/NPP/annual/global/maps/

Recommended citation: Zhao, M., S. W. Running, F. A. Heinsch, R. R. Nemani. (2008). Terrestrial Primary Production from MODIS. In Land Remote Sensing and Global Environmental Change: NASA's EOS and the Science of ASTER and MODIS.. Edited by C. Justice, M. Abrams, Springer, (in press).

Implementation notes: This is the folder containing the maps MODIS_NPP_2000.tif ... MODIS_NPP_2006.tif of annual NPP.

4. Results and Conclusions

4.1 Results

The brief analysis of the NPP model outputs brought the results that call for further reflections.

(1) Deviations from the Miami model's world view

Estimates of average productivity of major biomes produced with the Miami model lie below its temperature and humidity curves (Figure 9.6) that set certain limits for NPP. However, estimates produced with other models do not. BEAMS (Figure 9.1), MODIS-NPP (Figure 9.7) and TGER-NPP (Figure 9.12) implies that these limits are not valid for larch forests and taiga. Biome-BGC adds tundra to them (Figure 9.2), and the Montreal NPP (Figure 9.8) adds sub-humid forests and shrublands to the list of deviations. TsuBiMo 1 (Figure 9.13) removes taiga, tundra and shrublands from this list, but adds raingreen tropical forests. Sim-CYCLE (Figure 9.11) implies that these limits are too low for larch forests, taiga, summergreen broadleaf forests, evergreen broadleaf forests, and subhumid forests. VEGAS (Figure 9.14) adds grasslands to this list. GLO-PEM (Figure 9.3) suggests that all these limits should be 20-30% higher. All models, excepting Madison NPP, agree that the Miami model underestimates the productivity of larch forests.

(2) Effects of structural uncertainty

The Miami NPP, Montreal NPP, TGER-NPP and TsuBiMo 1 NPP were derived from the same measurements - Osnabruck database of measured NPP. Nevertheless they differ on the global pattern of productivity (Figure 8.5, 8.7, 8.11, 8.12).

(3) Effects of using more observations

The Madison NPP was derived from a larger database of measured NPP, but it gives quite similar estimates of productivity (Figure 9.5, 8.4). Thus, having more data does not imply different results.

(4) Evolutional stability of Normative NPP

The sequence of NormativeNPP versions (1.5 -1.14) demonstrates evolutional stability of the normative data on terrestrial productivity [61]. The totals (i.e. the estimates of the total terrestrial NPP corresponding to different versions of the Normative NPP grid) vary in a very narrow range: from 58.76 to 59.14 PgC y^{-1}. Sub-totals characterizing productivity of major vegetation zones never differ by more than 7 gC m^{-2} y^{-1}. A new model may change sub-totals by 1% at most.

(5) Emerging alternatives

The sequence of Alternative NPP versions (1.6-1.14) shows large variations of totals: from 64 to 91.7 PgC y^{-1} [61]. In the final version, the total is 70 PgC y^{-1} and sub-totals deviate greatly from the Miami model projections (Figure 9.17) implying an alternative global pattern of productivity (Figure 8.16). This pattern may be characterized in general as "seasonality sensitive". Productivity of larch forest zone (14) is comparable to that of taiga (36), and productivity of rain-green forest (3) is comparable to that of tropical rainforest (8) emphasizing that conditions of the growing season, not of the whole year, are crucial.

4.2 Conclusions

Modern computational and observational tools have caused an explosion of scientific data related to biosphere studies. This will eventually improve the consistency of biosphere models through creating multiple constraints for positioning 'true' values for model parameters. Thus, the limiting factor is the rate of building consensus on interpretation of the model outputs that will result from the new observations.

The purpose of *Carbon Sink Archives* is to facilitate internalization of the new model results that may deviate from the existing consensus on biosphere characteristics. The efficiency of this web-based service depends mainly on the attitude of biosphere modellers, their inclination "to harness collective, net-enabled intelligence" for coping with the dynamism of the data circulating in their research community.

5. Appendix. Maps, charts and plots

5.1 Web-portal

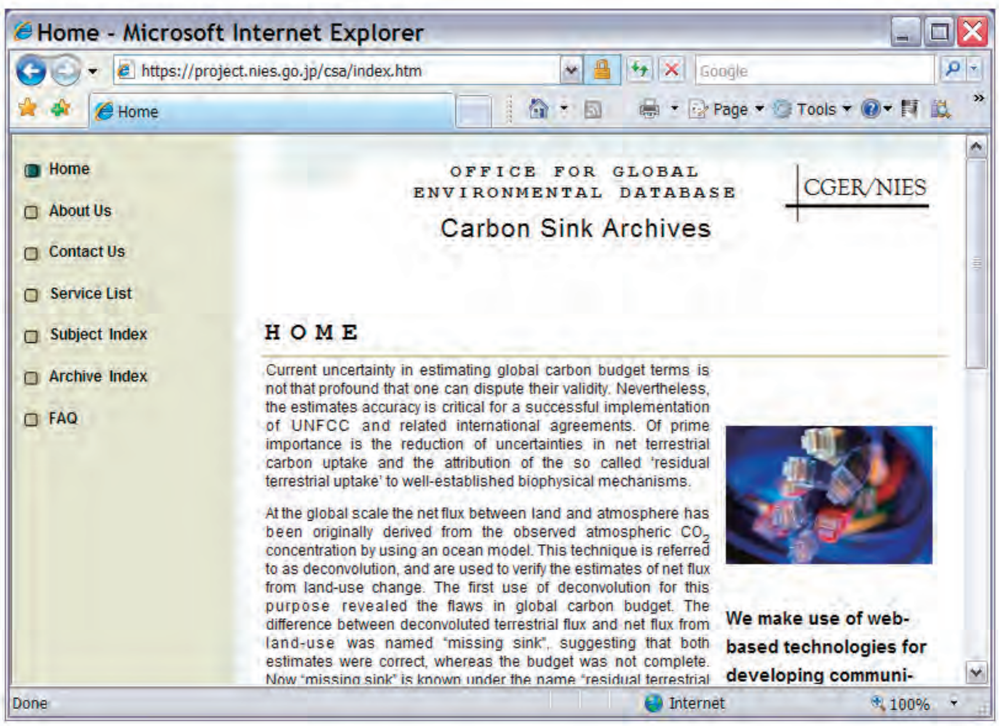

Figure 1.1 - Screenshot of the starting page of the *Carbon Sink Archives* web-portal.

Figure 1.2 - Screenshot of the directory of web-based services.

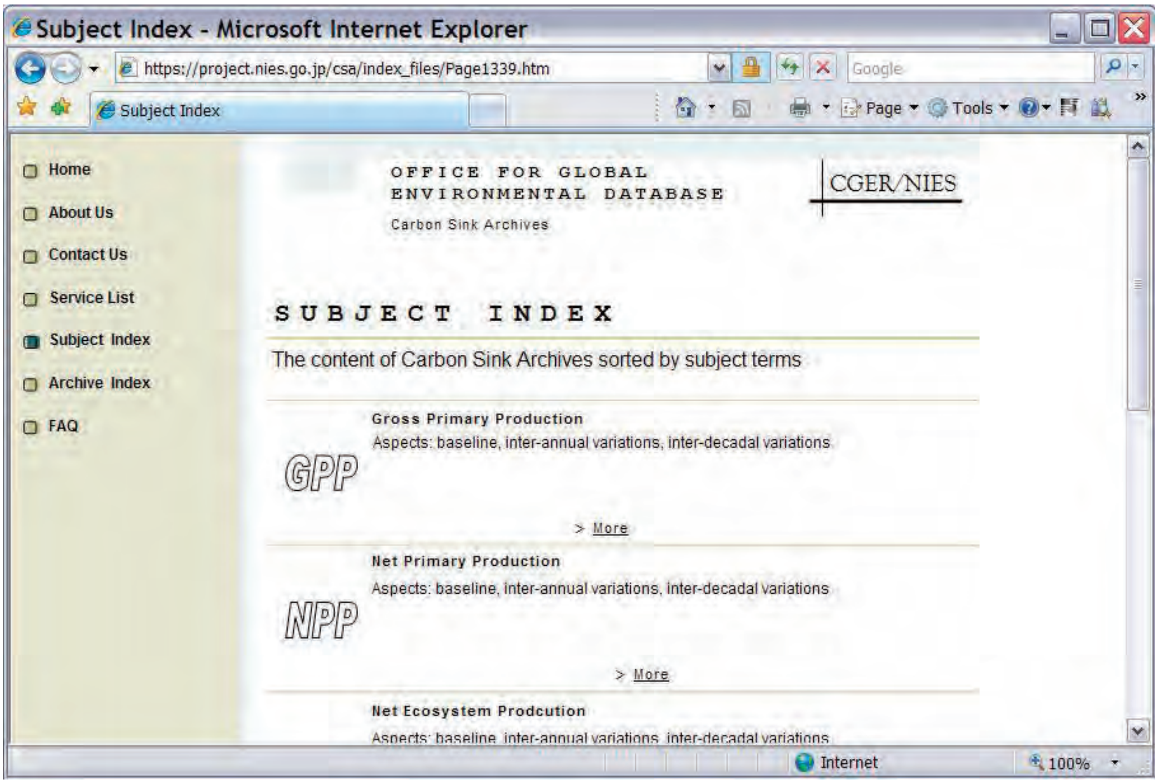

Figure 1.3 - Screenshot of the subject index.

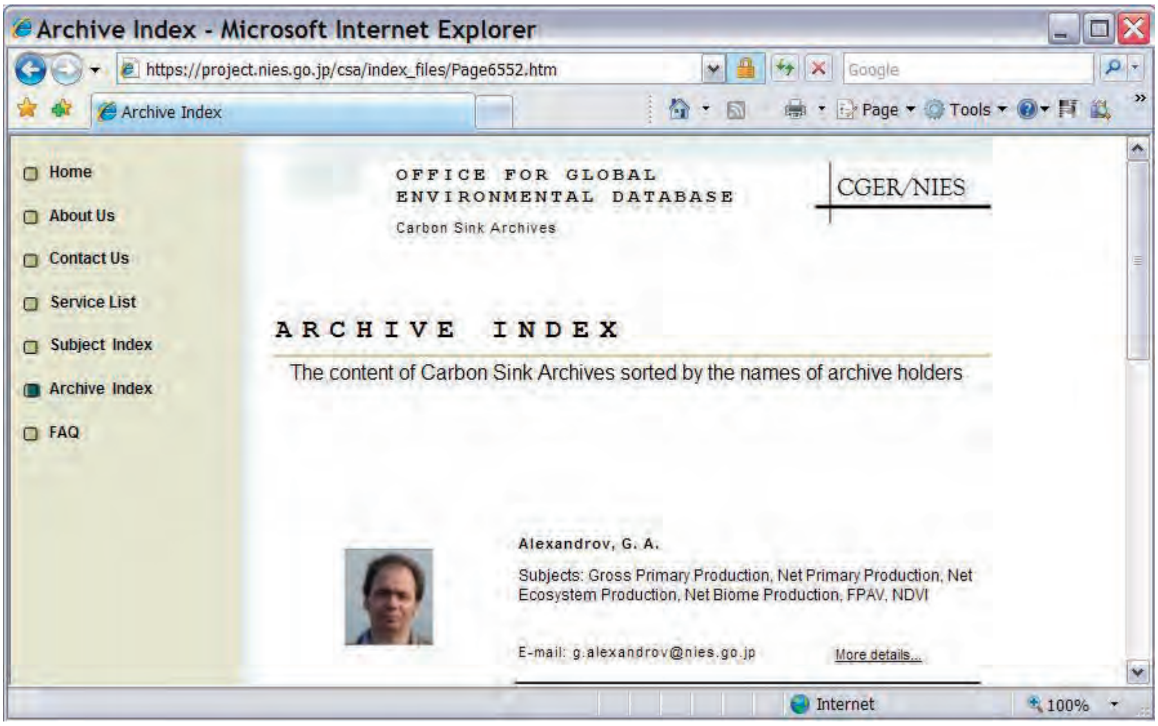

Figure 1.4 - Screenshot of the directory of subscribers.

5.2 Database of file references

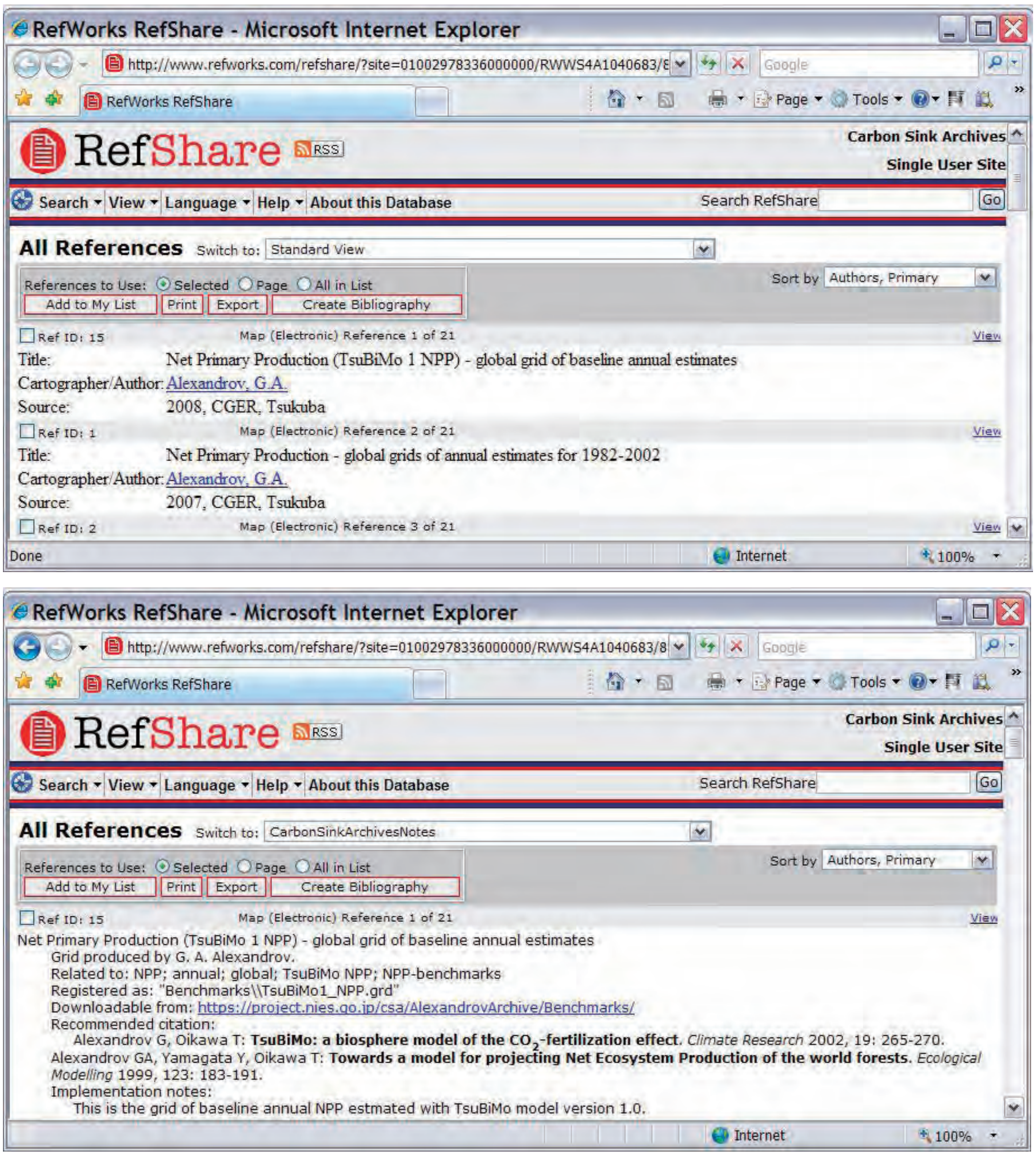

Figure 2.1 - The custom view of the database of file references.

The standard view (upper window) of the database of file references can be changed to custom view (lower window) using "switch to" window.

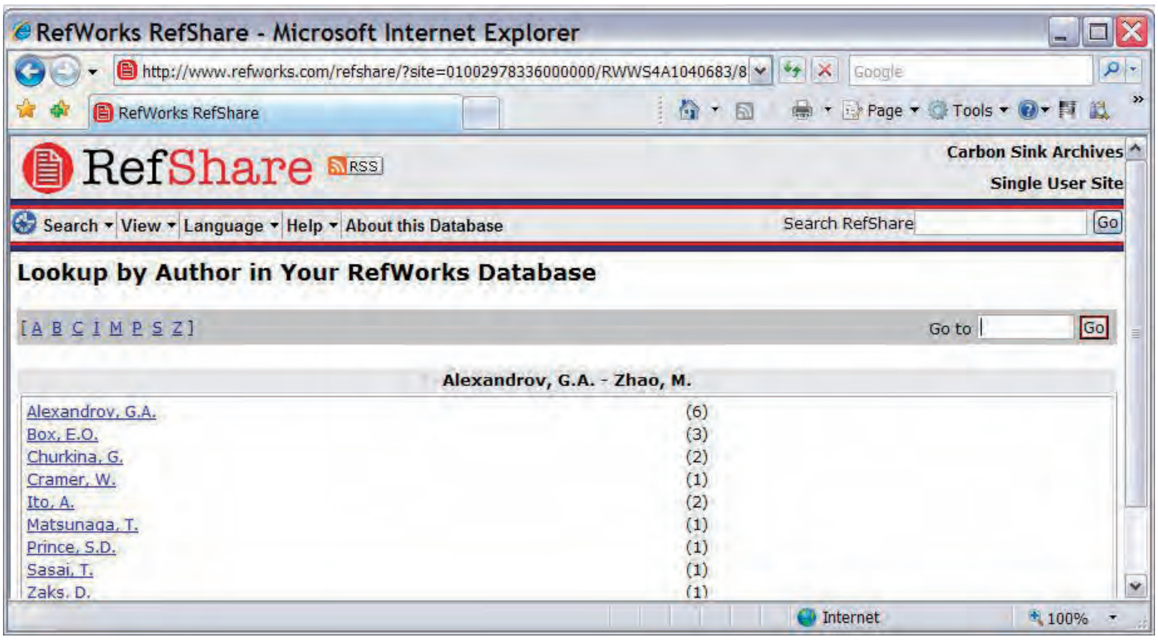

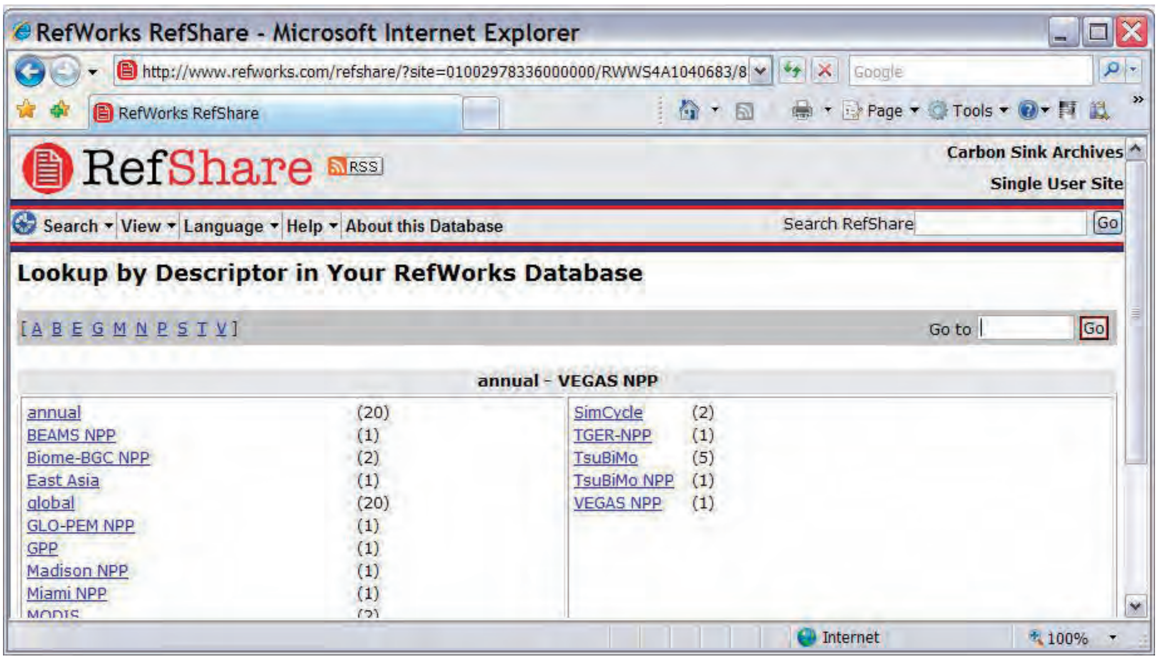

Figure 2.2 - The lookup of the database of file references.

One may select either the Author lookup (upper window) or the Descriptor lookup (lower window) in the “View” pop-up menu.

5.3 Web tools

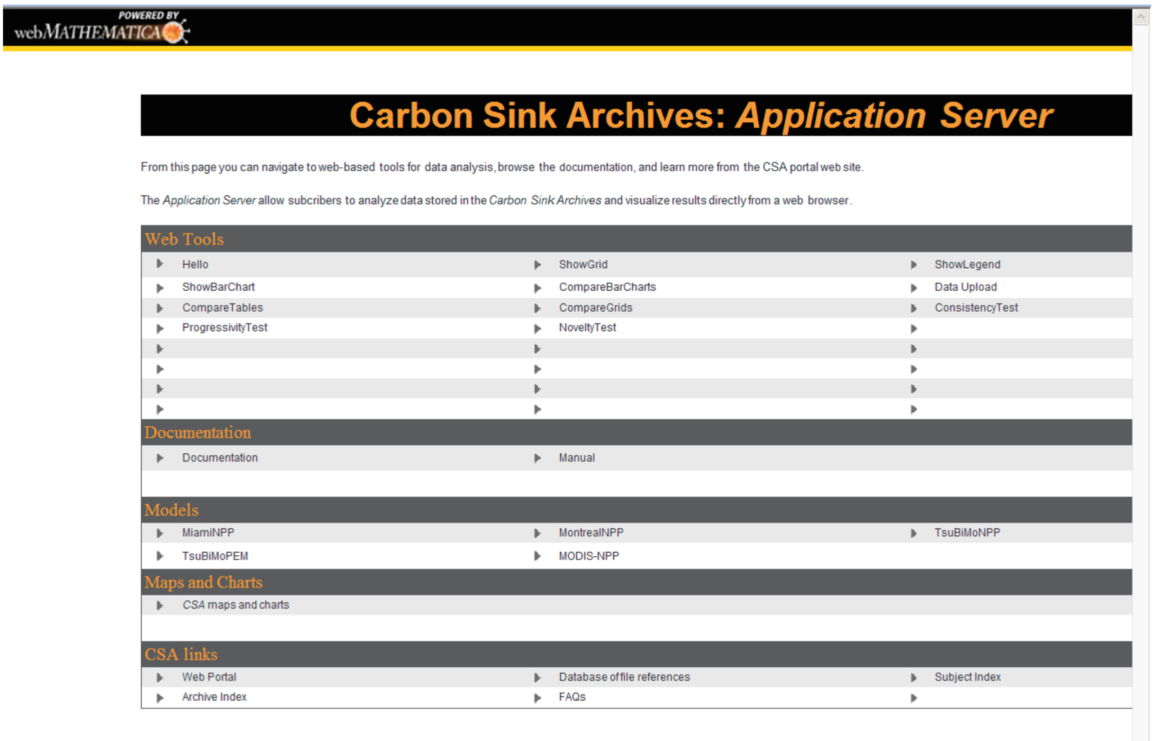

Figure 3.1 - Screenshot of the web-tools index.

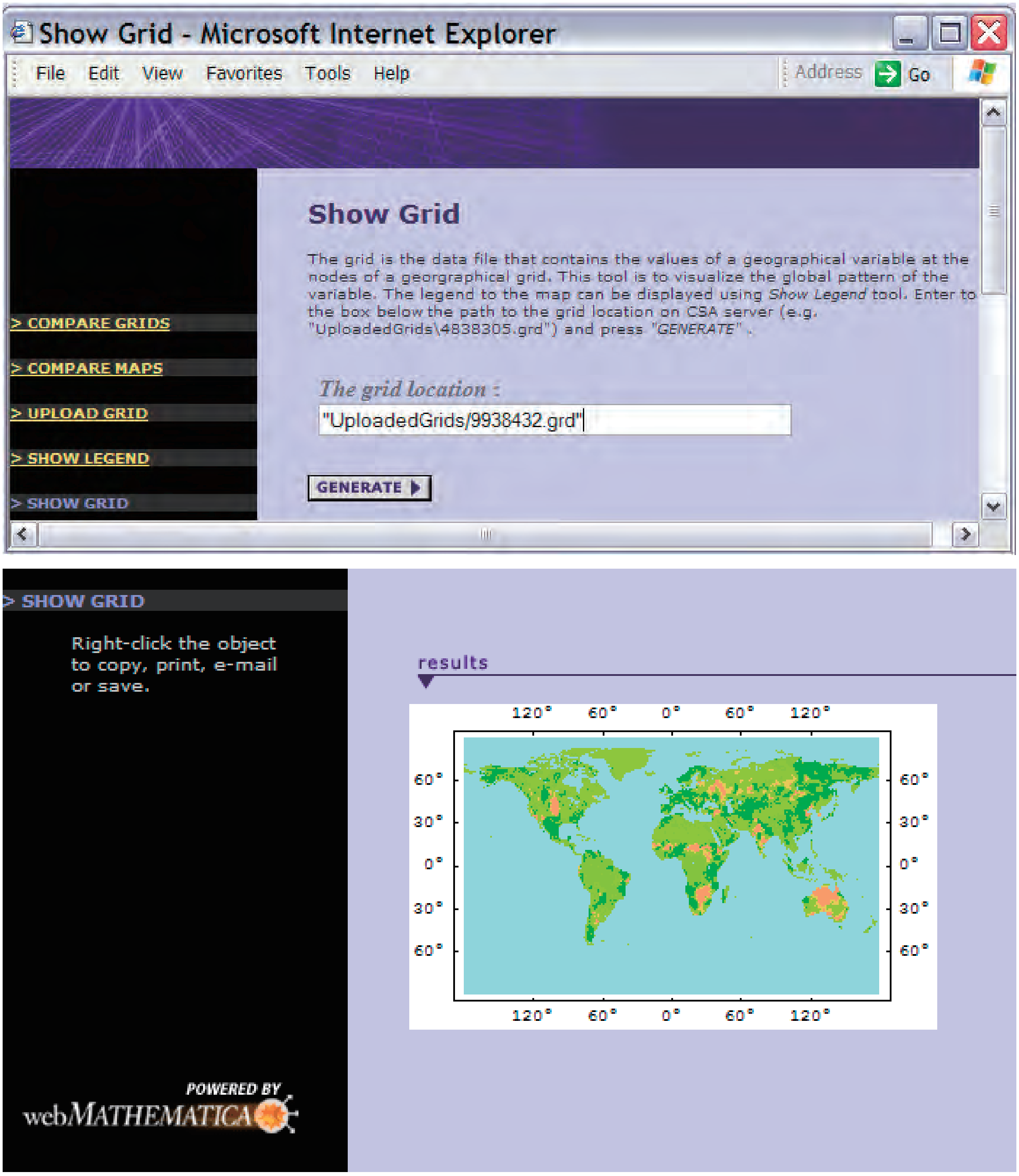

Figure 3.2 - Screenshots illustrating the usage of Show Grid tool.

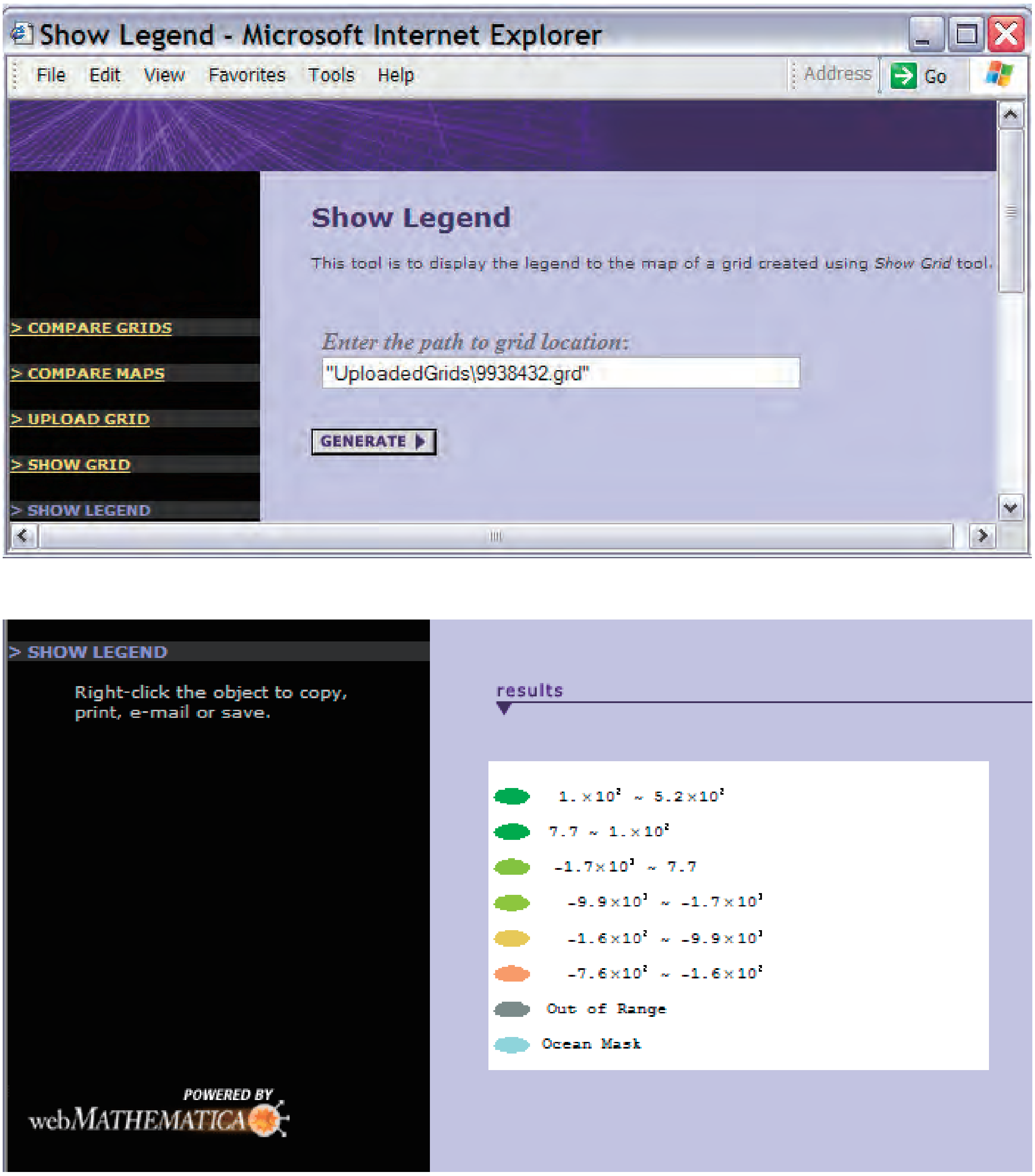

Figure 3.3 - Screenshots illustrating the usage of Show Legend tool.

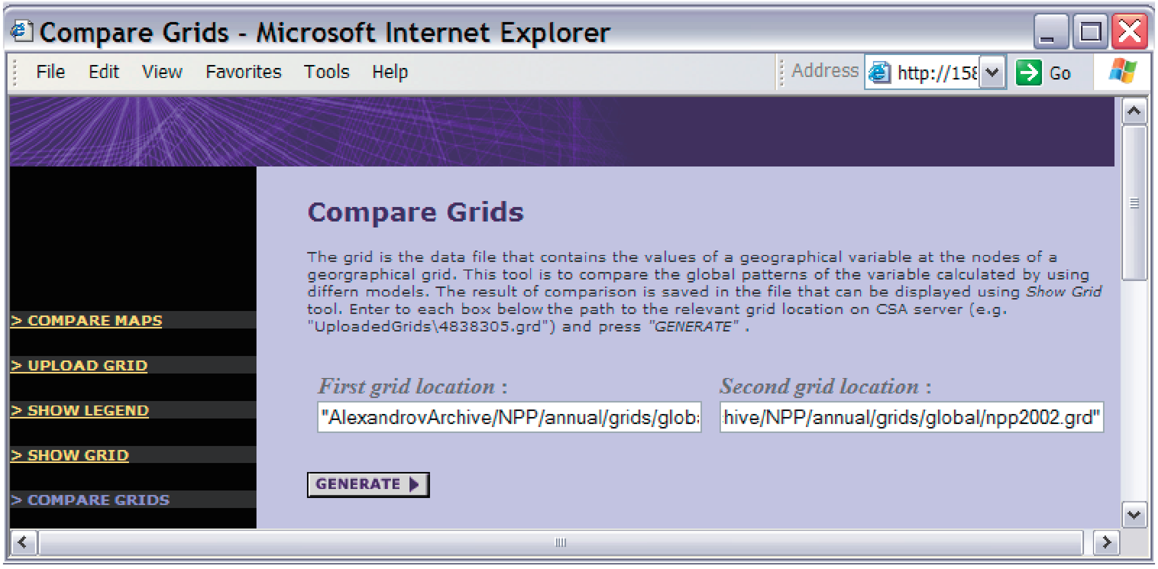

Figure 3.4 - Screenshots illustrating the usage of Compare Grids tool.

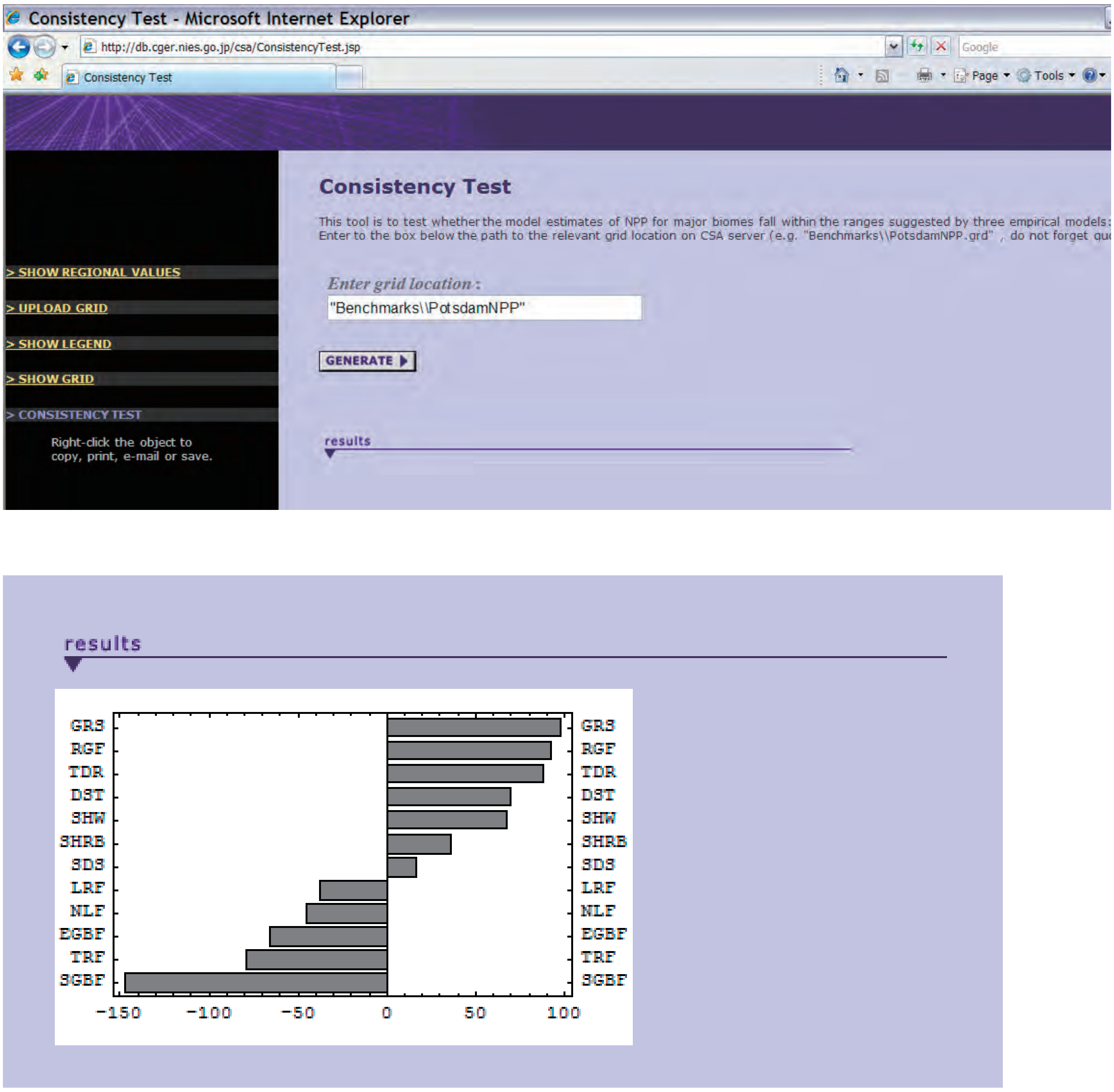

Figure 3.5 - Screenshots illustrating the usage of Consistency Test tool.

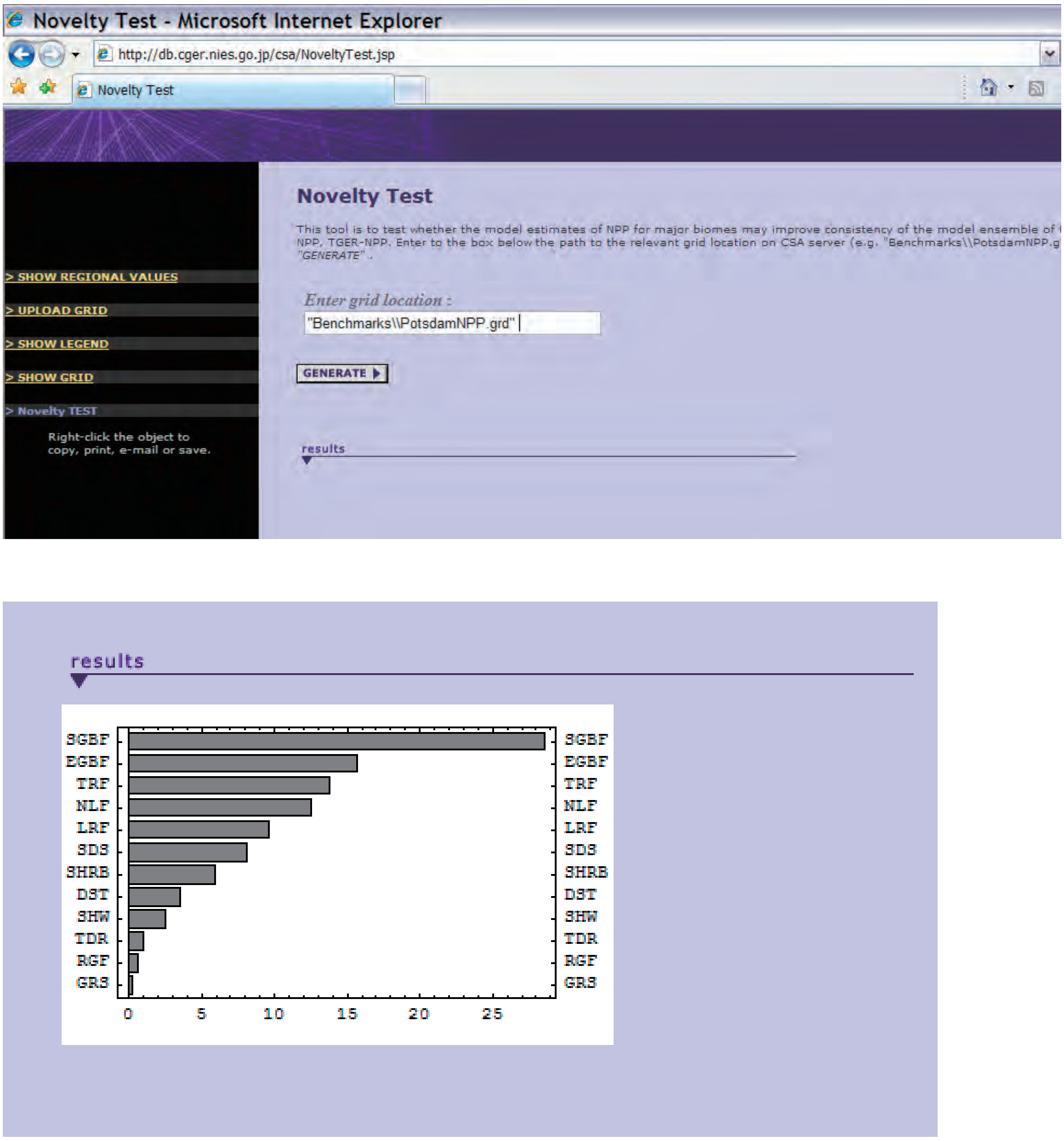

Figure 3.6 - Screenshots illustrating the usage of Novelty Test tool.

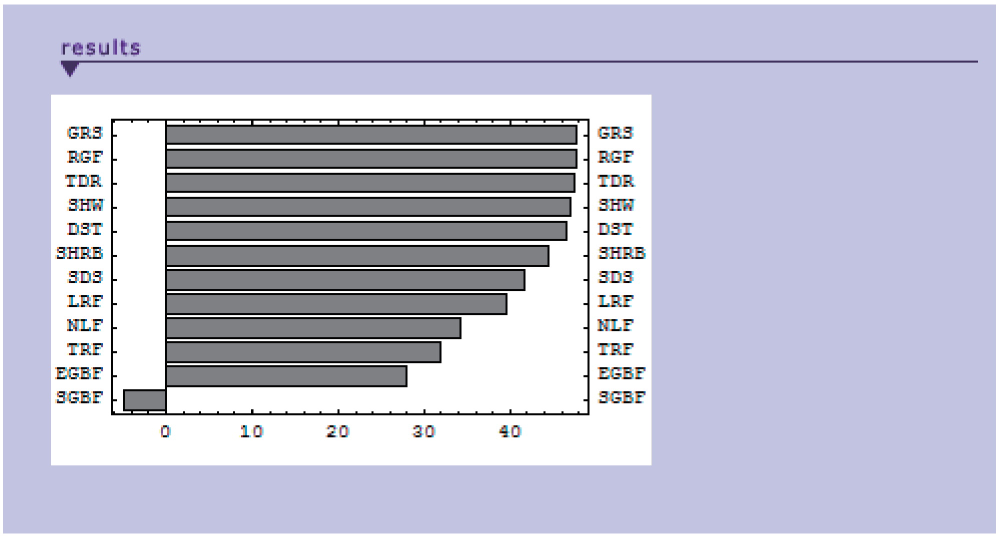

Figure 3.7 - Screenshots illustrating the usage of Progressivity Test tool.

5.4 NPP models

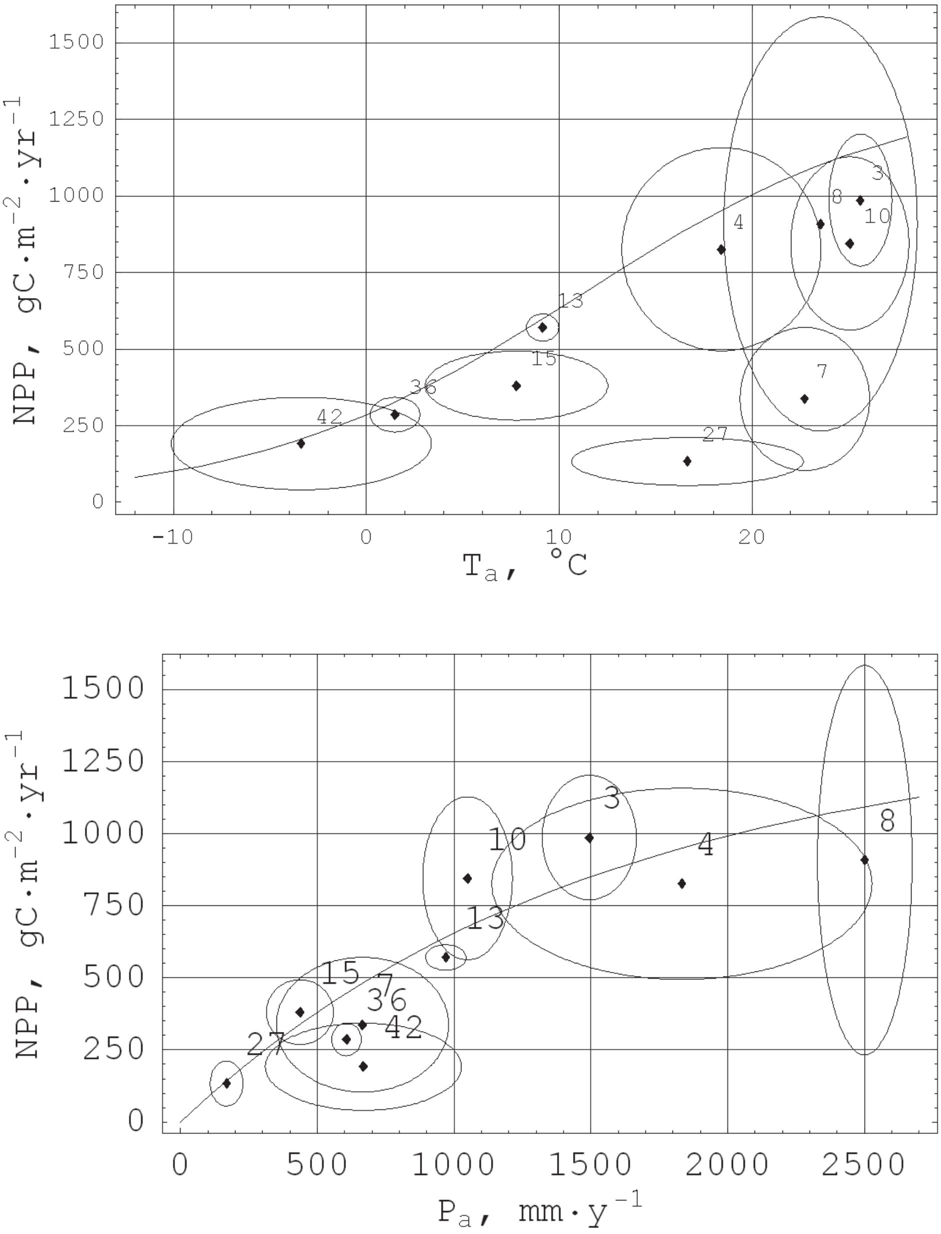

Figure 4.1 - Miami model curves plotted against measured NPP.

Legend: 42 - tundra, 14 - larch forests, 36 - needle-leaf forests, 13 - summer-green broad-leaved forests, 4 - evergreen broad-leaved forests, 8 - tropical rainforests, 6 - deserts, 27 - semi-desert scrubs, 7 - shrublands, 15 - grasslands, 10 - subhumid woodlands, 3 - rain green forests. Points mark mean values, ellipses delineate standard deviations from the mean values, and lines represent the temperature curve and humidity curve of the Miami NPP model, respectively. (*See also* [34].)

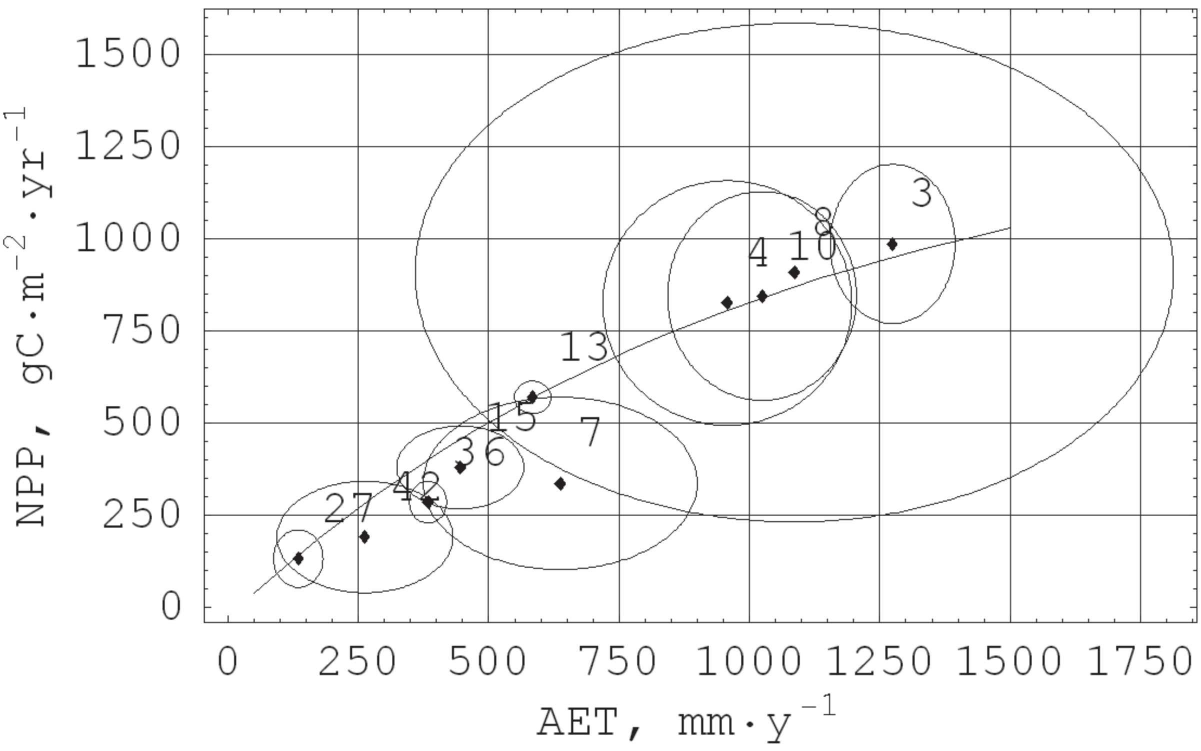

Figure 4.2 - The Montreal model curve plotted against measured NPP.

Legend: 42 - tundra, 14 - larch forests, 36 - needle-leaf forests, 13 - summer-green broad-leaved forests, 4 - evergreen broad-leaved forests, 8 - tropical rainforests, 6 - deserts, 27 - semi-desert scrubs, 7 - shrublands, 15 - grasslands, 10 - subhumid woodlands, 3 - rain green forests. Points mark mean values, ellipses delineate standard deviations from the mean values, and lines represent the temperature curve and humidity curve of the Miami NPP model, respectively. (*See also* [34].)

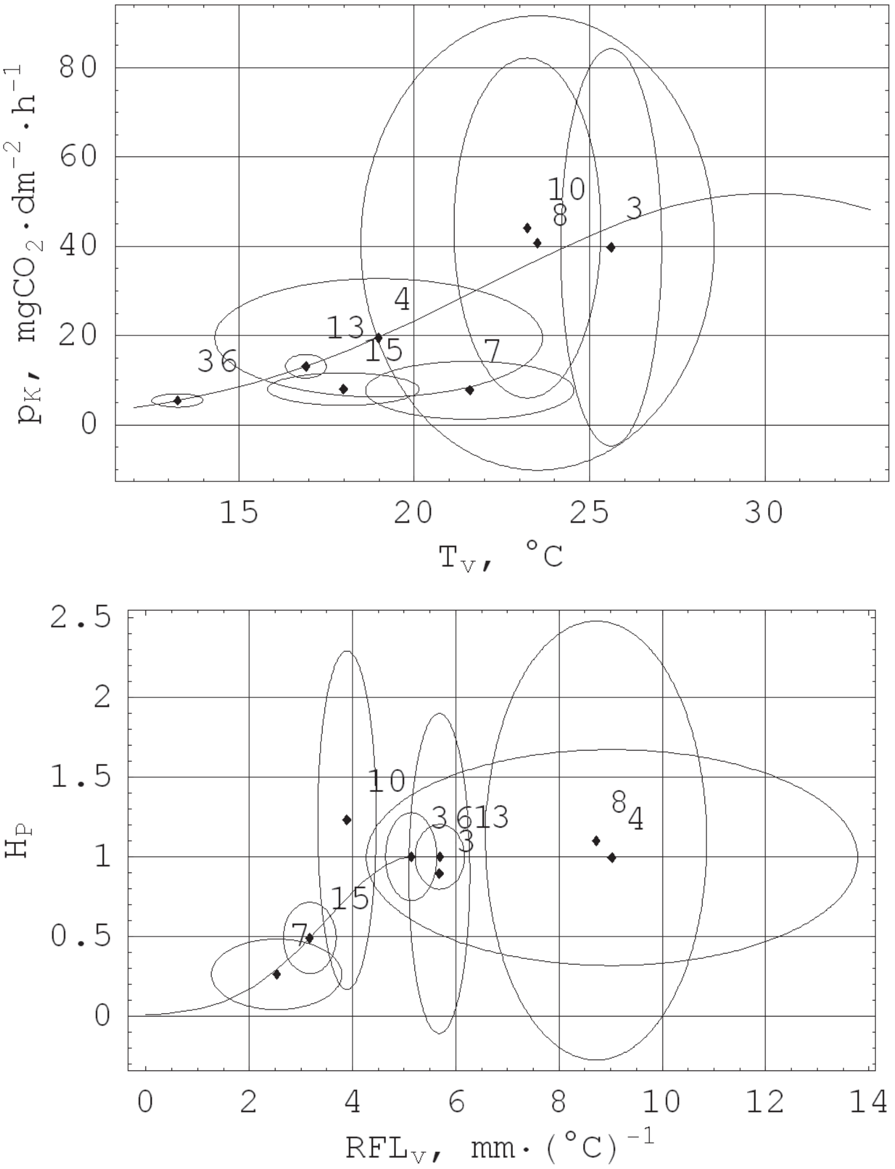

Figure 4.3 - The single lumped parameter of TsuBiMo plotted against the values derived from measured NPP.

The upper panel displays temperature dependence, and the lower panel displays humidity factor. (*See also* [34].)

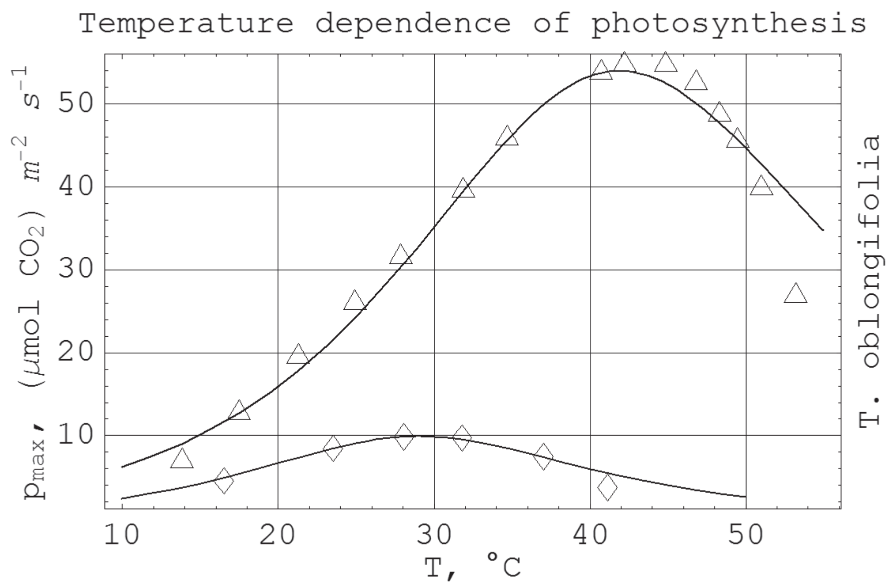

Figure 4.4 - Temperature dependence of light-saturated photosynthesis as modelled by the generalized Arrhenius function.

See also [44].

5.5 Consistency charts

This section contains figures displaying the results of consistency tests

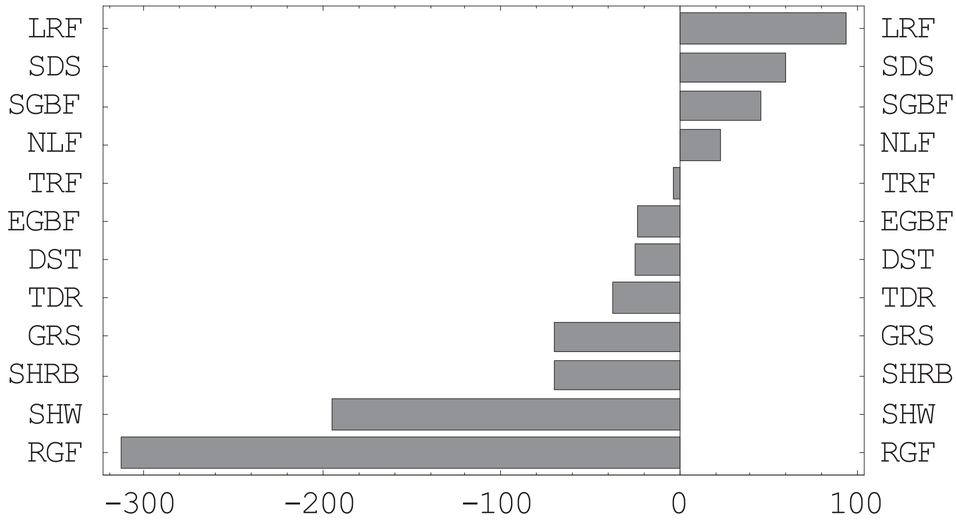

Figure 5.1 - Consistency chart for TsuBiMoNPP-1; reference ensemble "ToyBiMoPlus".

Legend: EGBF - evergreen broad-leaved forests, RGF - raingreen forests, TRF - tropical rainforests, SGBF - summer-green broad-leaved forests, SHW - subhumid woodlands, TDR - tundra, GRS - grasslands, NLF - needle-leaf forests, SDS - semi-desert scrubs, DST - deserts, SHRB - shrublands, LRF - larch forests.

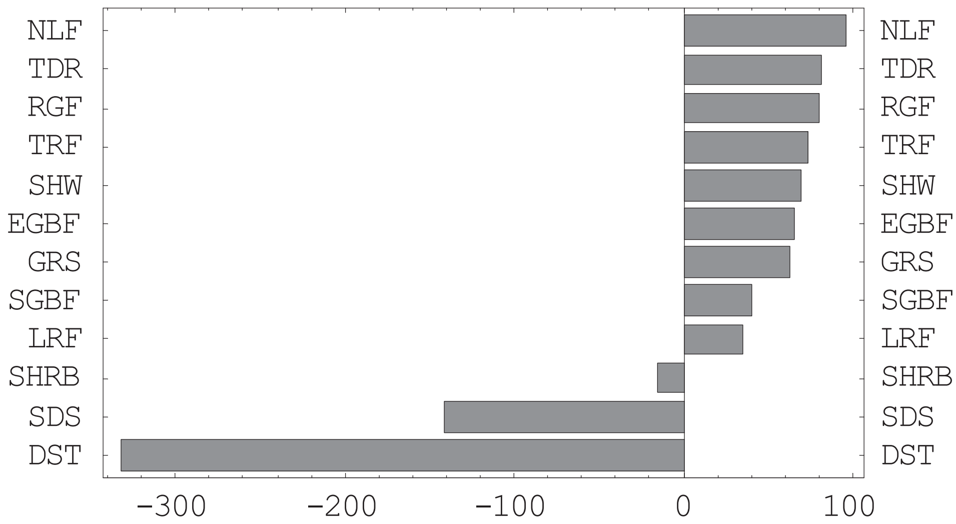

Figure 5.2 - Consistency chart for Madison NPP; reference ensemble "ToyBiMoPlus".

Legend: EGBF - evergreen broad-leaved forests, RGF - raingreen forests, TRF - tropical rainforests, SGBF - summer-green broad-leaved forests, SHW - subhumid woodlands, TDR - tundra, GRS - grasslands, NLF - needle-leaf forests, SDS - semi-desert scrubs, DST - deserts, SHRB - shrublands, LRF - larch forests

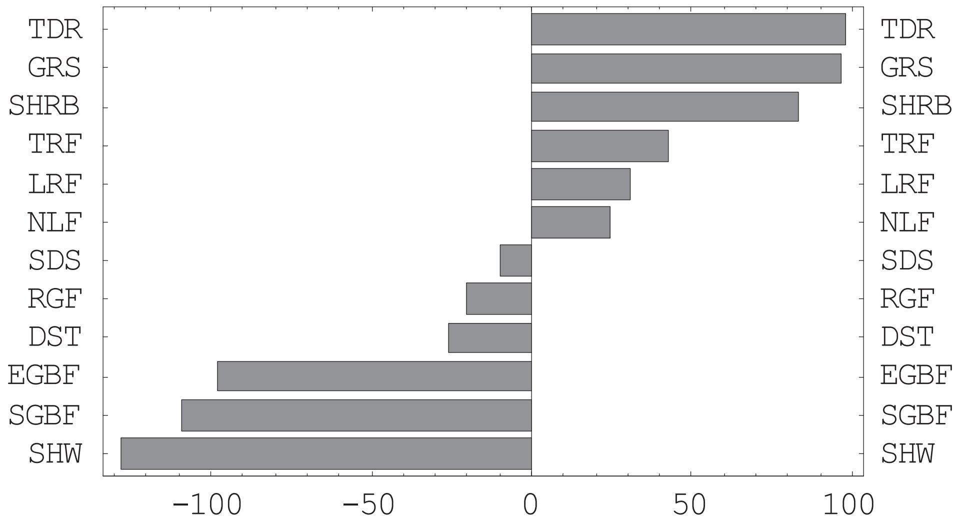

Figure 5.3 - Consistency chart for Sim-CYCLE(rev); reference ensemble "ToyBiMoPlus".

Legend: EGBF - evergreen broad-leaved forests, RGF - raingreen forests, TRF - tropical rainforests, SGBF - summer-green broad-leaved forests, SHW - subhumid woodlands, TDR - tundra, GRS - grasslands, NLF - needle-leaf forests, SDS - semi-desert scrubs, DST - deserts, SHRB - shrublands, LRF - larch forests.

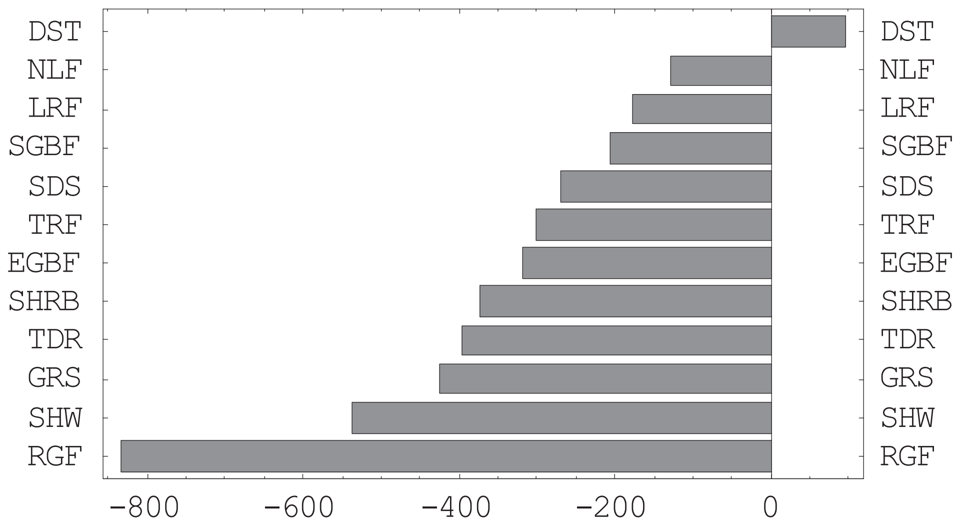

Figure 5.4 - Consistency chart for GLO-PEM; reference ensemble "ToyBiMoPlus".

Legend: EGBF - evergreen broad-leaved forests, RGF - raingreen forests, TRF - tropical rainforests, SGBF - summer-green broad-leaved forests, SHW - subhumid woodlands, TDR - tundra, GRS - grasslands, NLF - needle-leaf forests, SDS - semi-desert scrubs, DST - deserts, SHRB - shrublands, LRF - larch forests.

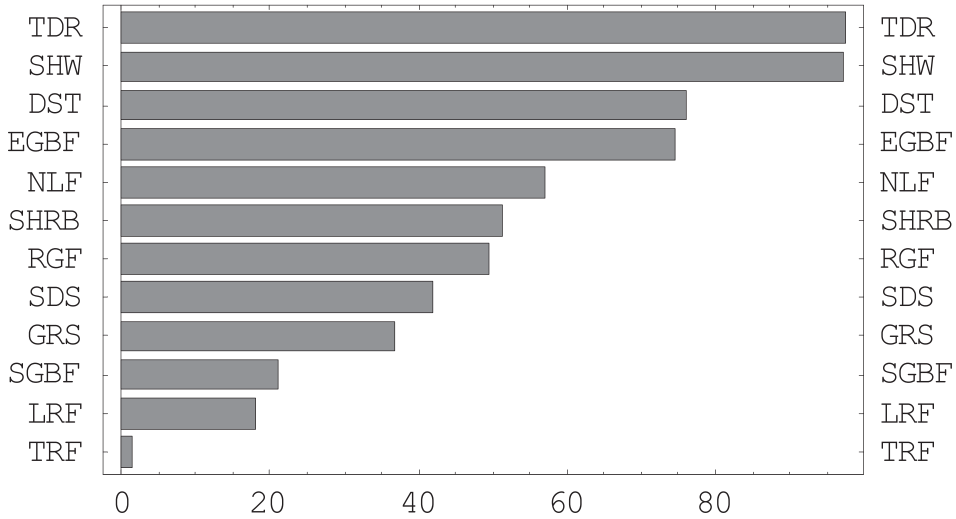

Figure 5.5 - Consistency chart for BEAMS; reference ensemble "ToyBiMoPlus".

Legend: EGBF - evergreen broad-leaved forests, RGF - raingreen forests, TRF - tropical rainforests, SGBF - summer-green broad-leaved forests, SHW - subhumid woodlands, TDR - tundra, GRS - grasslands, NLF - needle-leaf forests, SDS - semi-desert scrubs, DST - deserts, SHRB - shrublands, LRF - larch forests.

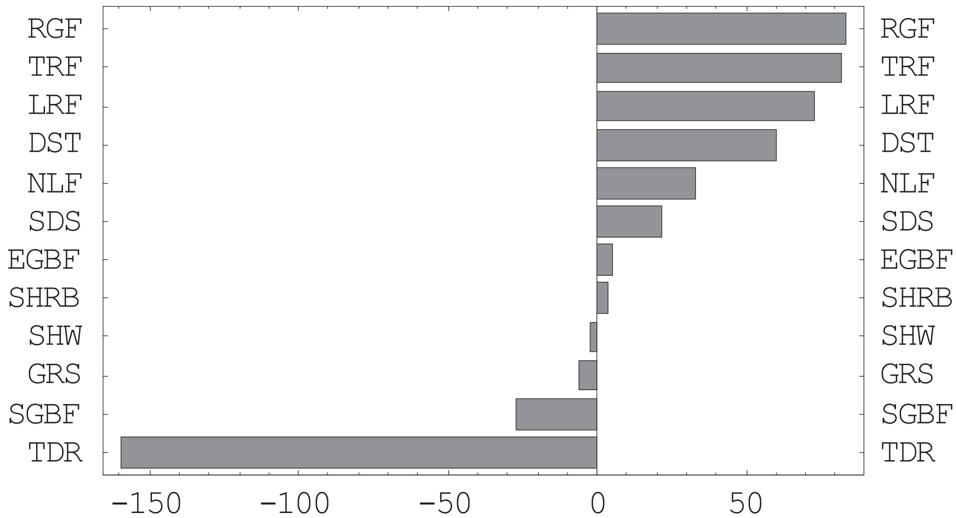

Figure 5.6 - Consistency chart for VEGAS; reference ensemble "ToyBiMoPlus".

Legend: EGBF - evergreen broad-leaved forests, RGF - raingreen forests, TRF - tropical rainforests, SGBF - summer-green broad-leaved forests, SHW - subhumid woodlands, TDR - tundra, GRS - grasslands, NLF - needle-leaf forests, SDS - semi-desert scrubs, DST - deserts, SHRB - shrublands, LRF - larch forests.

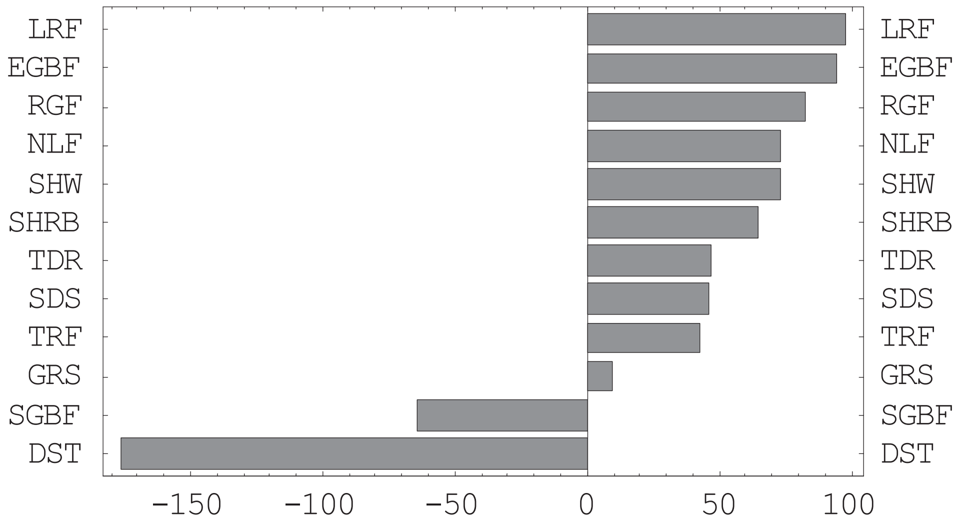

Figure 5.7 - Consistency chart for MODIS-NPP; reference ensemble "ToyBiMoPlus".

Legend: EGBF - evergreen broad-leaved forests, RGF - raingreen forests, TRF - tropical rainforests, SGBF - summer-green broad-leaved forests, SHW - subhumid woodlands, TDR - tundra, GRS - grasslands, NLF - needle-leaf forests, SDS - semi-desert scrubs, DST - deserts, SHRB - shrublands, LRF - larch forests.

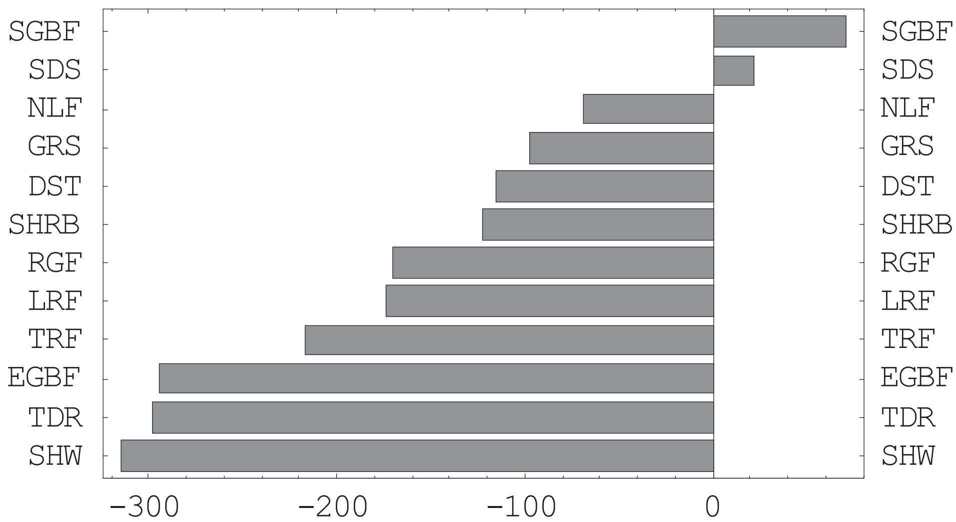

Figure 5.8 - Consistency chart for Biome-BGC 4.1.1; reference ensemble "ToyBiMoPlus".

Legend: EGBF - evergreen broad-leaved forests, RGF - raingreen forests, TRF - tropical rainforests, SGBF - summer-green broad-leaved forests, SHW - subhumid woodlands, TDR - tundra, GRS - grasslands, NLF - needle-leaf forests, SDS - semi-desert scrubs, DST - deserts, SHRB - shrublands, LRF - larch forests.

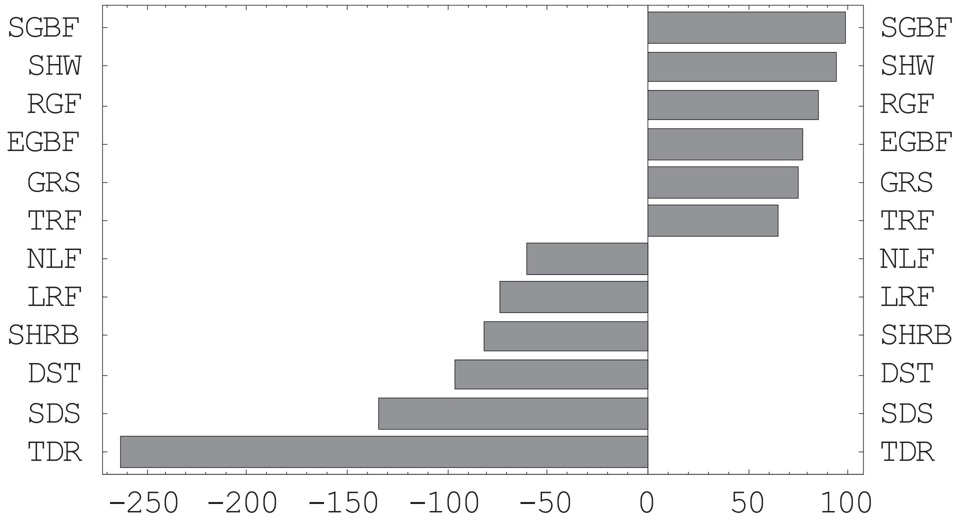

Figure 5.9 - Consistency chart for LPJ-NPP; reference ensemble "ToyBiMoPlus".

Legend: EGBF - evergreen broad-leaved forests, RGF - raingreen forests, TRF - tropical rainforests, SGBF - summer-green broad-leaved forests, SHW - subhumid woodlands, TDR - tundra, GRS - grasslands, NLF - needle-leaf forests, SDS - semi-desert scrubs, DST - deserts, SHRB - shrublands, LRF - larch forests.

5.6 Novelty charts

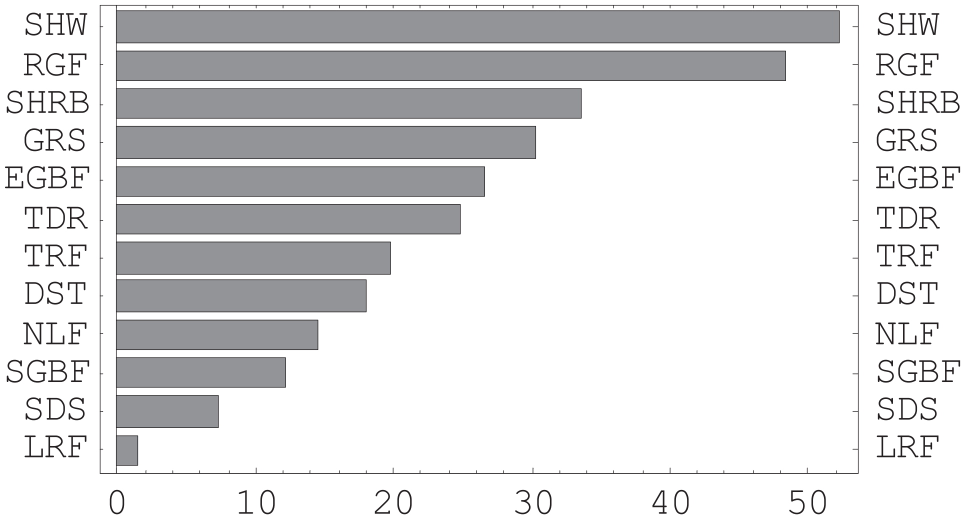

Figure 6.1 - Novelty chart for TsuBiMoNPP-1; reference ensemble "ToyBiMoPlus".

Legend: EGBF - evergreen broad-leaved forests, RGF - raingreen forests, TRF - tropical rainforests, SGBF - summer-green broad-leaved forests, SHW - subhumid woodlands, TDR - tundra, GRS - grasslands, NLF - needle-leaf forests, SDS - semi-desert scrubs, DST - deserts, SHRB - shrublands, LRF - larch forests.

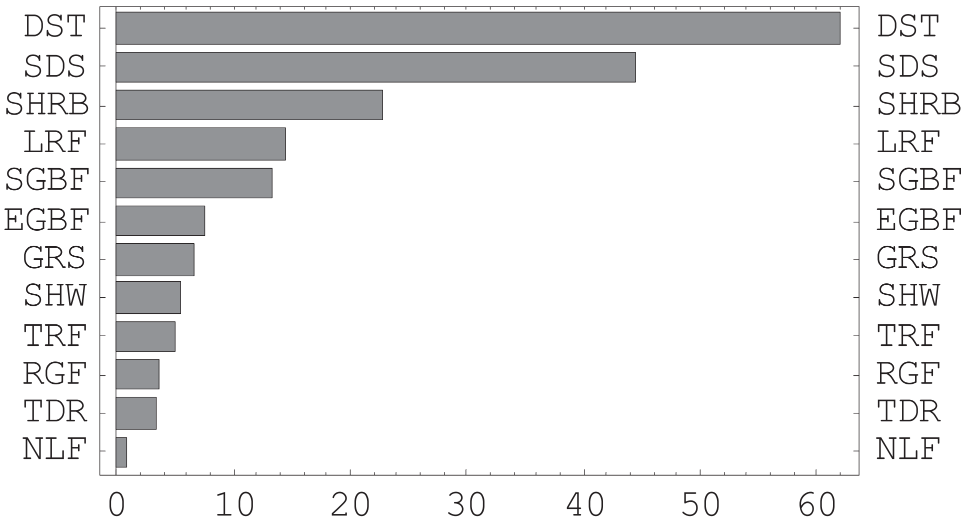

Figure 6.2 - Novelty chart for Madison NPP; reference ensemble "ToyBiMoPlus".

Legend: EGBF - evergreen broad-leaved forests, RGF - raingreen forests, TRF - tropical rainforests, SGBF - summer-green broad-leaved forests, SHW - subhumid woodlands, TDR - tundra, GRS - grasslands, NLF - needle-leaf forests, SDS - semi-desert scrubs, DST - deserts, SHRB - shrublands, LRF - larch forests.

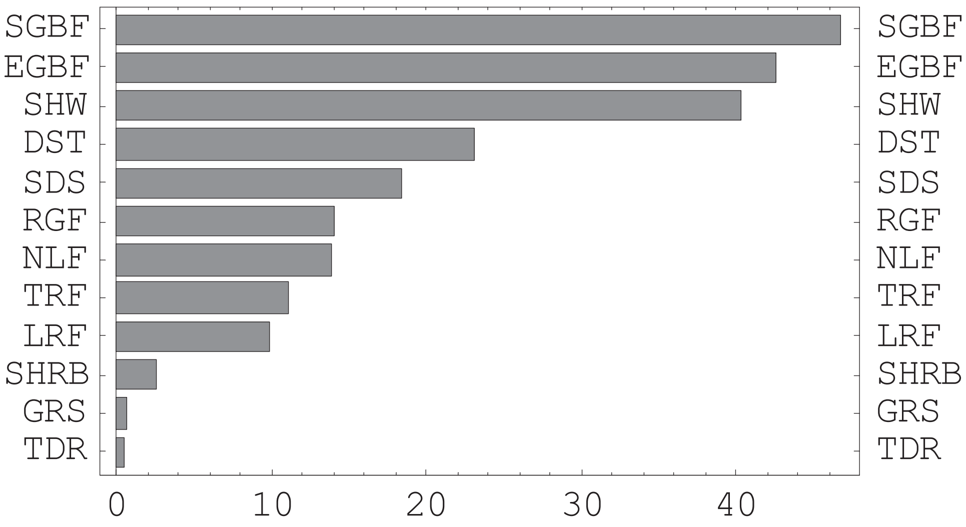

Figure 6.3 - Novelty chart for Sim-CYCLE(rev); reference ensemble "ToyBiMoPlus".

Legend: EGBF - evergreen broad-leaved forests, RGF - raingreen forests, TRF - tropical rainforests, SGBF - summer-green broad-leaved forests, SHW - subhumid woodlands, TDR - tundra, GRS - grasslands, NLF - needle-leaf forests, SDS - semi-desert scrubs, DST - deserts, SHRB - shrublands, LRF - larch forests.

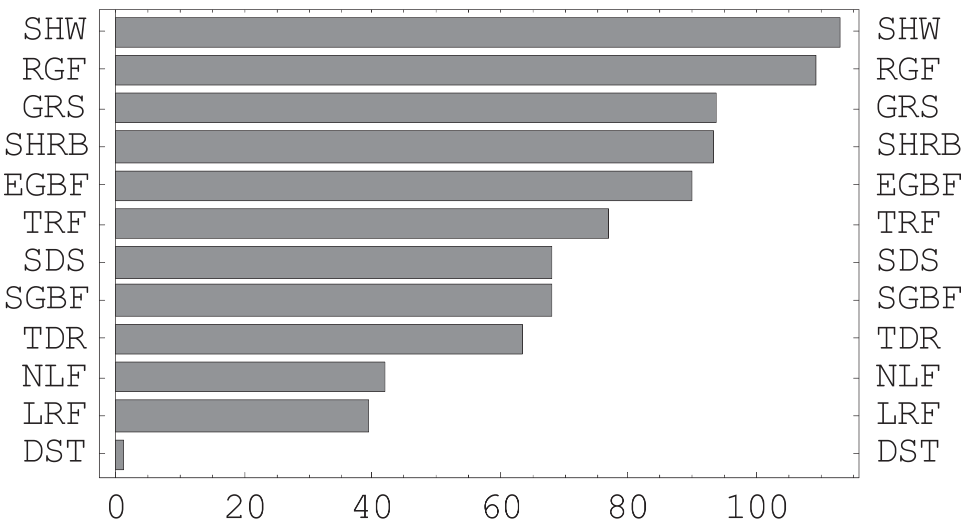

Figure 6.4 - Novelty chart for GLO-PEM; reference ensemble "ToyBiMoPlus".

Legend: EGBF - evergreen broad-leaved forests, RGF - raingreen forests, TRF - tropical rainforests, SGBF - summer-green broad-leaved forests, SHW - subhumid woodlands, TDR - tundra, GRS - grasslands, NLF - needle-leaf forests, SDS - semi-desert scrubs, DST - deserts, SHRB - shrublands, LRF - larch forests.

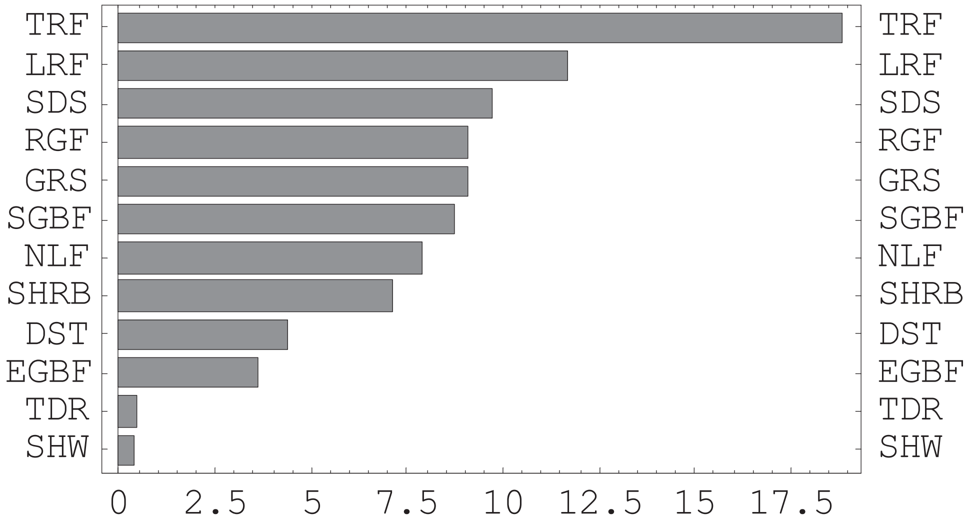

Figure 6.5 - Novelty chart for BEAMS; reference ensemble “ToyBiMoPlus”.

Legend: EGBF - evergreen broad-leaved forests, RGF - raingreen forests, TRF - tropical rainforests, SGBF - summer-green broad-leaved forests, SHW - subhumid woodlands, TDR - tundra, GRS - grasslands, NLF - needle-leaf forests, SDS - semi-desert scrubs, DST - deserts, SHRB - shrublands, LRF - larch forests.

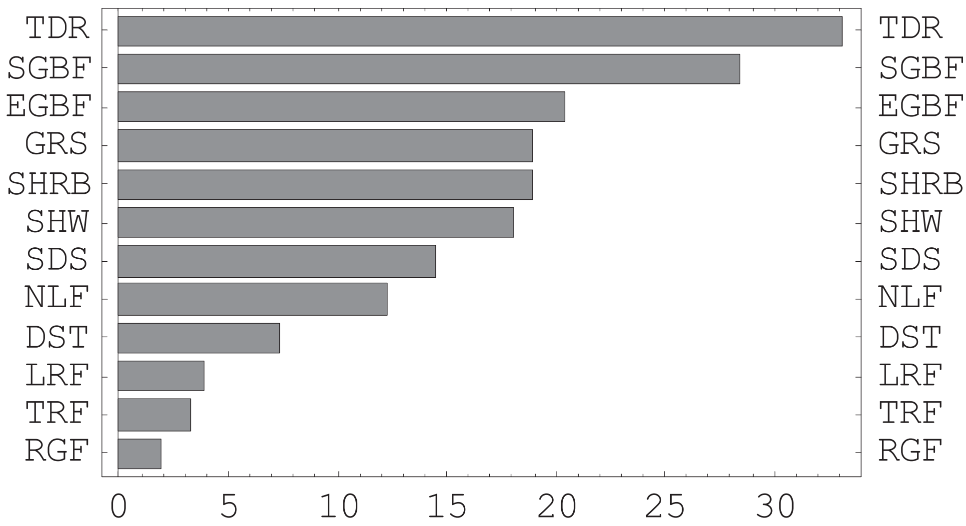

Figure 6.6 - Novelty chart for VEGAS; reference ensemble “ToyBiMoPlus”.

Legend: EGBF - evergreen broad-leaved forests, RGF - raingreen forests, TRF - tropical rainforests, SGBF - summer-green broad-leaved forests, SHW - subhumid woodlands, TDR - tundra, GRS - grasslands, NLF - needle-leaf forests, SDS - semi-desert scrubs, DST - deserts, SHRB - shrublands, LRF - larch forests.

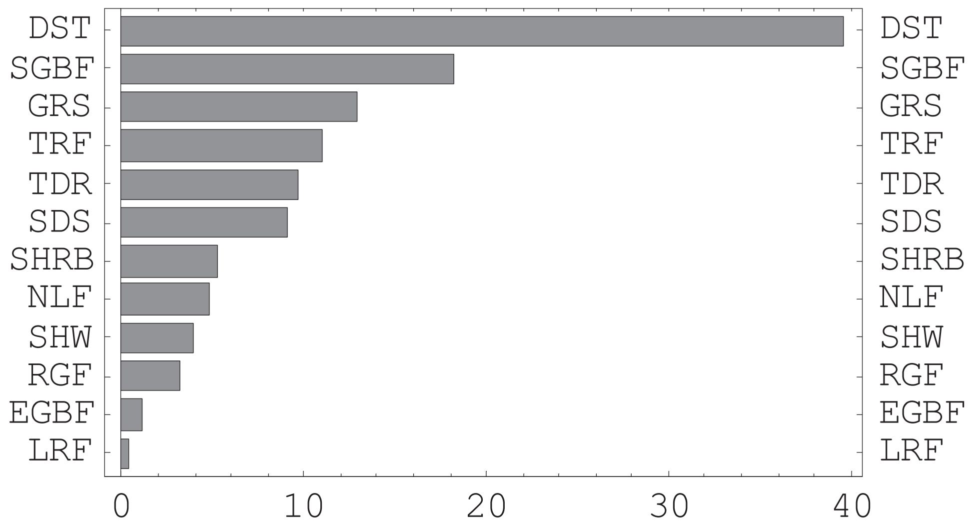

Figure 6.7 - Novelty chart for MODIS-NPP; reference ensemble "ToyBiMoPlus".

Legend: EGBF - evergreen broad-leaved forests, RGF - raingreen forests, TRF - tropical rainforests, SGBF - summer-green broad-leaved forests, SHW - subhumid woodlands, TDR - tundra, GRS - grasslands, NLF - needle-leaf forests, SDS - semi-desert scrubs, DST - deserts, SHRB - shrublands, LRF - larch forests.

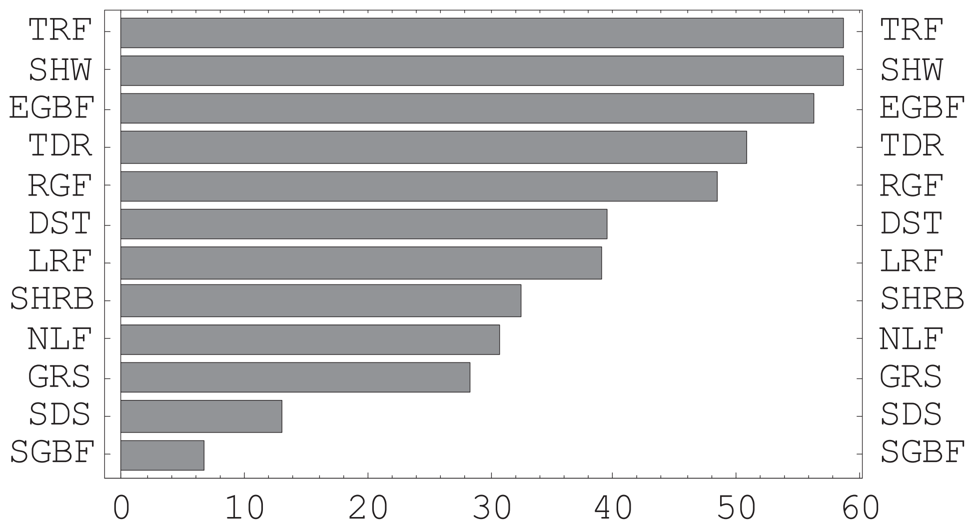

Figure 6.8 - Novelty chart for Biome-BGC 4.1.1; reference ensemble "ToyBiMoPlus".

Legend: EGBF - evergreen broad-leaved forests, RGF - raingreen forests, TRF - tropical rainforests, SGBF - summer-green broad-leaved forests, SHW - subhumid woodlands, TDR - tundra, GRS - grasslands, NLF - needle-leaf forests, SDS - semi-desert scrubs, DST - deserts, SHRB - shrublands, LRF - larch forests.

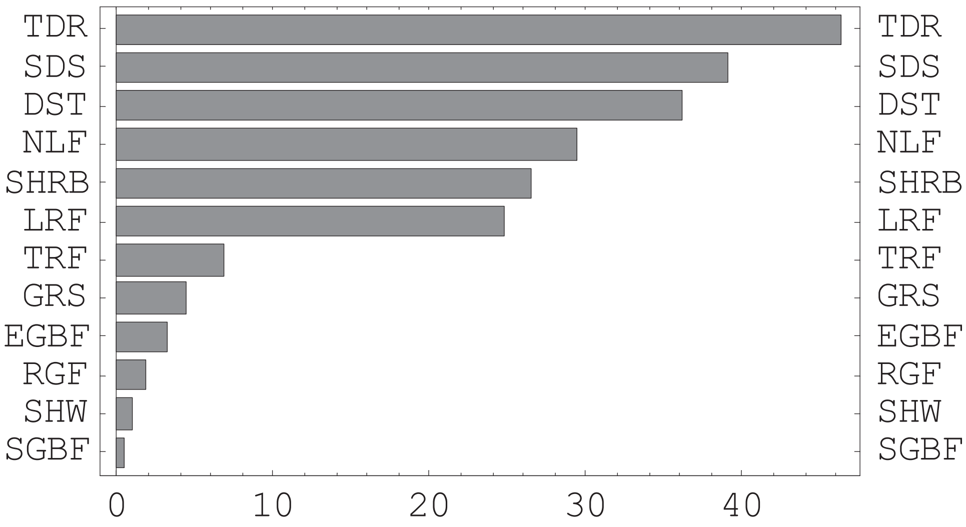

Figure 6.9 - Novelty chart for LPJ-NPP; reference ensemble “ToyBiMoPlus”.

Legend: EGBF - evergreen broad-leaved forests, RGF - raingreen forests, TRF - tropical rainforests, SGBF - summer-green broad-leaved forests, SHW - subhumid woodlands, TDR - tundra, GRS - grasslands, NLF - needle-leaf forests, SDS - semi-desert scrubs, DST - deserts, SHRB - shrublands, LRF - larch forests.

5.7 Progressivity charts

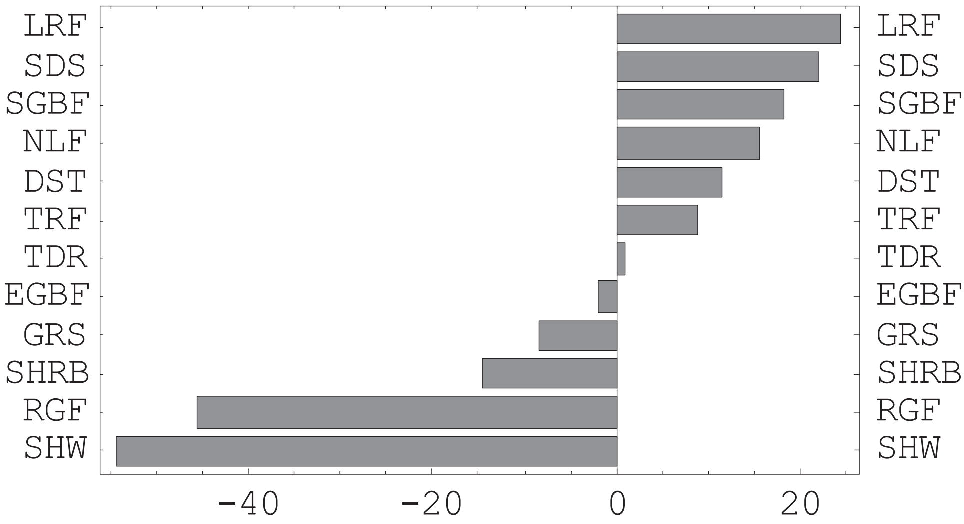

Figure 7.1 - Progressivity chart for TsuBiMoNPP-1, reference ensemble "ToyBiMoPlus".

Legend: EGBF - evergreen broad-leaved forests, RGF - raingreen forests, TRF - tropical rainforests, SGBF - summer-green broad-leaved forests, SHW - subhumid woodlands, TDR - tundra, GRS - grasslands, NLF - needle-leaf forests, SDS - semi-desert scrubs, DST - deserts, SHRB - shrublands, LRF - larch forests.

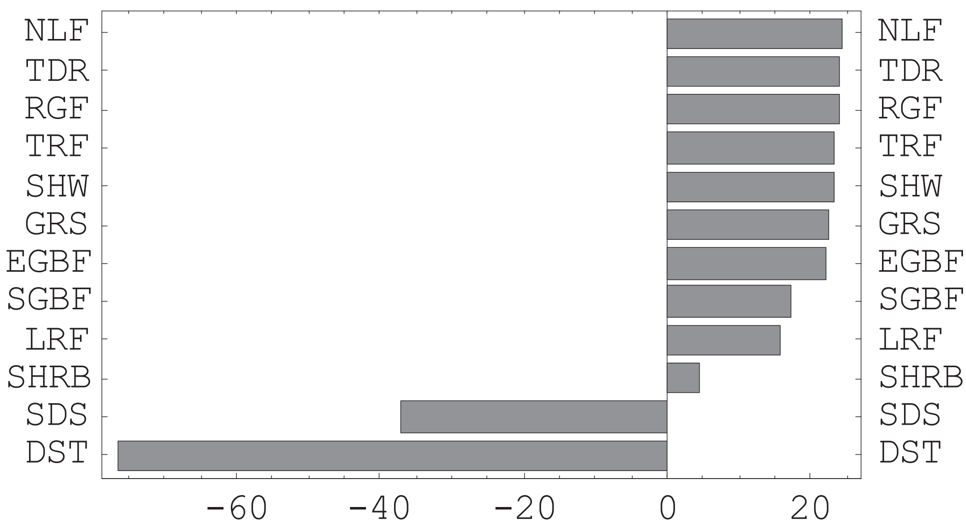

Figure 7.2 - Progressivity chart for Madison NPP; reference ensemble "ToyBiMoPlus".

Legend: EGBF - evergreen broad-leaved forests, RGF - raingreen forests, TRF - tropical rainforests, SGBF - summer-green broad-leaved forests, SHW - subhumid woodlands, TDR - tundra, GRS - grasslands, NLF - needle-leaf forests, SDS - semi-desert scrubs, DST - deserts, SHRB - shrublands, LRF - larch forests.

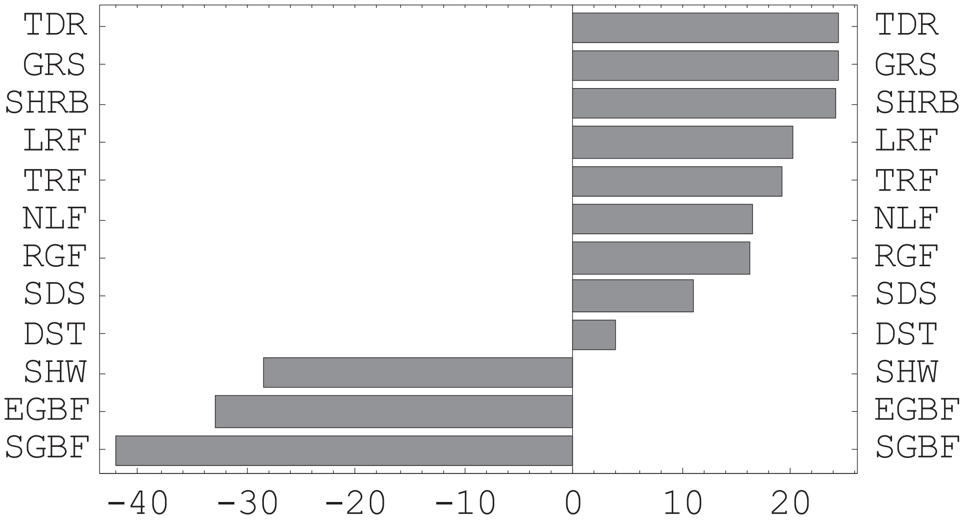

Figure 7.3 - Progressivity chart for Sim-CYCLE(rev); reference ensemble "ToyBiMoPlus".

Legend: EGBF - evergreen broad-leaved forests, RGF - raingreen forests, TRF - tropical rainforests, SGBF - summer-green broad-leaved forests, SHW - subhumid woodlands, TDR - tundra, GRS - grasslands, NLF - needle-leaf forests, SDS - semi-desert scrubs, DST - deserts, SHRB - shrublands, LRF - larch forests.

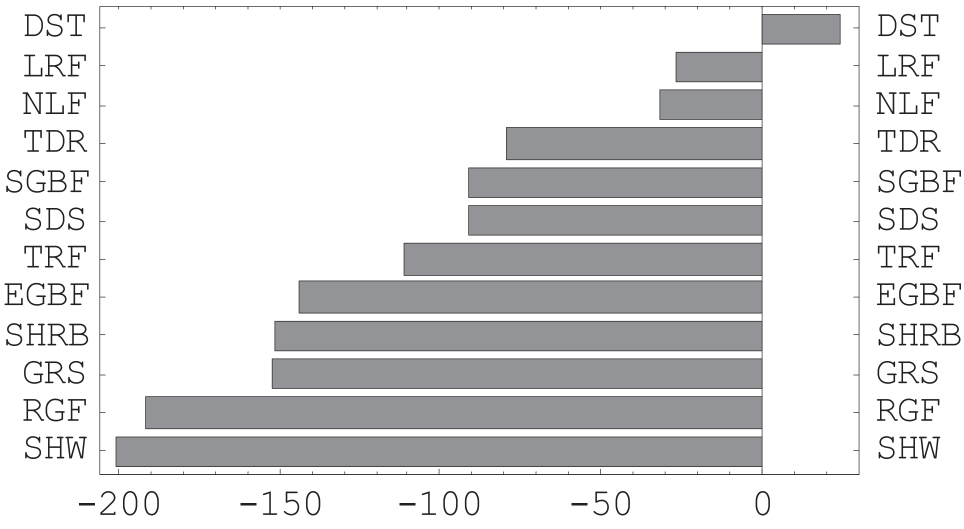

Figure 7.4 - Progressivity chart for GLO-PEM; reference ensemble "ToyBiMoPlus".

Legend: EGBF - evergreen broad-leaved forests, RGF - raingreen forests, TRF - tropical rainforests, SGBF - summer-green broad-leaved forests, SHW - subhumid woodlands, TDR - tundra, GRS - grasslands, NLF - needle-leaf forests, SDS - semi-desert scrubs, DST - deserts, SHRB - shrublands, LRF - larch forests.

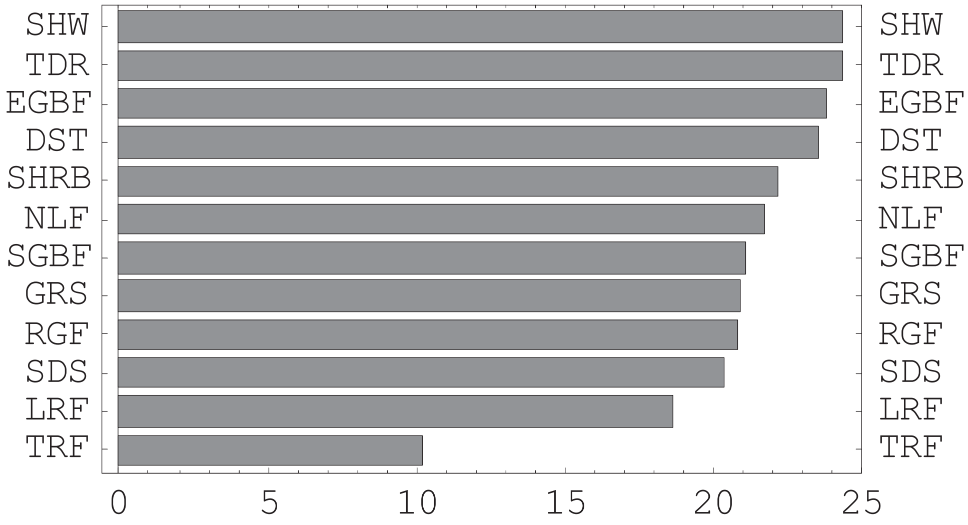

Figure 7.5 - Progressivity chart for BEAMS; reference ensemble "ToyBiMoPlus".

Legend: EGBF - evergreen broad-leaved forests, RGF - raingreen forests, TRF - tropical rainforests, SGBF - summer-green broad-leaved forests, SHW - subhumid woodlands, TDR - tundra, GRS - grasslands, NLF - needle-leaf forests, SDS - semi-desert scrubs, DST - deserts, SHRB - shrublands, LRF - larch forests.

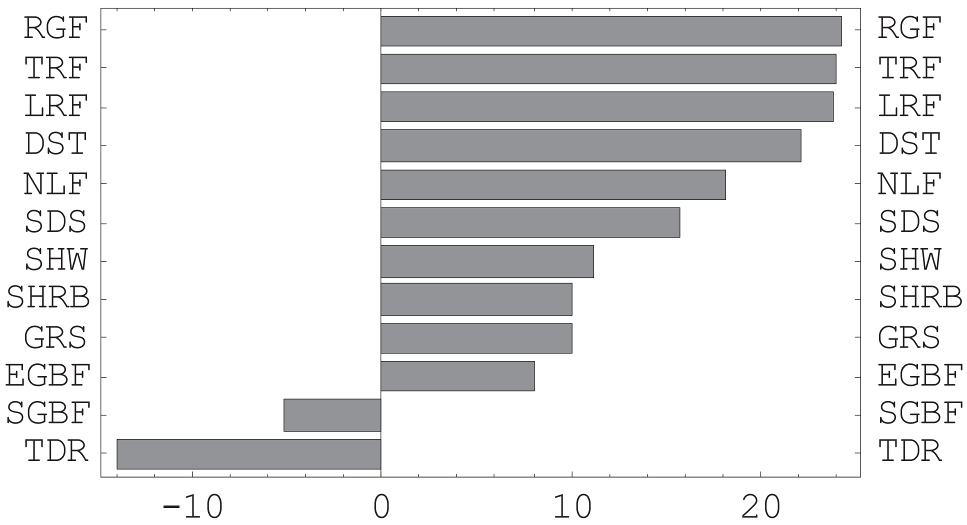

Figure 7.6 - Progressivity chart for VEGAS; reference ensemble "ToyBiMoPlus".

Legend: EGBF - evergreen broad-leaved forests, RGF - raingreen forests, TRF - tropical rainforests, SGBF - summer-green broad-leaved forests, SHW - subhumid woodlands, TDR - tundra, GRS - grasslands, NLF - needle-leaf forests, SDS - semi-desert scrubs, DST - deserts, SHRB - shrublands, LRF - larch forests.

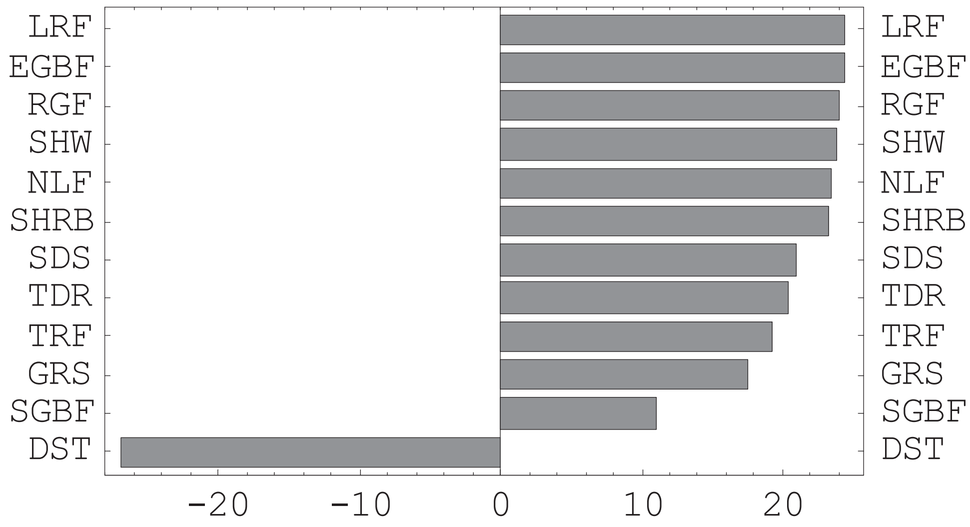

Figure 7.7 - Progressivity chart for MODIS-NPP; reference ensemble "ToyBiMoPlus".

Legend: EGBF - evergreen broad-leaved forests, RGF - raingreen forests, TRF - tropical rainforests, SGBF - summer-green broad-leaved forests, SHW - subhumid woodlands, TDR - tundra, GRS - grasslands, NLF - needle-leaf forests, SDS - semi-desert scrubs, DST - deserts, SHRB - shrublands, LRF - larch forests.

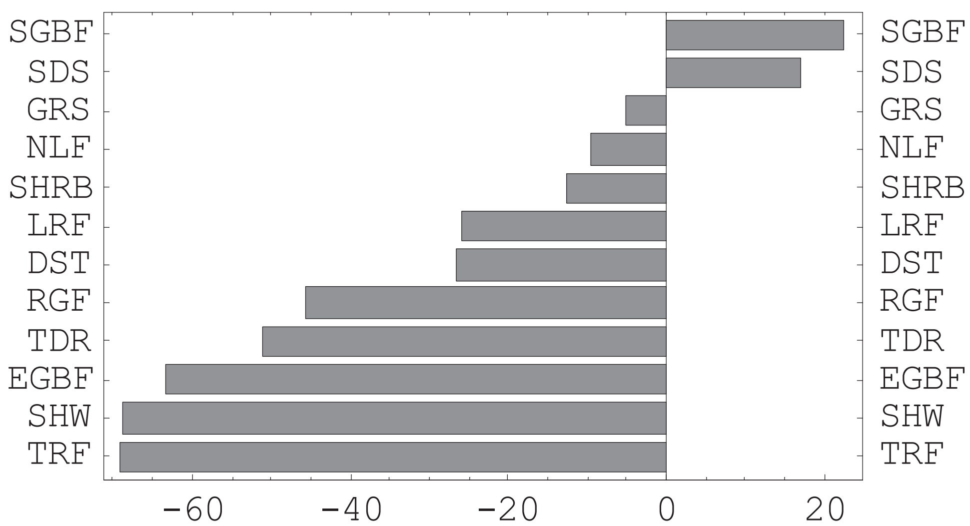

Figure 7.8 - Progressivity chart for Biome-BGC 4.1.1; reference ensemble "ToyBiMoPlus".

Legend: EGBF - evergreen broad-leaved forests, RGF - raingreen forests, TRF - tropical rainforests, SGBF - summer-green broad-leaved forests, SHW - subhumid woodlands, TDR - tundra, GRS - grasslands, NLF - needle-leaf forests, SDS - semi-desert scrubs, DST - deserts, SHRB - shrublands, LRF - larch forests.

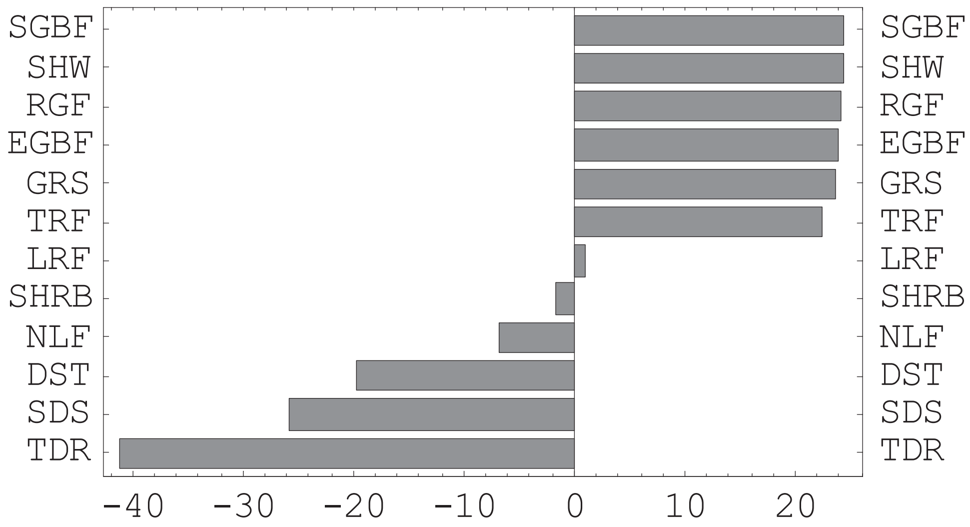

Figure 7.9 - Progressivity chart for LPJ-NPP; reference ensemble "ToyBiMoPlus".

Legend: EGBF - evergreen broad-leaved forests, RGF - raingreen forests, TRF - tropical rainforests, SGBF - summer-green broad-leaved forests, SHW - subhumid woodlands, TDR - tundra, GRS - grasslands, NLF - needle-leaf forests, SDS - semi-desert scrubs, DST - deserts, SHRB - shrublands, LRF - larch forests.

5.8 Model outputs: Maps

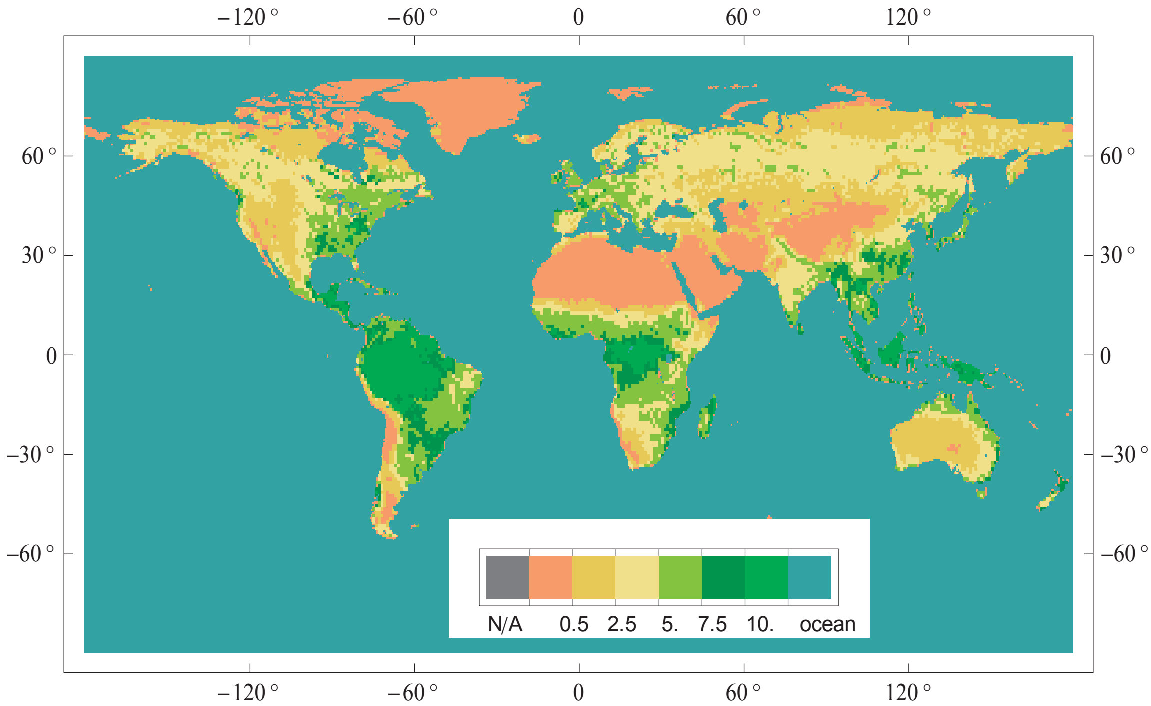

Figure 8.1 - BEAMS NPP, Units: tC ha^{-1} y^{-1} .

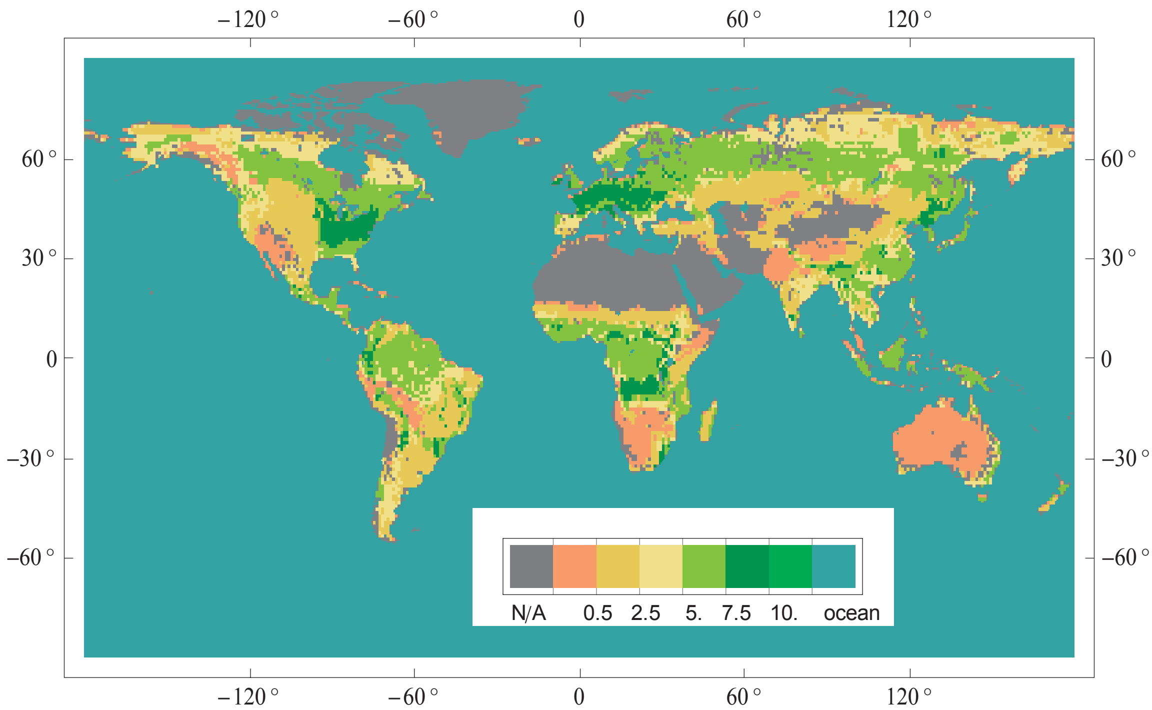

Figure 8.2 - Biome-BGC NPP, Units: tC ha^{-1} y^{-1} .

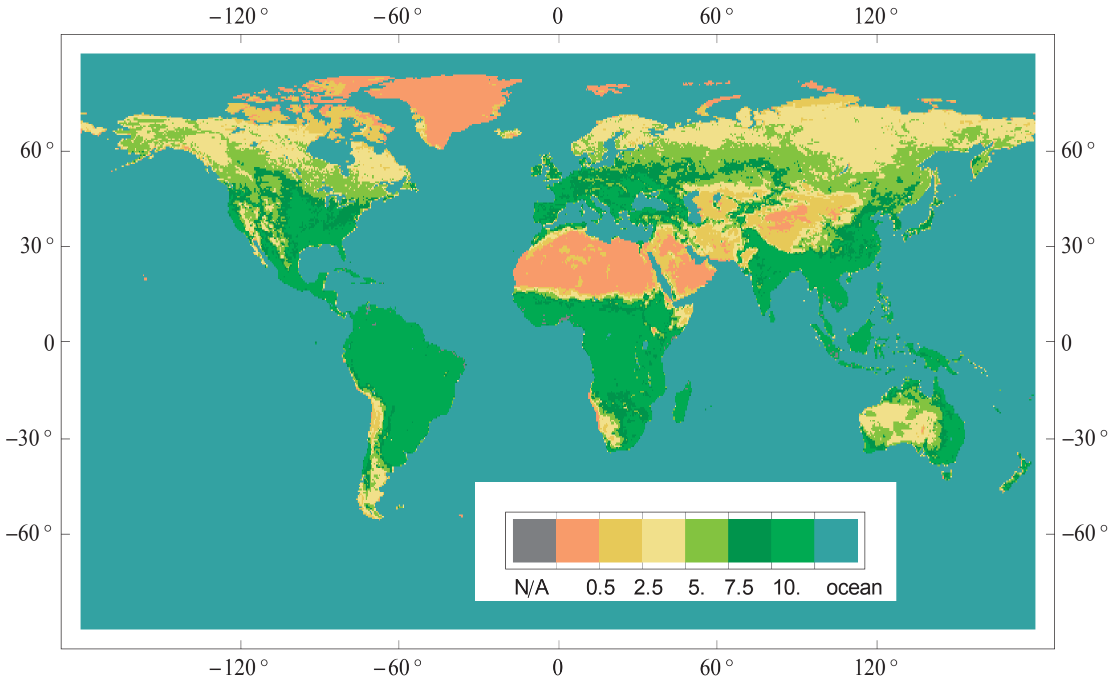

Figure 8.3 - GLO-PEM NPP, units: tC ha^{-1} y^{-1}.

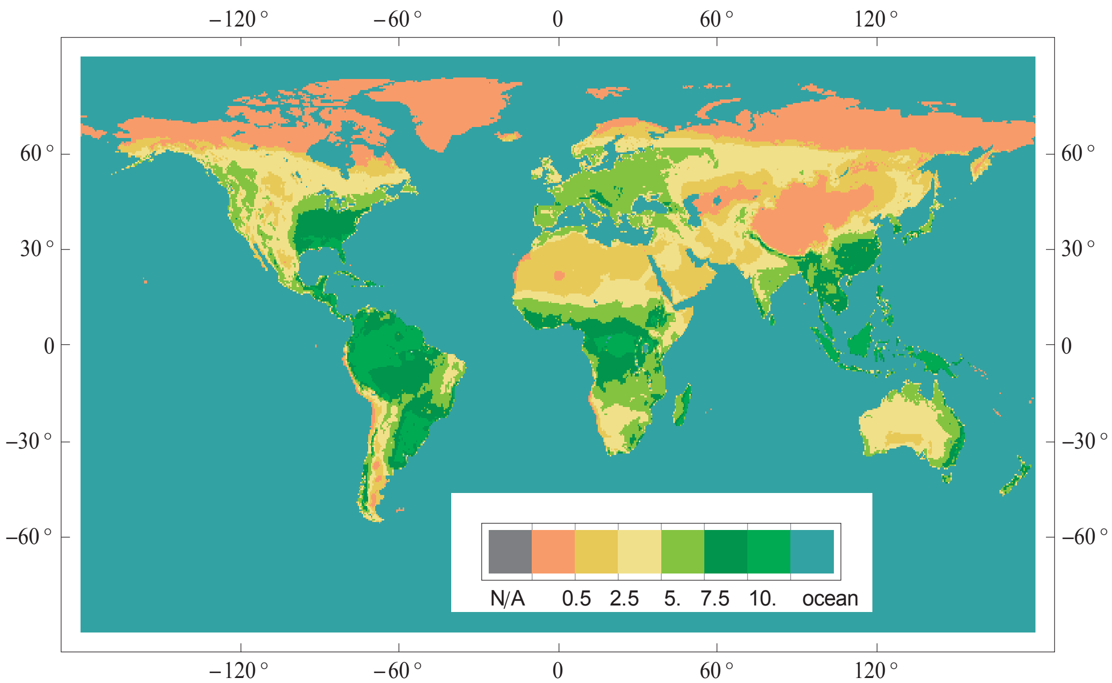

Figure 8.4 - Madison NPP, units: tC ha^{-1} y^{-1}.

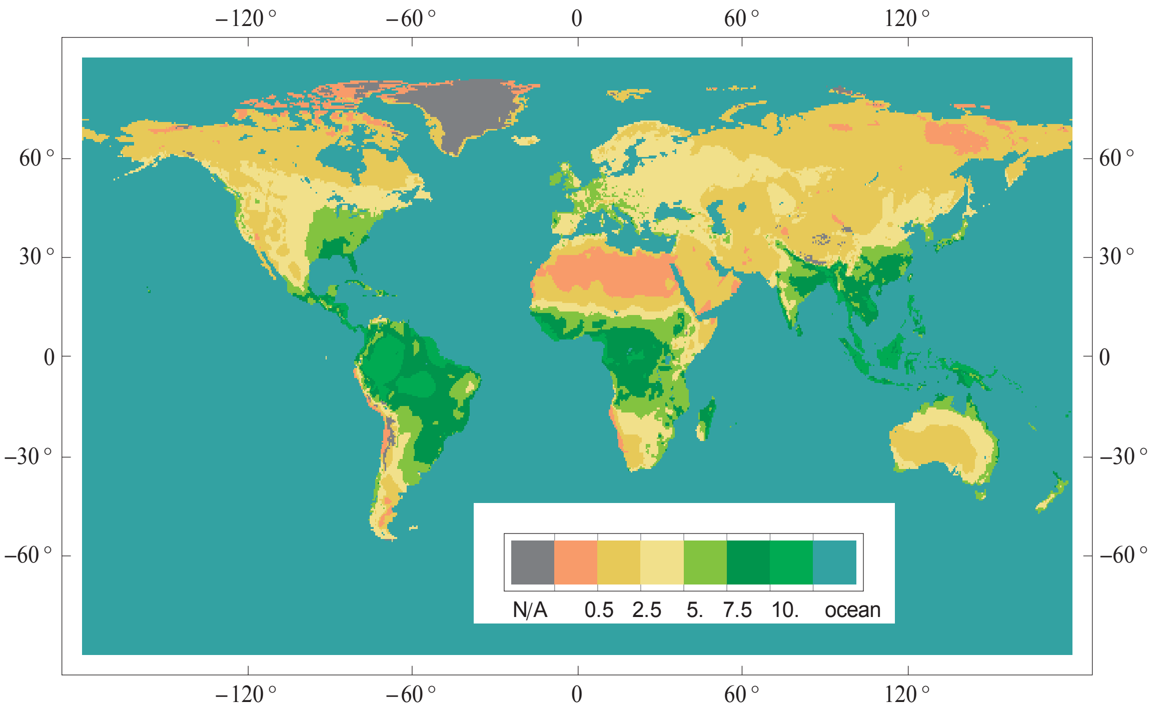

Figure 8.5 - Miami NPP, units: tC ha^{-1} y^{-1}.

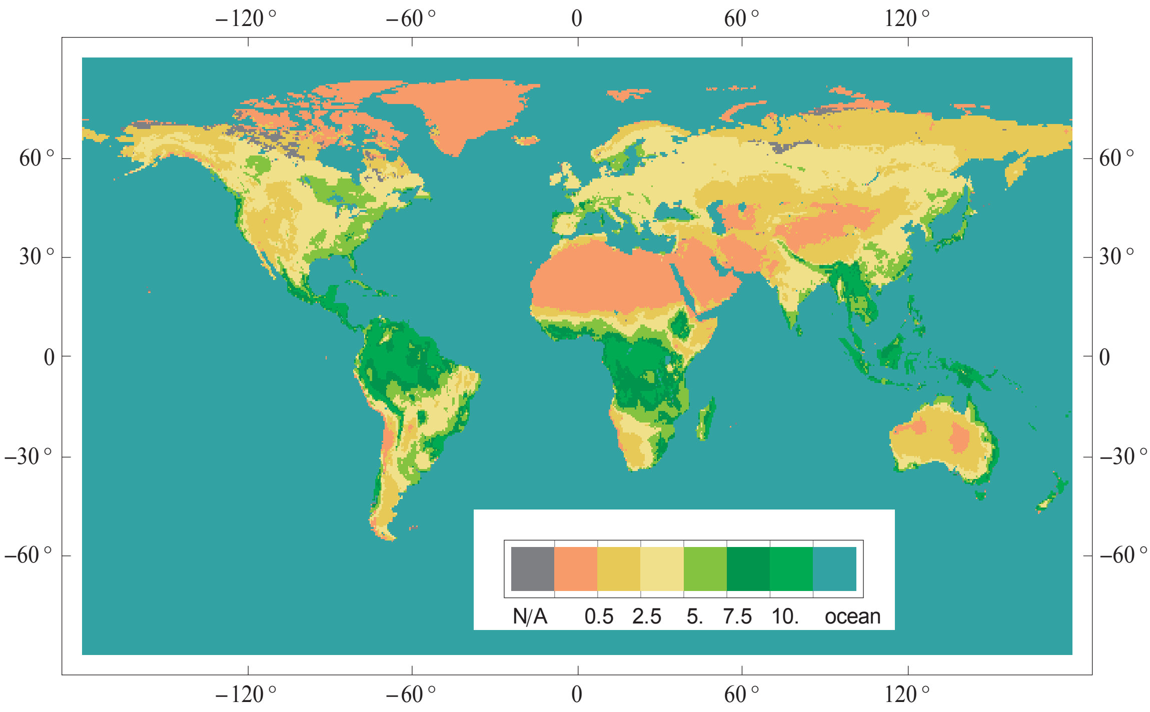

Figure 8.6 - MODIS-NPP, units: tC ha^{-1} y^{-1}.

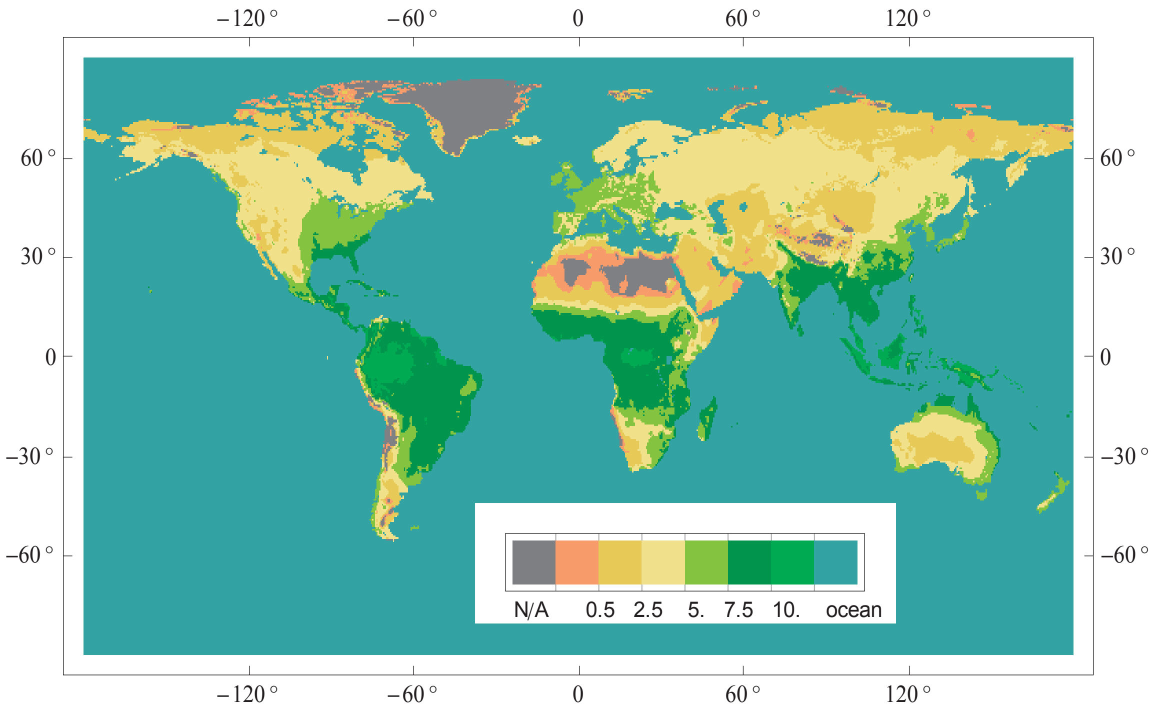

Figure 8.7 - Montreal NPP, units: tC ha^{-1} y^{-1}.

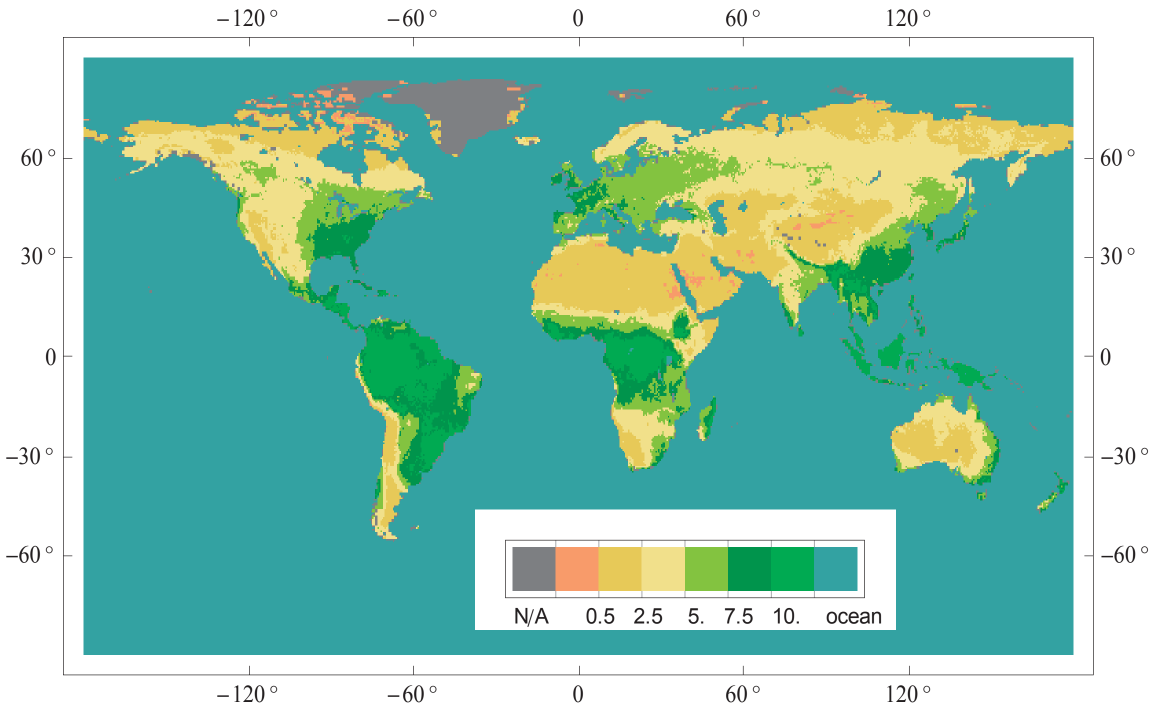

Figure 8.8 - Potsdam NPP (high), units: tC ha^{-1} y^{-1}.

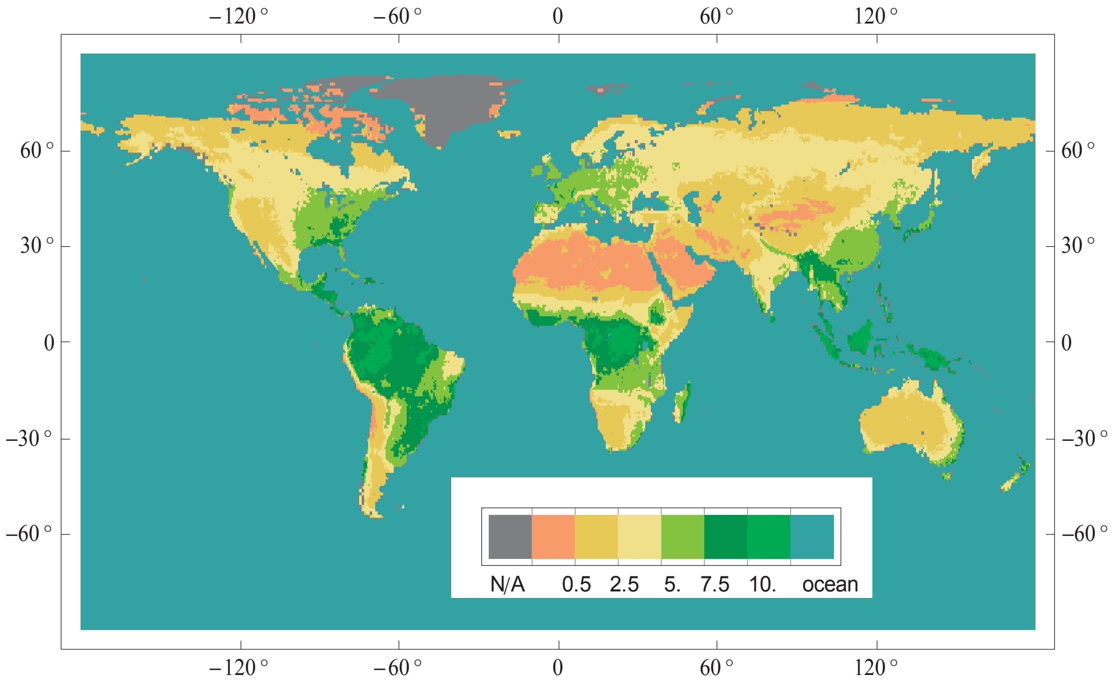

Figure 8.9 - Potsdam NPP (low), units: tC ha^{-1} y^{-1}.

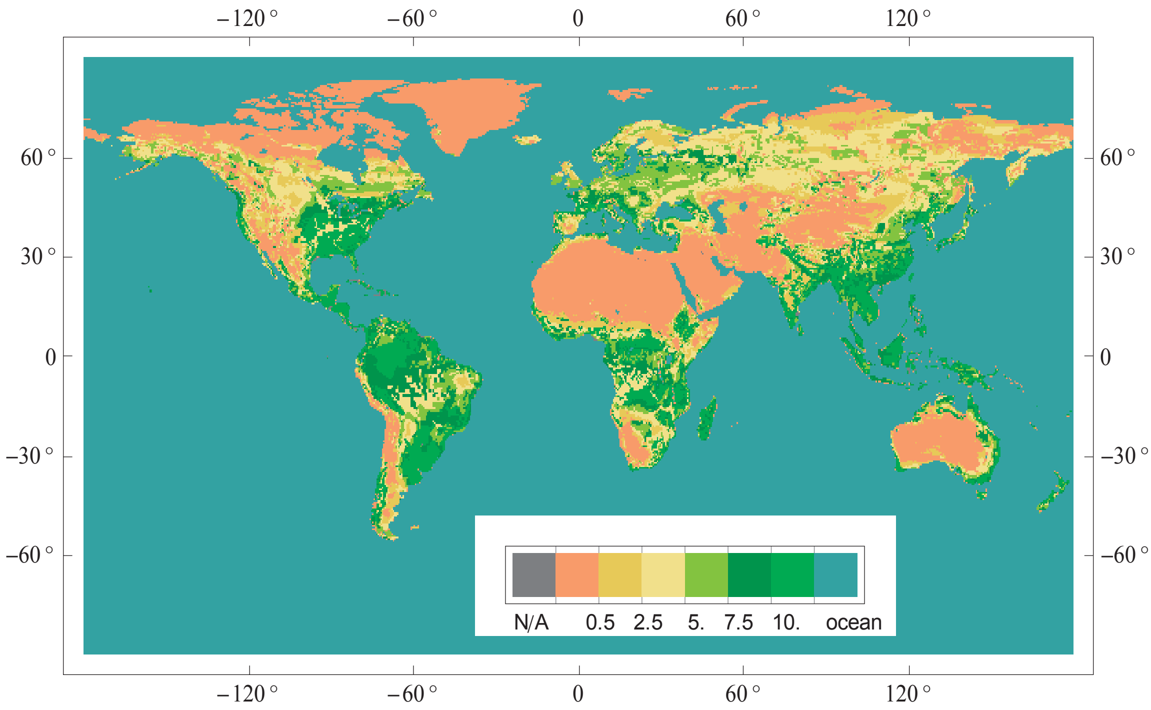

Figure 8.10 - Sim-CYCLE (rev) NPP, units: tC ha^{-1} y^{-1}.

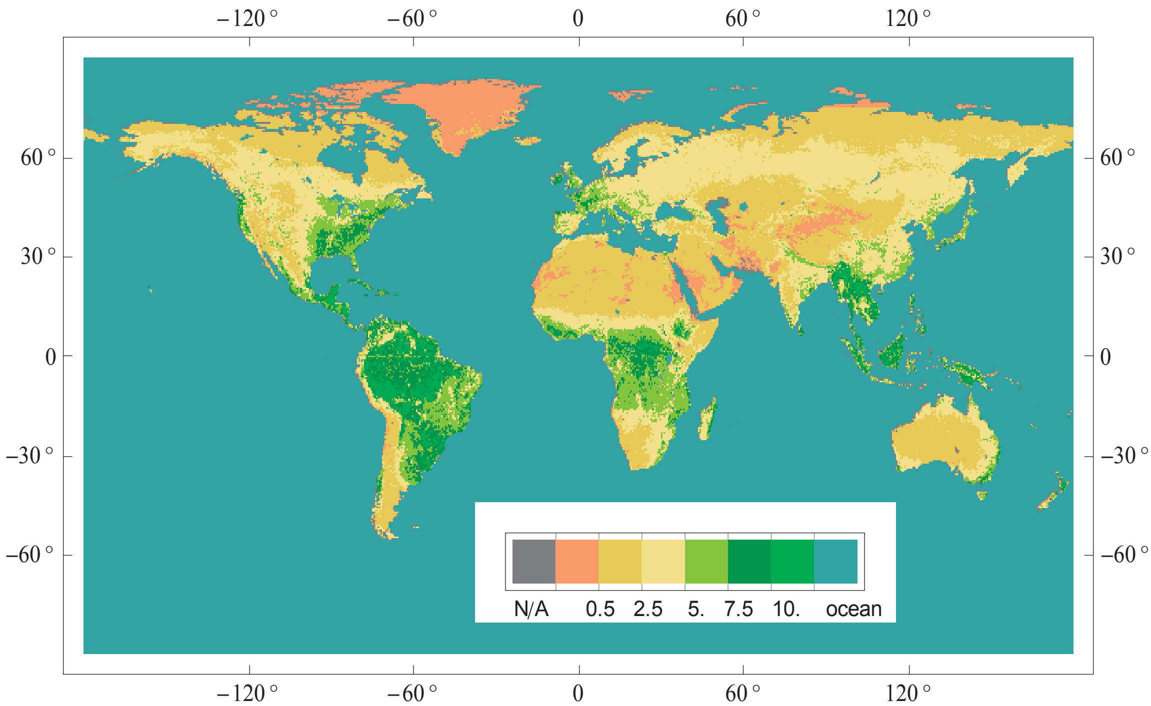

Figure 8.11 - TGER- NPP, units: tC ha^{-1} y^{-1}.

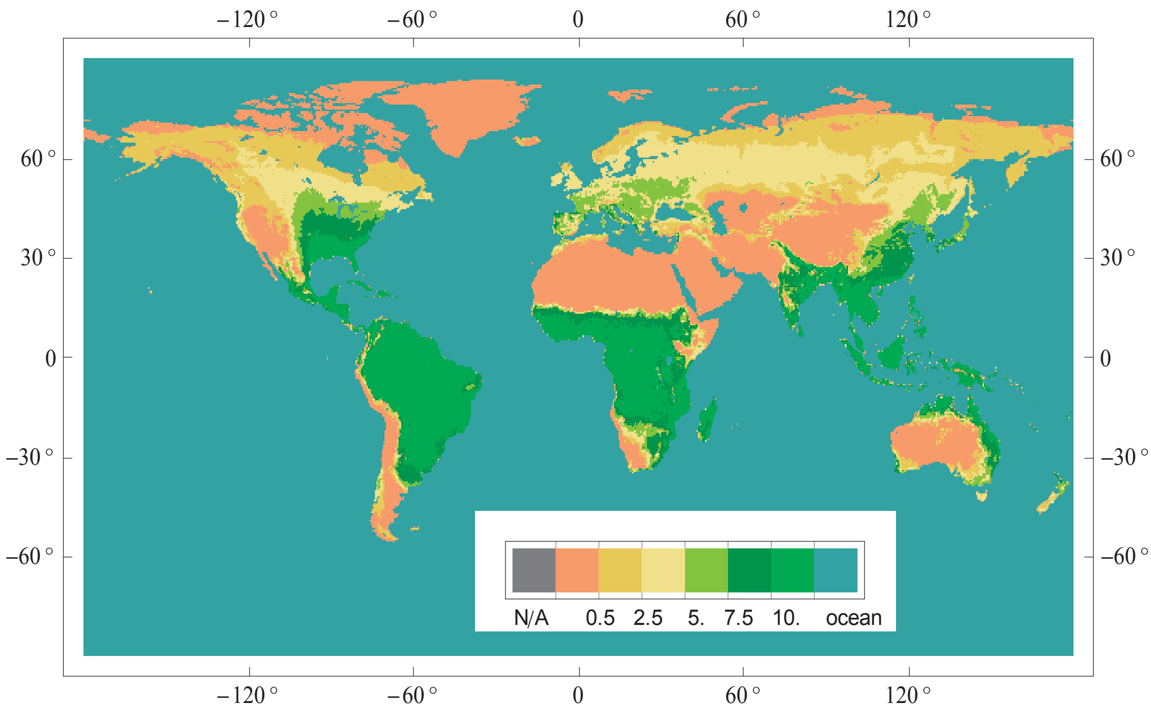

Figure 8.12 - TsuBiMo 1 NPP, units: tC ha^{-1} y^{-1}.

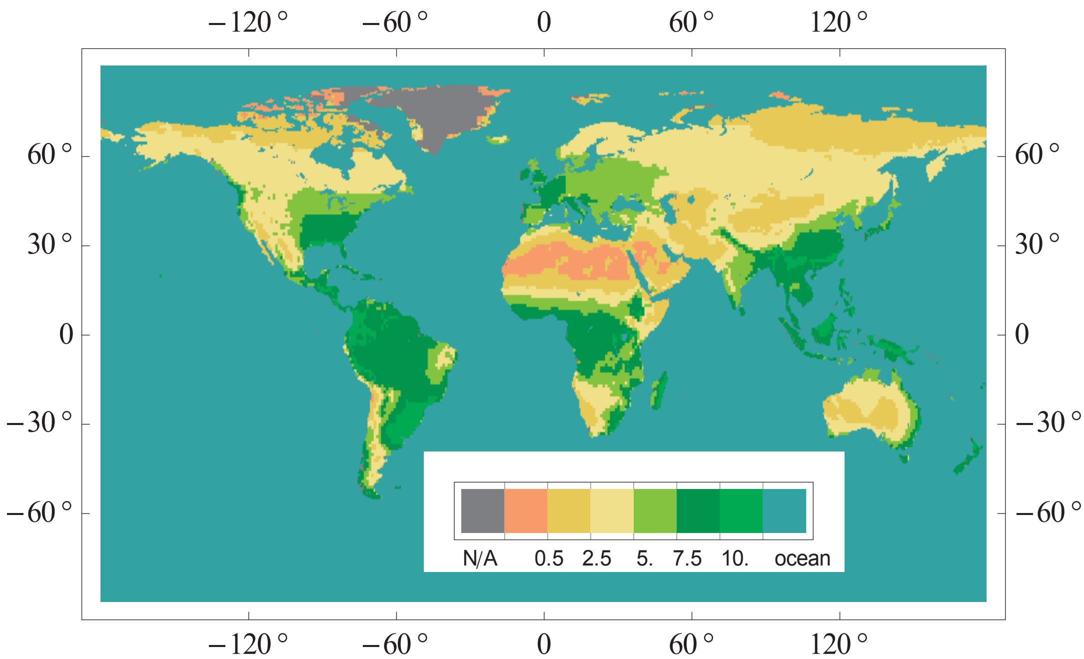

Figure 8.13 - VEGAS NPP, units: tC ha^{-1} y^{-1}.

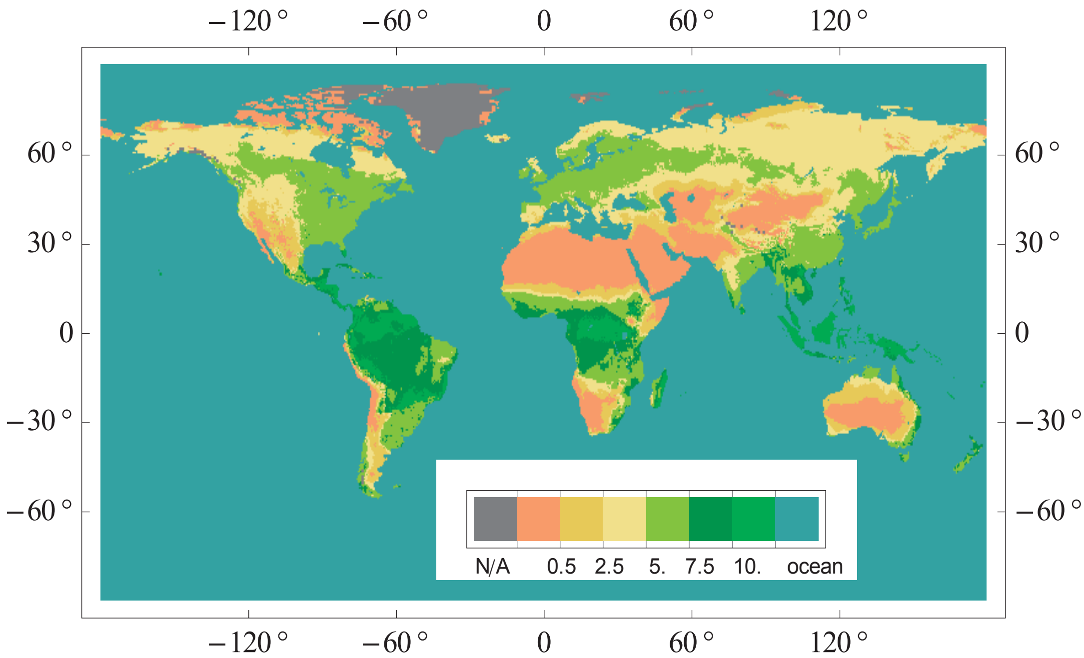

Figure 8.14 - LPJ-NPP, units: tC ha^{-1} y^{-1}.

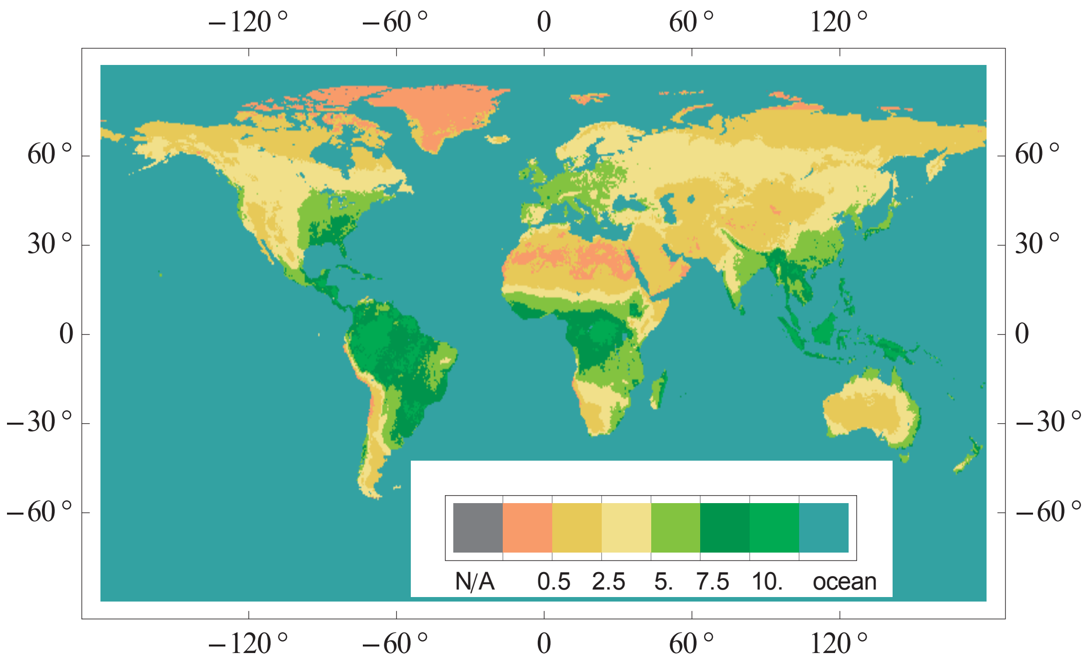

Figure 8.15 - Normative NPP 1.14.1, units: tC ha^{-1} y^{-1}.

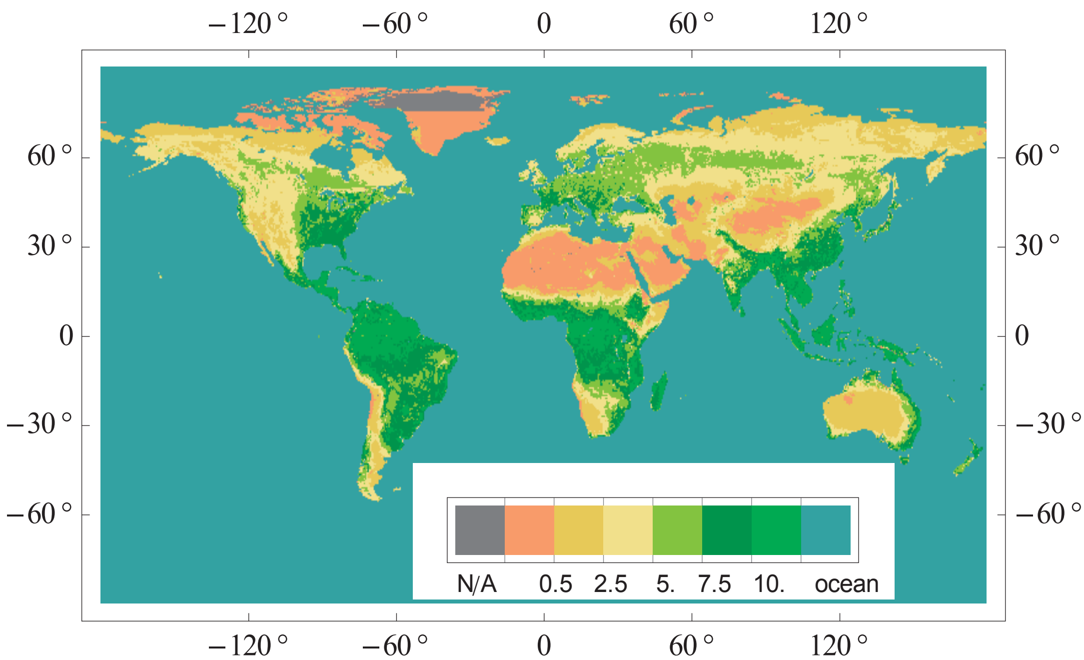

Figure 8.16 - Alternative NPP 1.14.1, units: tC ha^{-1} y^{-1}.

5.9 Model outputs: Charts

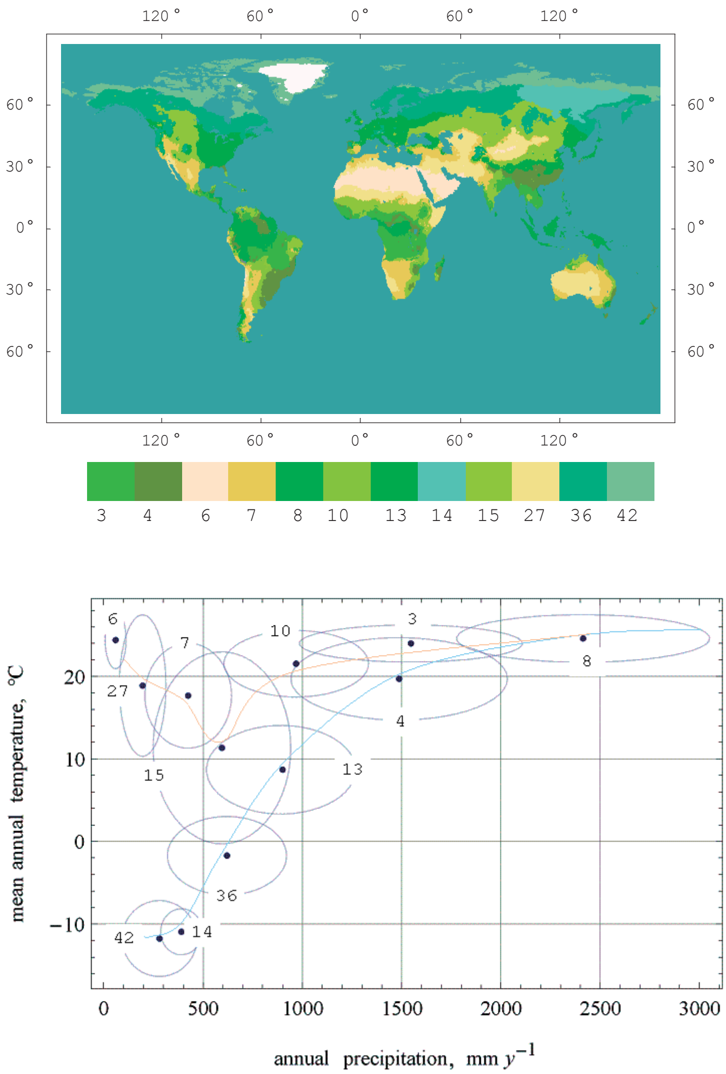

Figure 9.1 - The map and climatic characteristics of the vegetation zones.

Legend: 42 - tundra, 14 - larch forests, 36 -needle-leaf forests, 13 - summer-green broad-leaved forests, 4 - evergreen broad-leaved forests, 8 - tropical rainforests, 6 - deserts, 27 - semi-desert scrubs, 7 - shrublands, 15 - grasslands, 10- subhumid woodlands, 3 - raingreen forests. Points mark mean values, ellipses delineate standard deviations from the mean values, and lines highlight ecological series (ecoclines). The blue line highlights the series of biomes succeeding each other along the gradient of mean annual temperature, and the red line highlights the series of biomes succeeding each other along the gradient of annual precipitation.

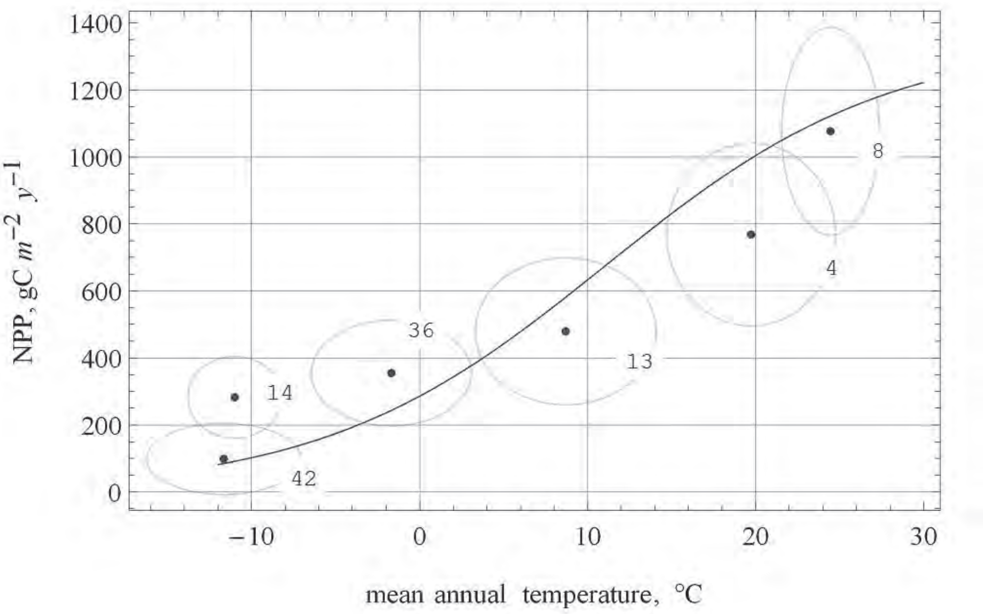

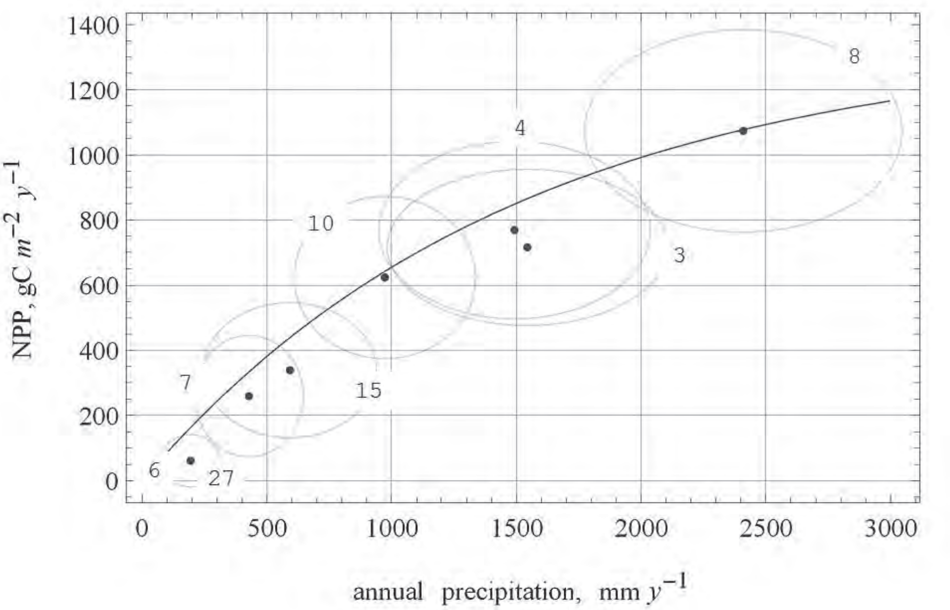

Figure 9.2 - BEAMS NPP of major vegetation zones.

Points mark mean values, ellipses delineate standard deviations from the mean values, and lines represent the temperature curve and humidity curve of the Miami NPP model, respectively. World total: 53.4 PgC y^{-1}

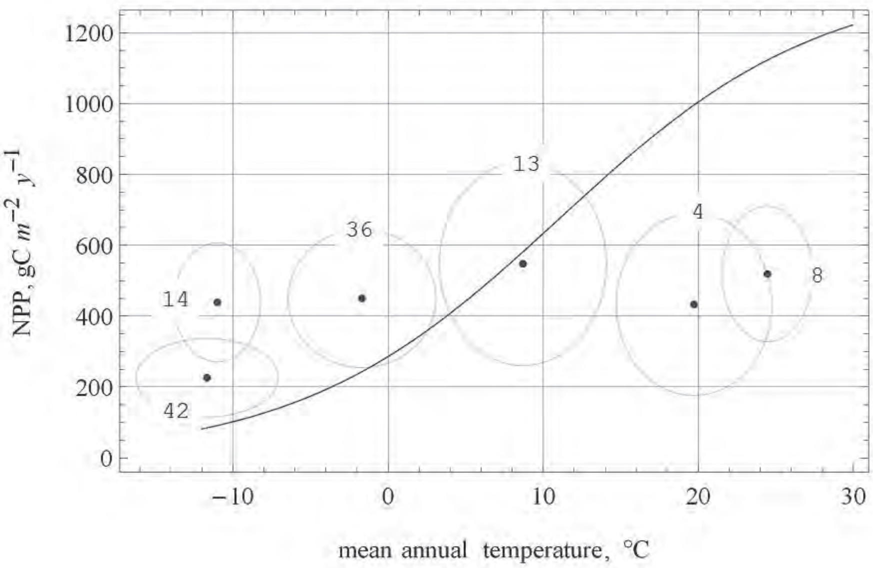

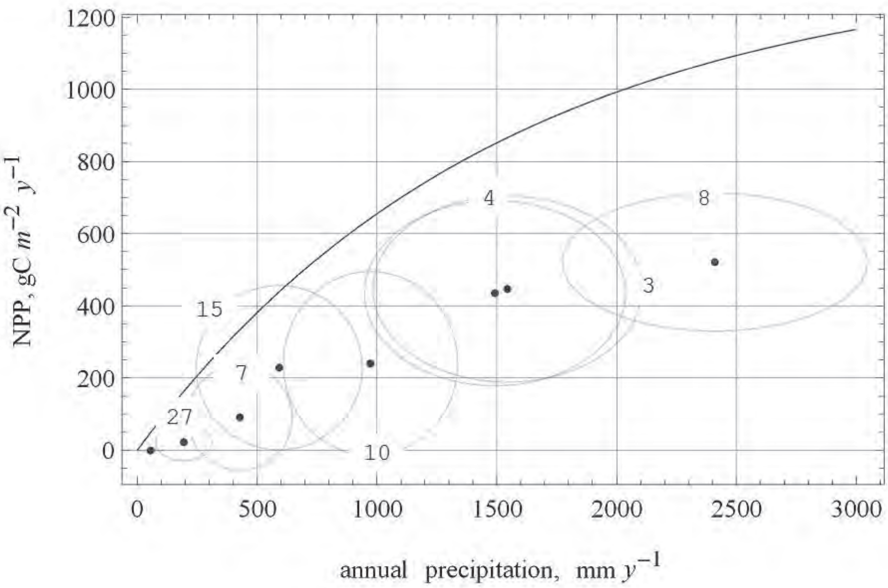

Figure 9.3 - Biome-BGC NPP of major vegetation zones.

Points mark mean values, ellipses delineate standard deviations from the mean values, and lines represent the temperature curve and humidity curve of the Miami NPP model, respectively. World total: 34.8 PgC y^{-1}

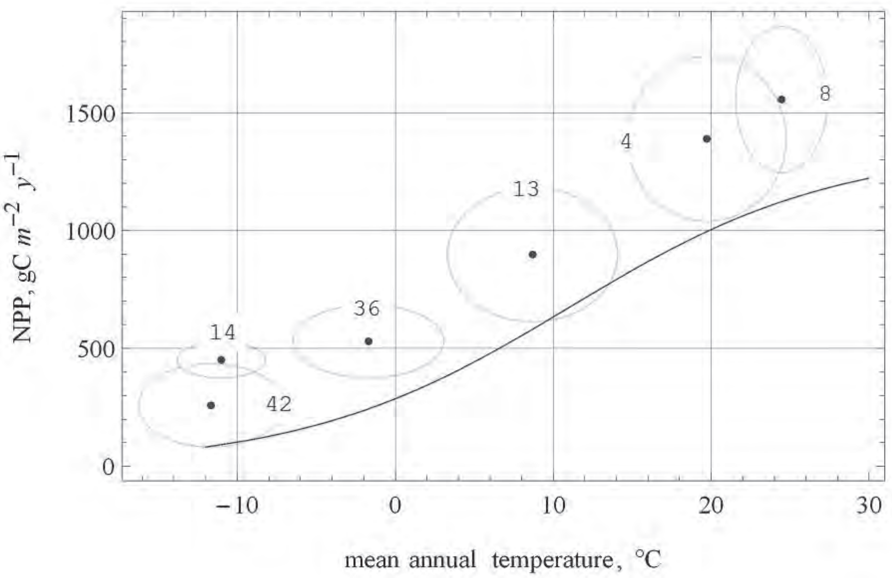

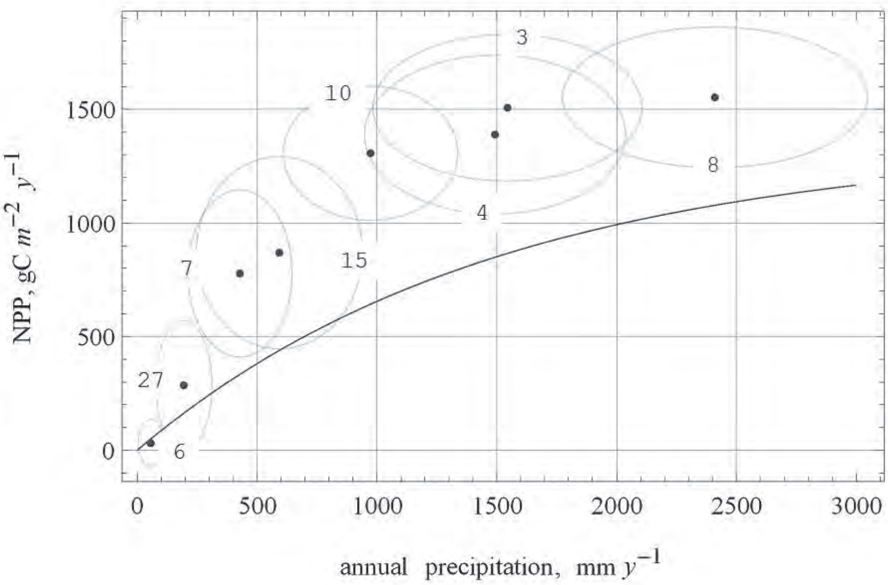

Figure 9.4 - GLO-PEM NPP of major vegetation zones.

Points mark mean values, ellipses delineate standard deviations from the mean values, and lines represent the temperature curve and humidity curve of the Miami NPP model, respectively. World total: 108.0 PgC y^{-1}

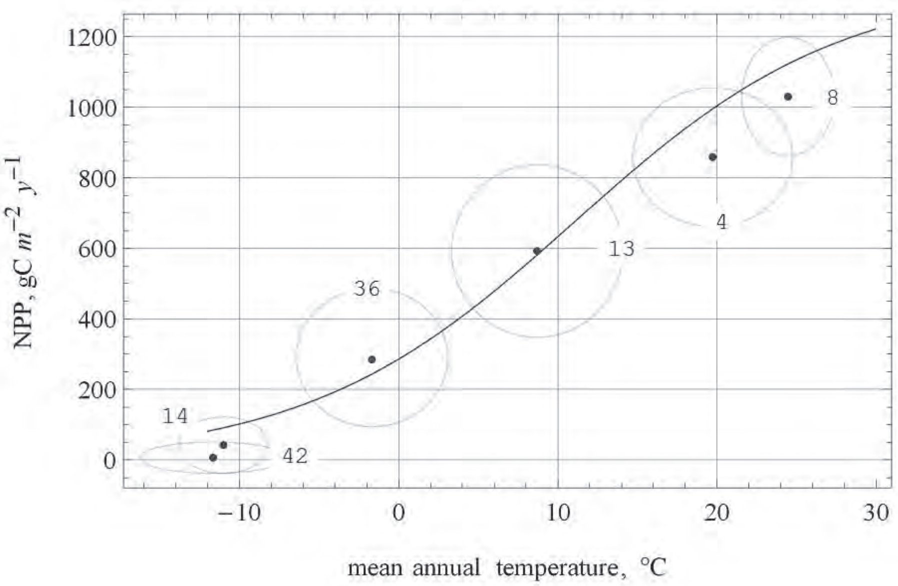

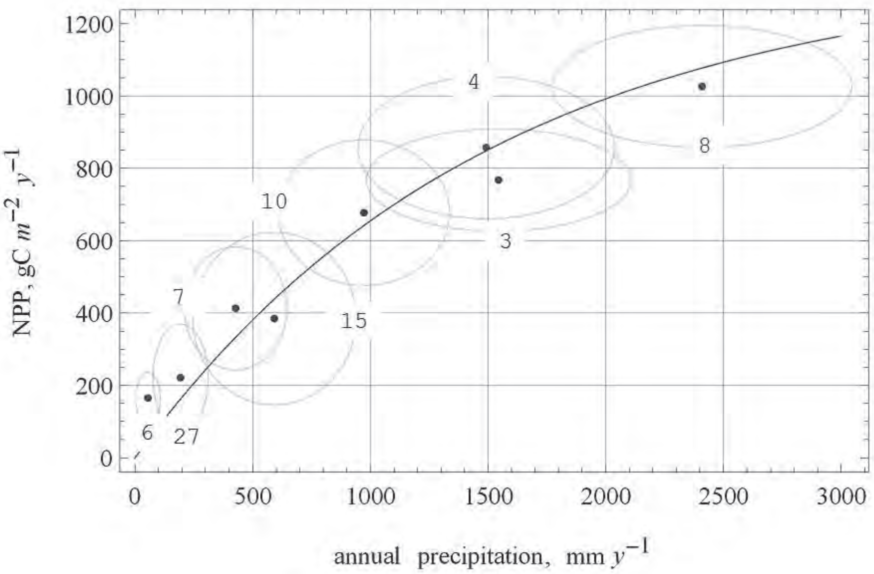

Figure 9.5 - Madison NPP of major vegetation zones.

Points mark mean values, ellipses delineate standard deviations from the mean values, and lines represent the temperature curve and humidity curve of the Miami NPP model, respectively. World total: 60.5 PgC y^{-1}

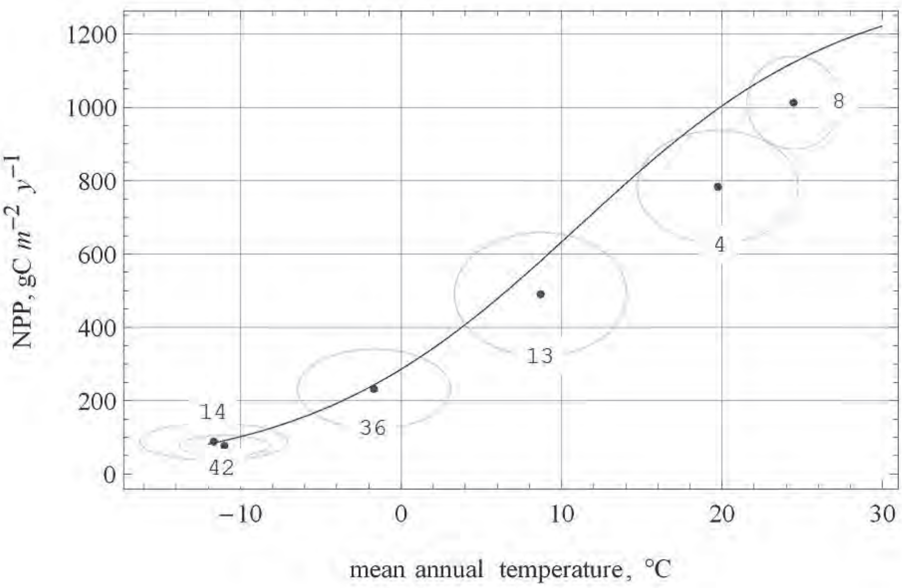

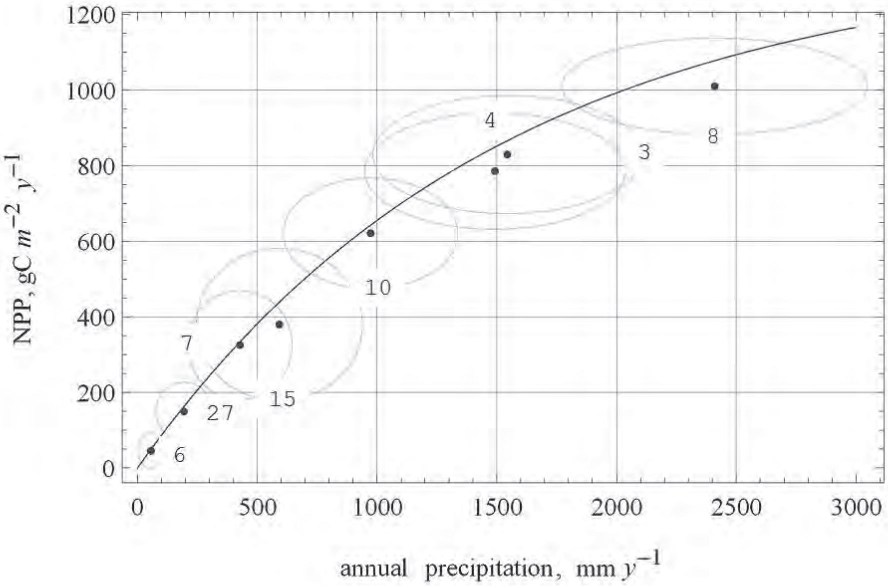

Figure 9.6 - Miami NPP of major vegetation zones.

Points mark mean values, ellipses delineate standard deviations from the mean values, and lines represent the temperature curve and humidity curve of the Miami NPP model, respectively. World total: 56.0 PgC y^{-1}

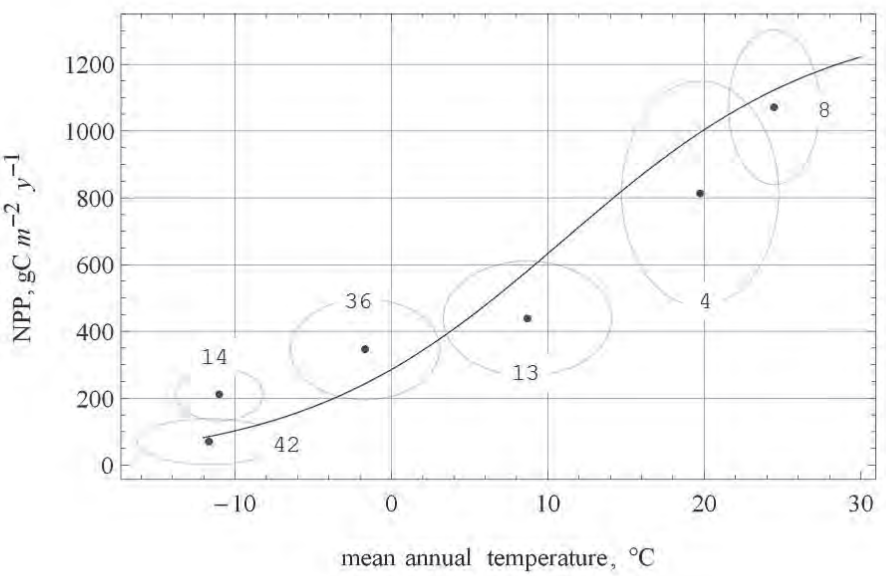

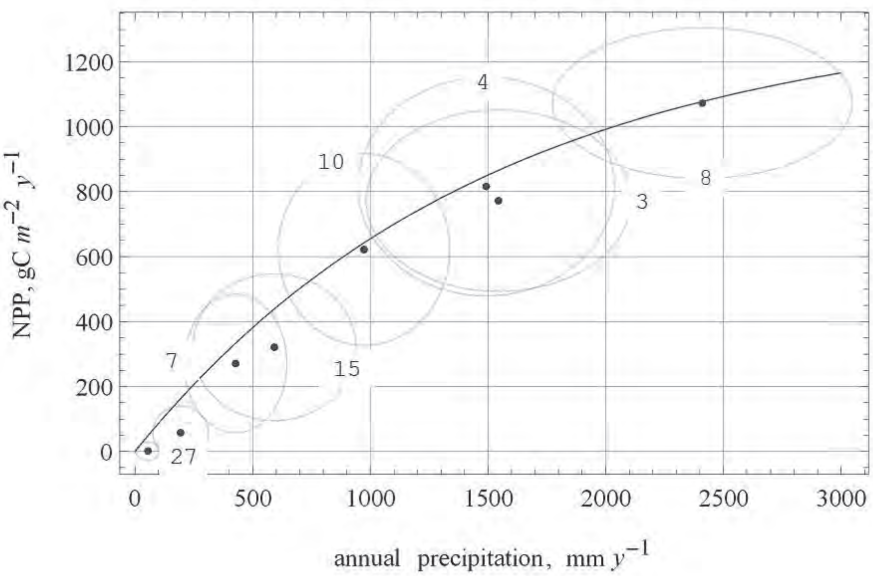

Figure 9.7 - MODIS-NPP of major vegetation zones.

Points mark mean values, ellipses delineate standard deviations from the mean values, and lines represent the temperature curve and humidity curve of the Miami NPP model, respectively. World total: 54.1 PgC y^{-1}

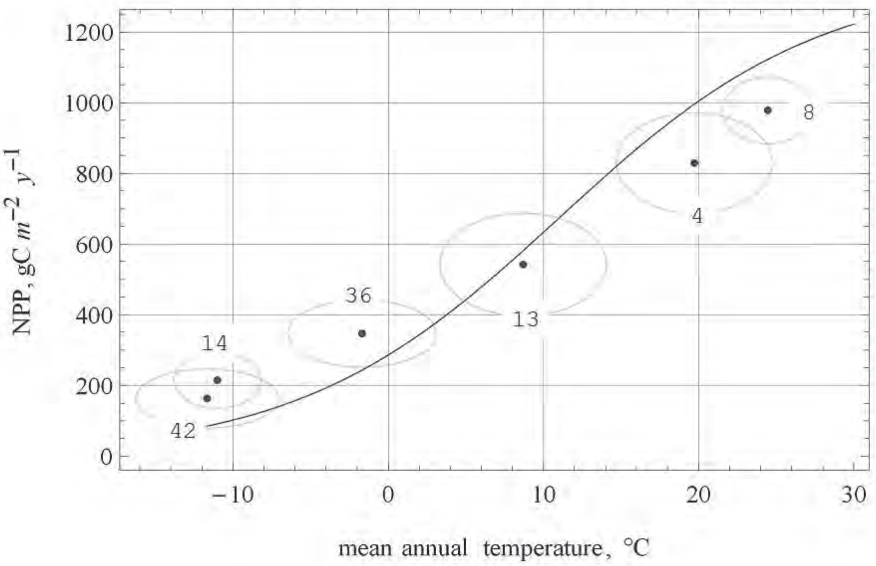

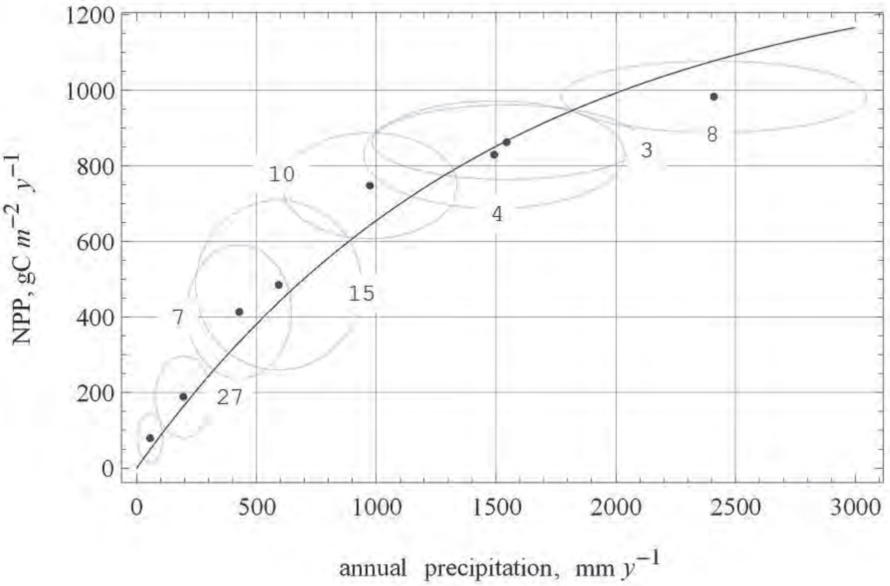

Figure 9.8 - Montreal NPP of major vegetation zones.

Points mark mean values, ellipses delineate standard deviations from the mean values, and lines represent the temperature curve and humidity curve of the Miami NPP model, respectively. World total: 64.2 PgC y^{-1}

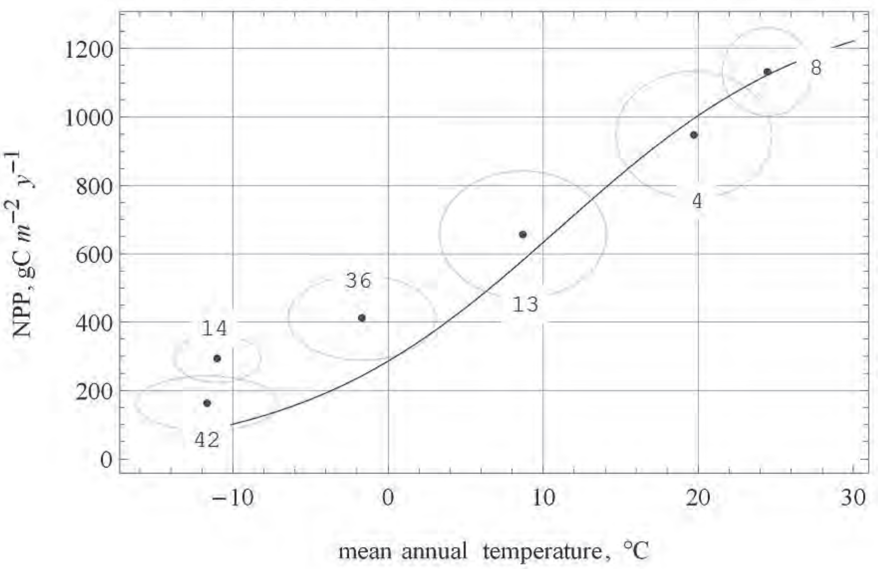

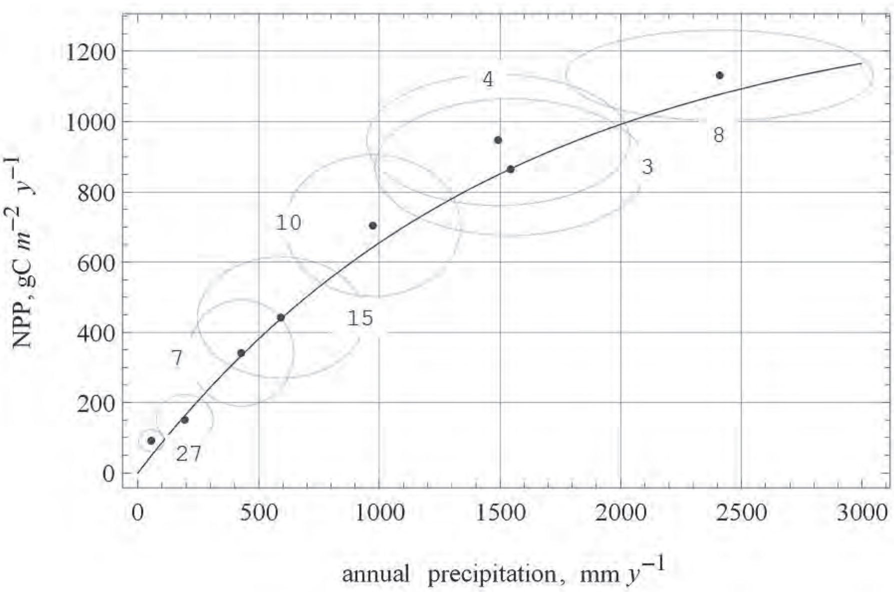

Figure 9.9- Potsdam NPP (high) of major vegetation.

Points mark mean values, ellipses delineate standard deviations from the mean values, and lines represent the temperature curve and humidity curve of the Miami NPP model, respectively. World total: 64.8 PgC y^{-1}

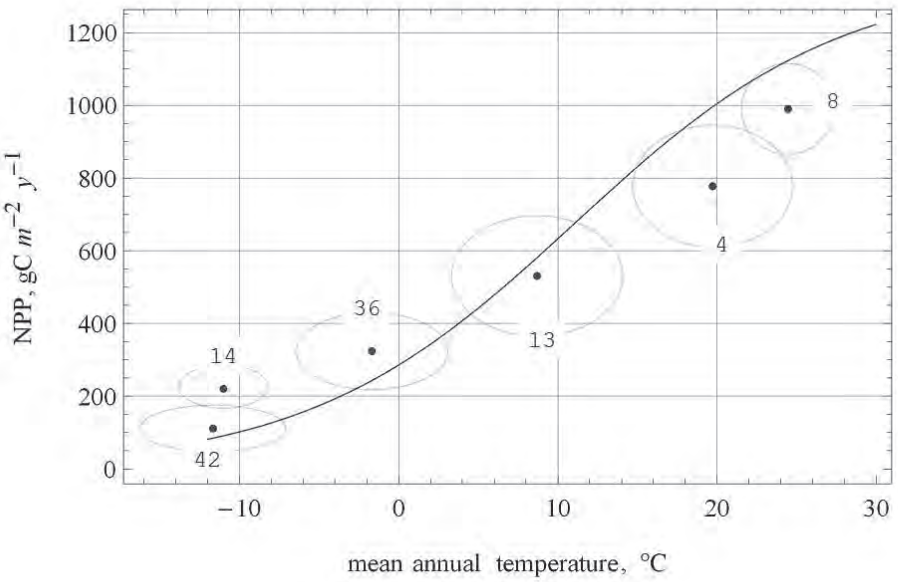

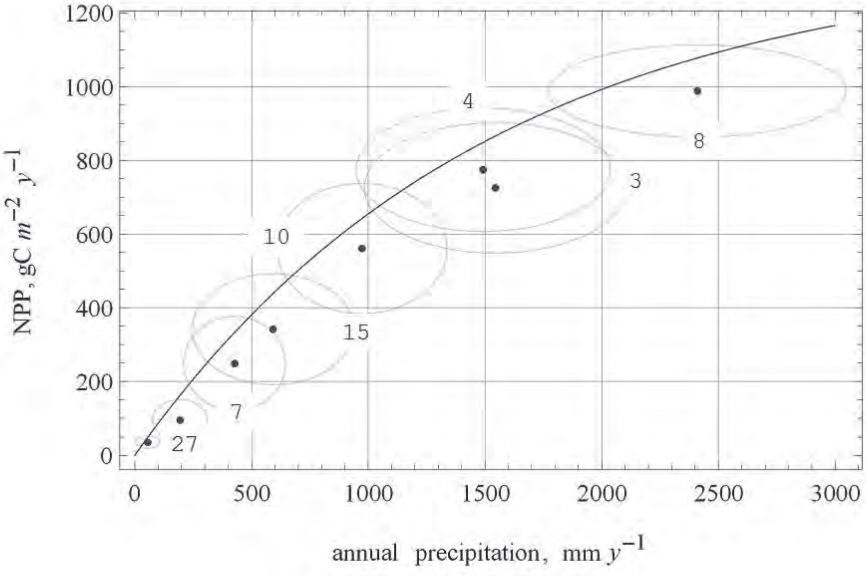

Figure 9.10- Potsdam NPP (low) of major vegetation.

Points mark mean values, ellipses delineate standard deviations from the mean values, and lines represent the temperature curve and humidity curve of the Miami NPP model, respectively. World total: 51.6 PgC y^{-1}

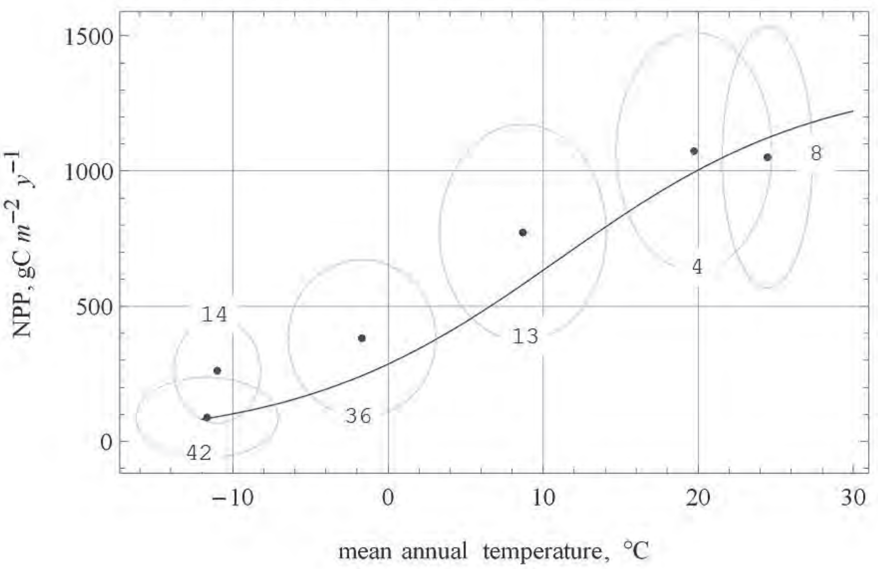

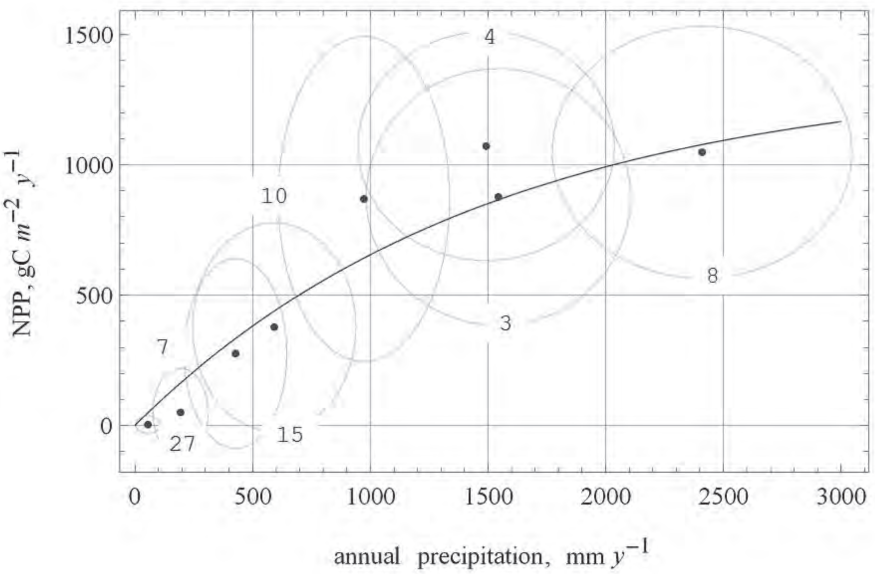

Figure 9.11 - Sim-CYCLE NPP (rev) of major vegetation zones.

Points mark mean values, ellipses delineate standard deviations from the mean values, and lines represent the temperature curve and humidity curve of the Miami NPP model, respectively. World total: 64.8 PgC y^{-1}

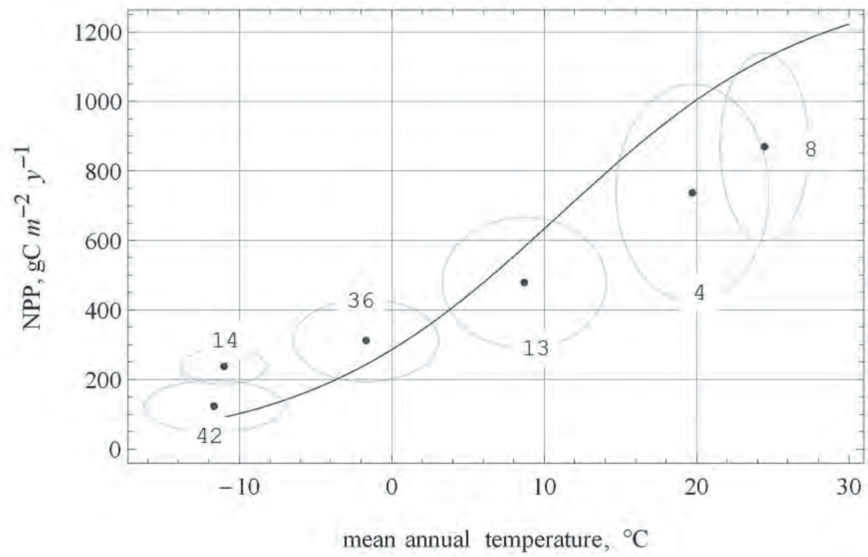

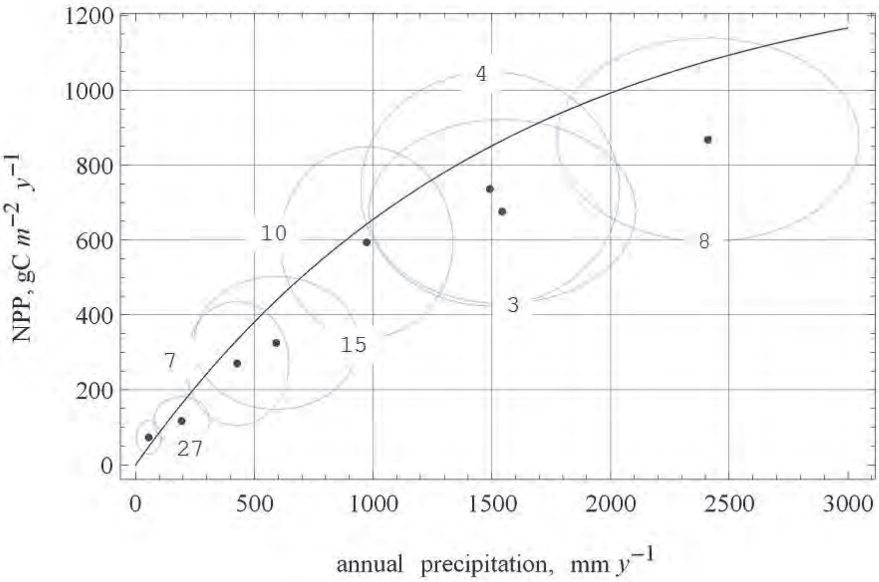

Figure 9.12 - TGER-NPP of major vegetation zones.

Points mark mean values, ellipses delineate standard deviations from the mean values, and lines represent temperature curve and humidity curve of the Miami NPP model, respectively. World total: 49.4 PgC y^{-1}

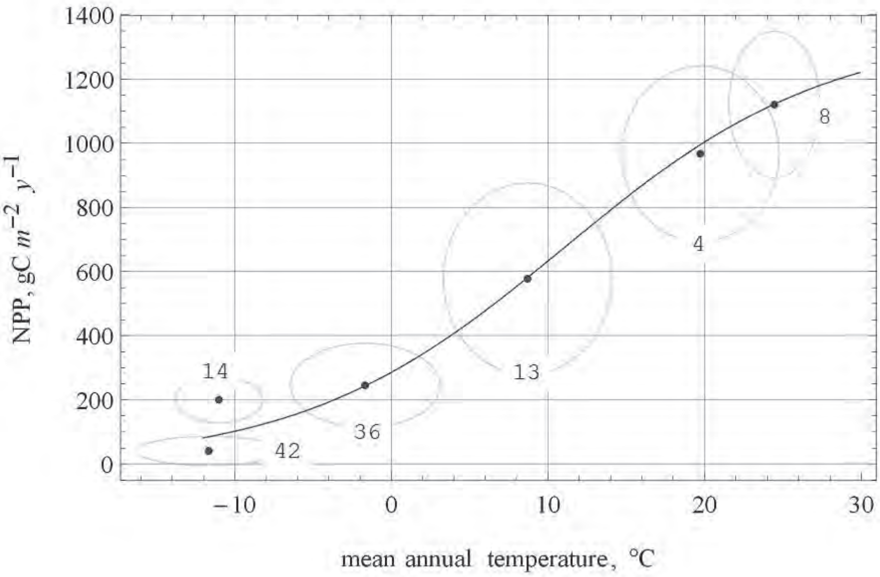

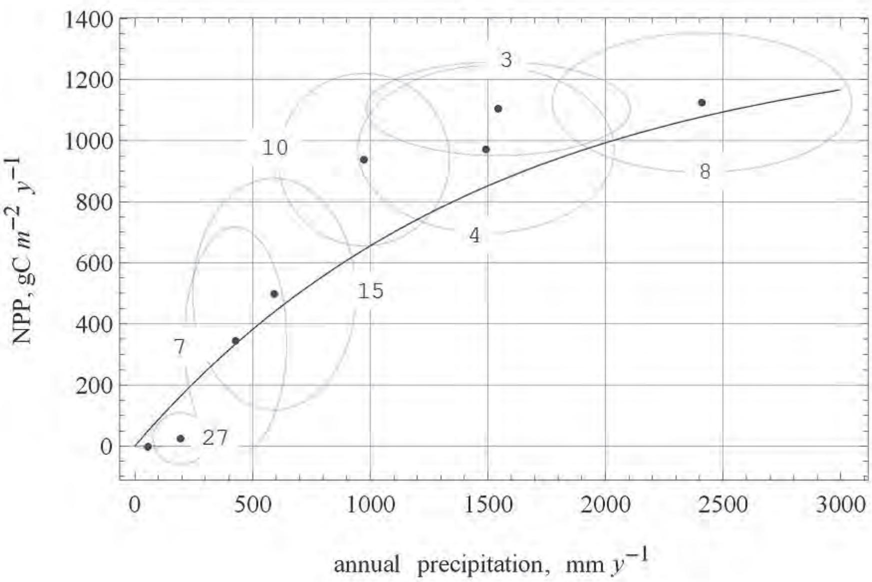

Figure 9.13 - TsuBiMo 1-NPP of major vegetation zones.

Points mark mean values, ellipses delineate standard deviations from the mean values, and lines represent the temperature curve and humidity curve of the Miami NPP model, respectively. World total: 64.4 PgC y^{-1}

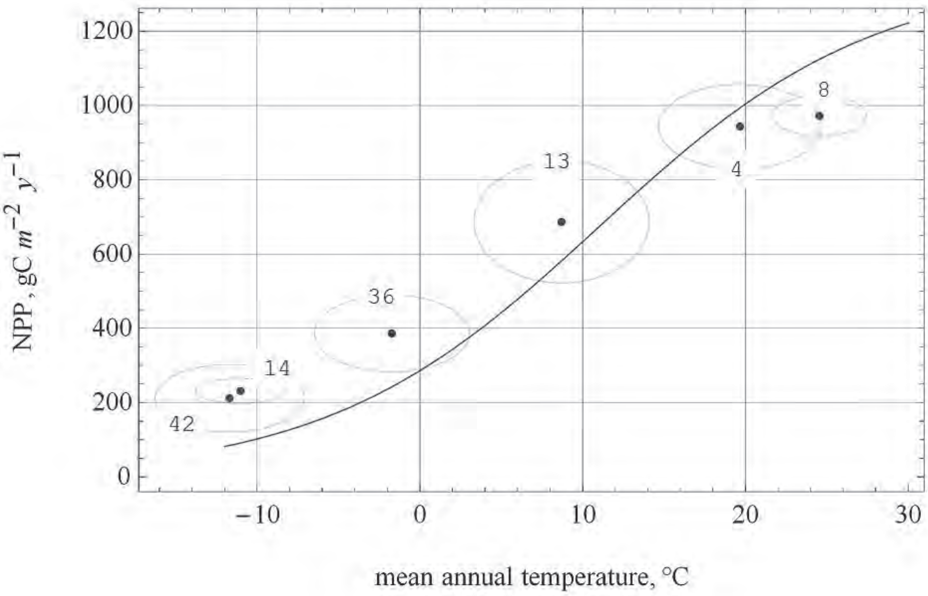

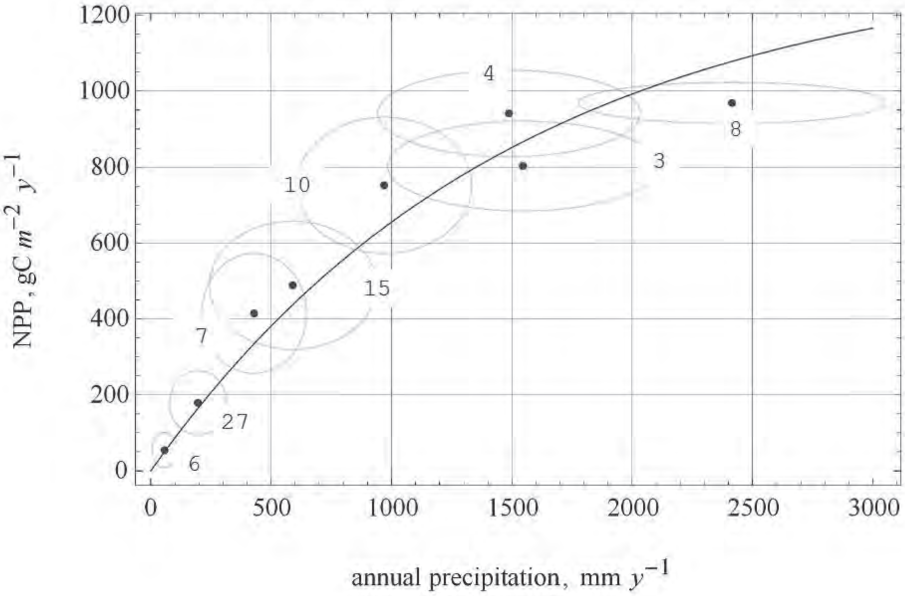

Figure 9.14 - VEGAS-NPP of major vegetation zones.

Points mark mean values, ellipses delineate standard deviations from the mean values, and lines represent the temperature curve and humidity curve of the Miami NPP model, respectively. World total: 67.1 PgC y^{-1}

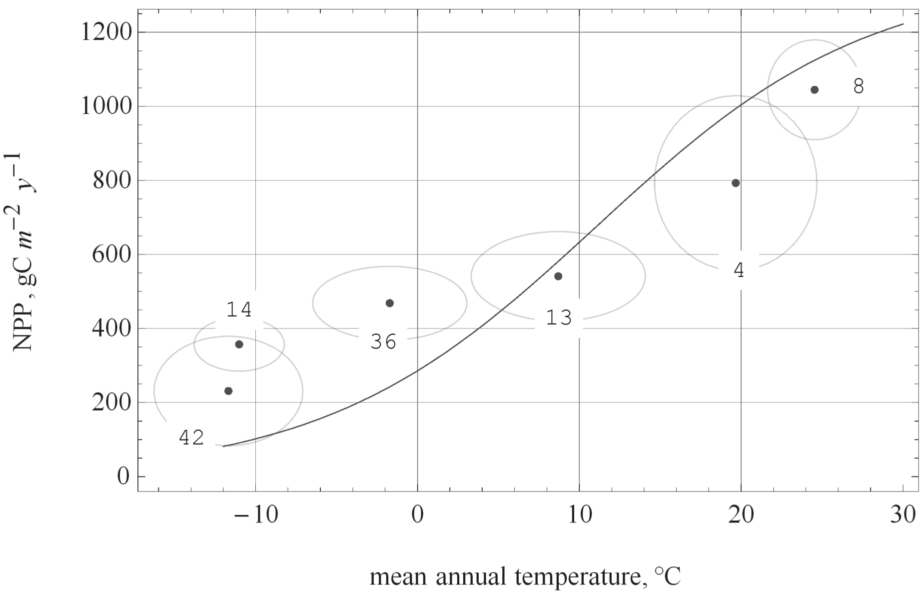

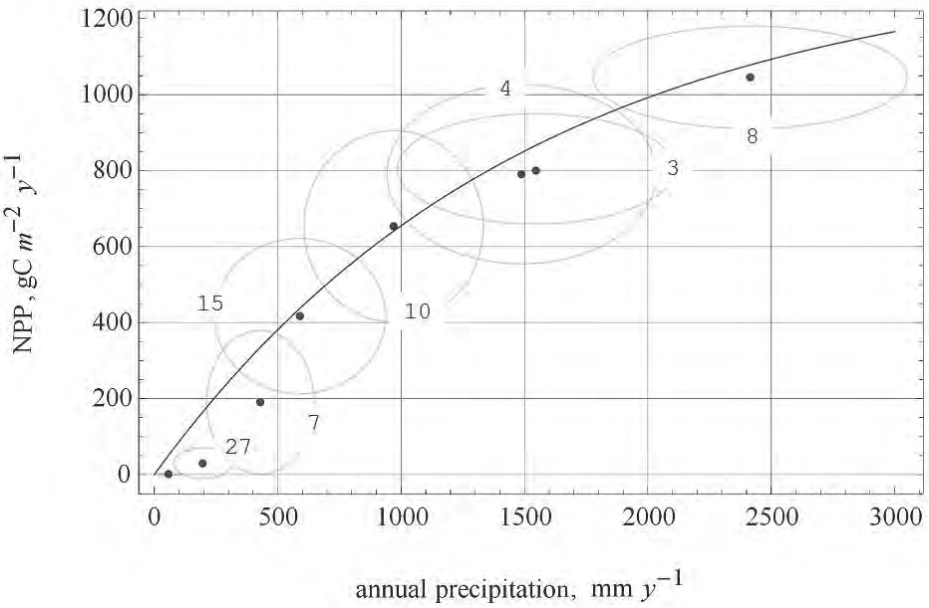

Figure 9.15 - LPJ-NPP of major vegetation zones.

Points mark mean values, ellipses delineate standard deviations from the mean values, and lines represent the temperature curve and humidity curve of the Miami NPP model, respectively. World total: 59.1 PgC y^{-1}

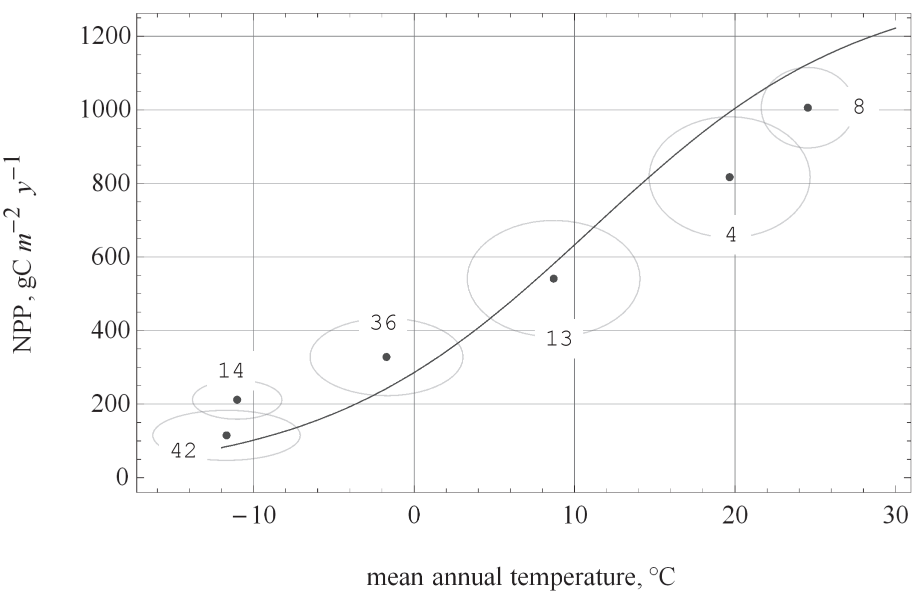

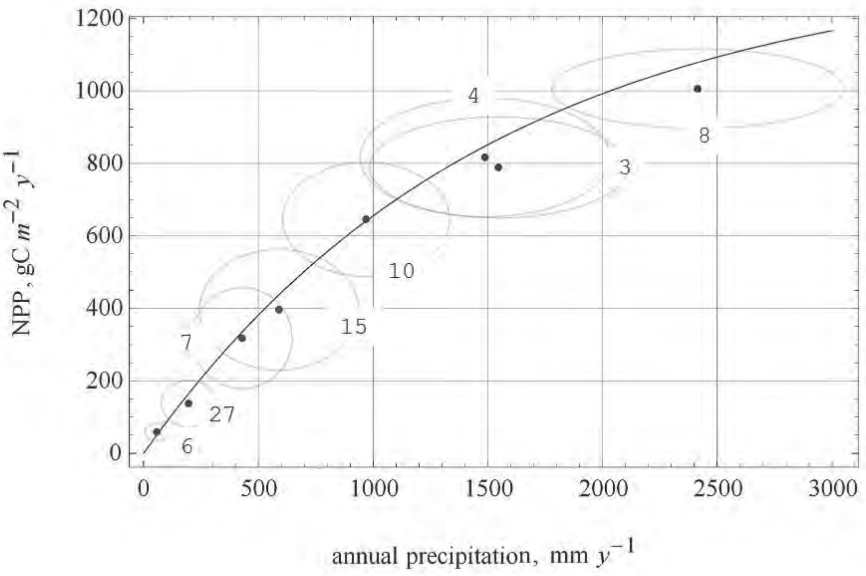

Figure 9.16 - Normative NPP (version 1.14.1) of major vegetation zones.

Points mark mean values, ellipses delineate standard deviations from the mean values, and lines represent the temperature curve and humidity curve of the Miami NPP model, respectively. World total: 59 PgC y^{-1}

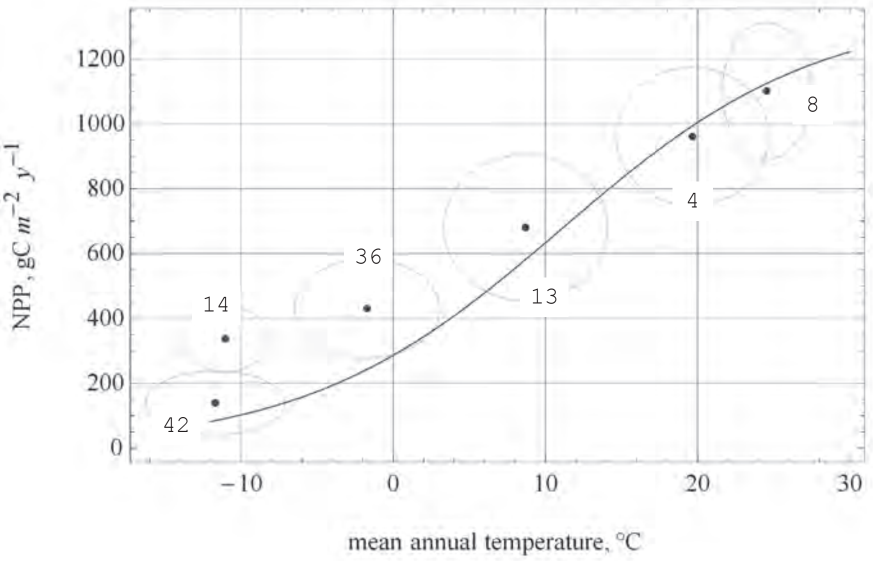

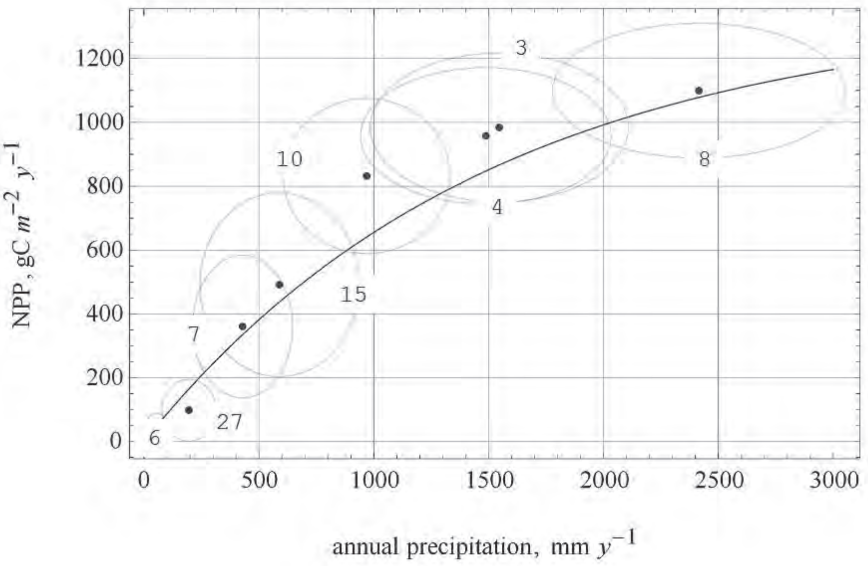

Figure 9.17 - Alternative NPP (version 1.14.1) of major vegetation zones.

Points mark mean values, ellipses delineate standard deviations from the mean values, and lines represent the temperature curve and humidity curve of the Miami NPP model, respectively. World total: 70 PgC y^{-1}

5.10 Alternatives to Normative NPP: maps

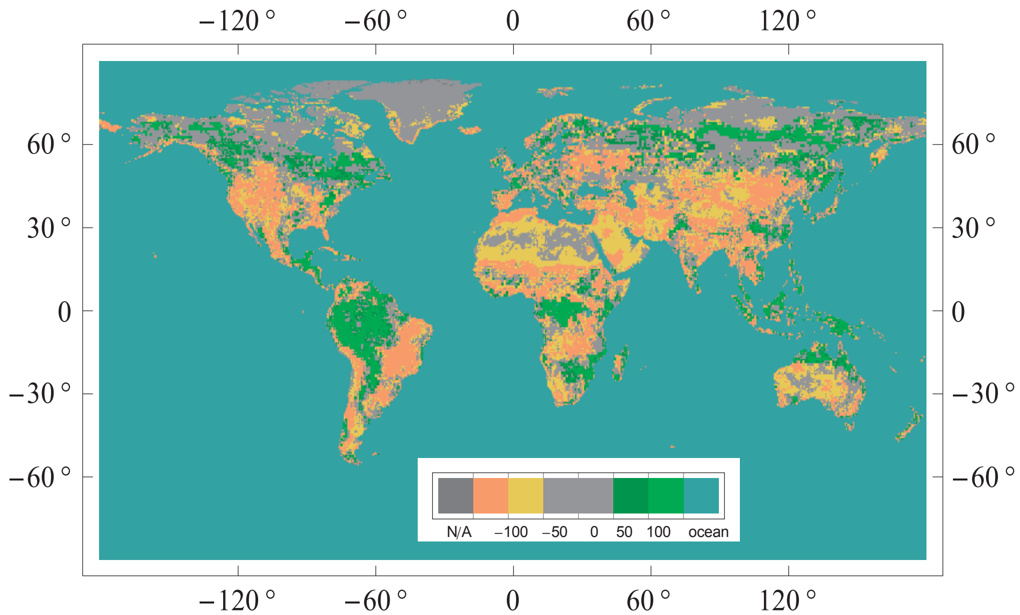

Figure 10.1 - BEAMS alternative to Normative NPP 1.14.1. Units: gC m^{-2} y^{-1}

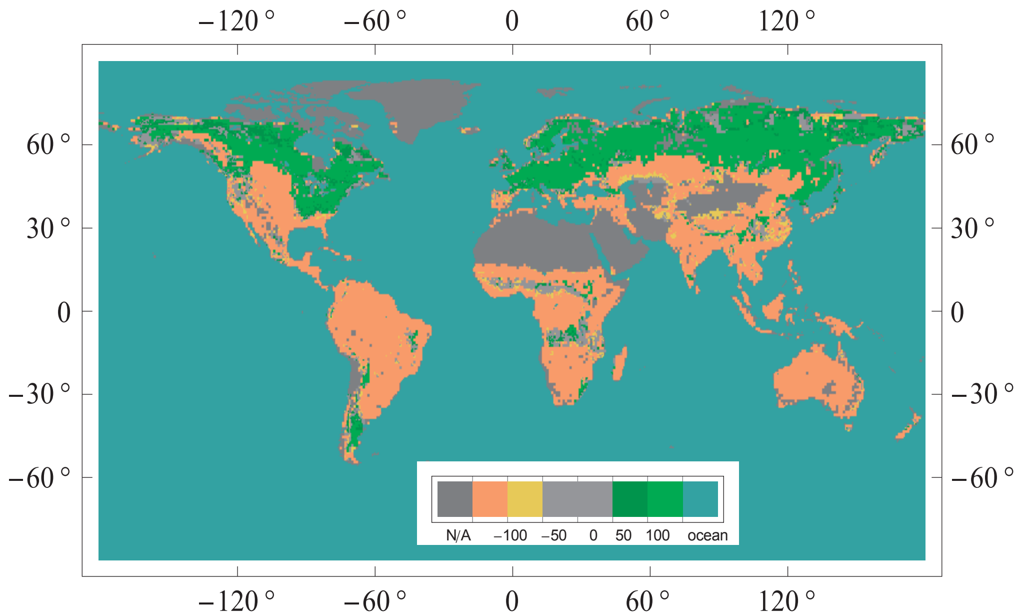

Figure 10.2 - Biome-BGC alternative to Normative NPP 1.14.1. Units: gC m^{-2} y^{-1}

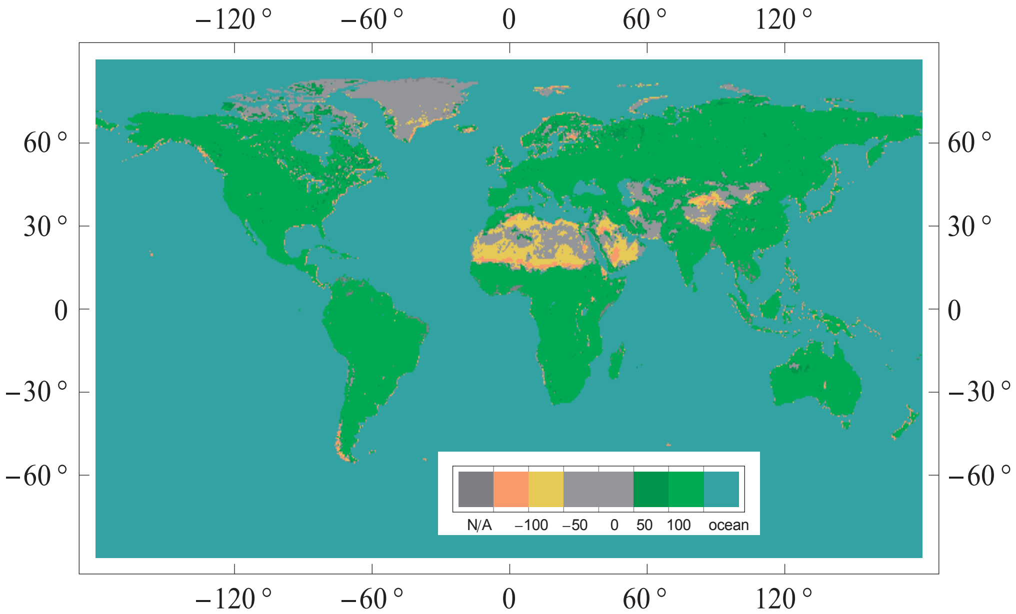

Figure 10.3 - GLO-PEM alternative to Normative NPP 1.14.1 Units: gC m^{-2} y^{-1}

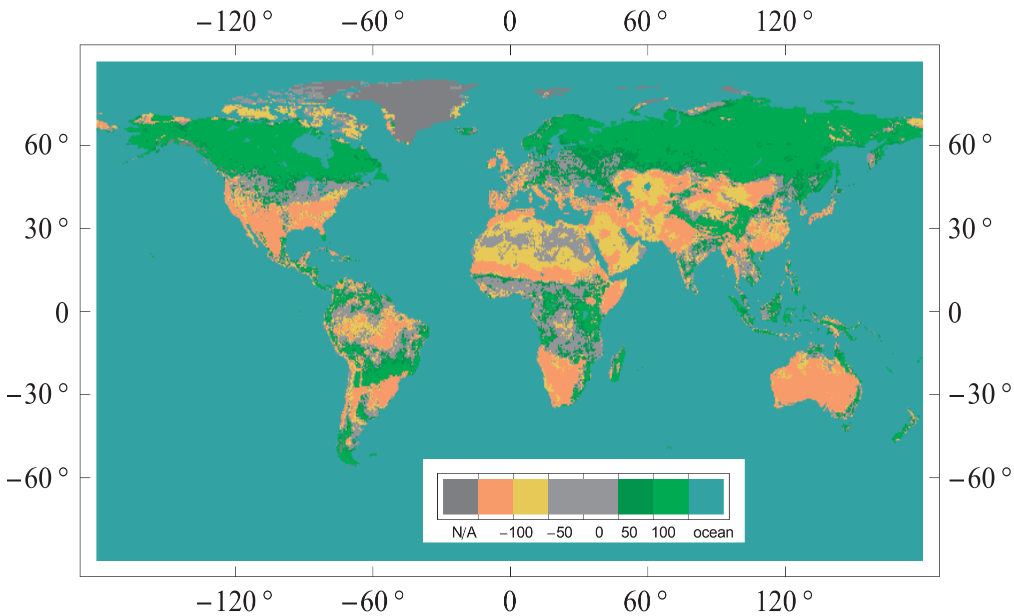

Figure 10.4 - LPJ NPP alternative to Normative NPP 1.14.1. Units: gC m^{-2} y^{-1}

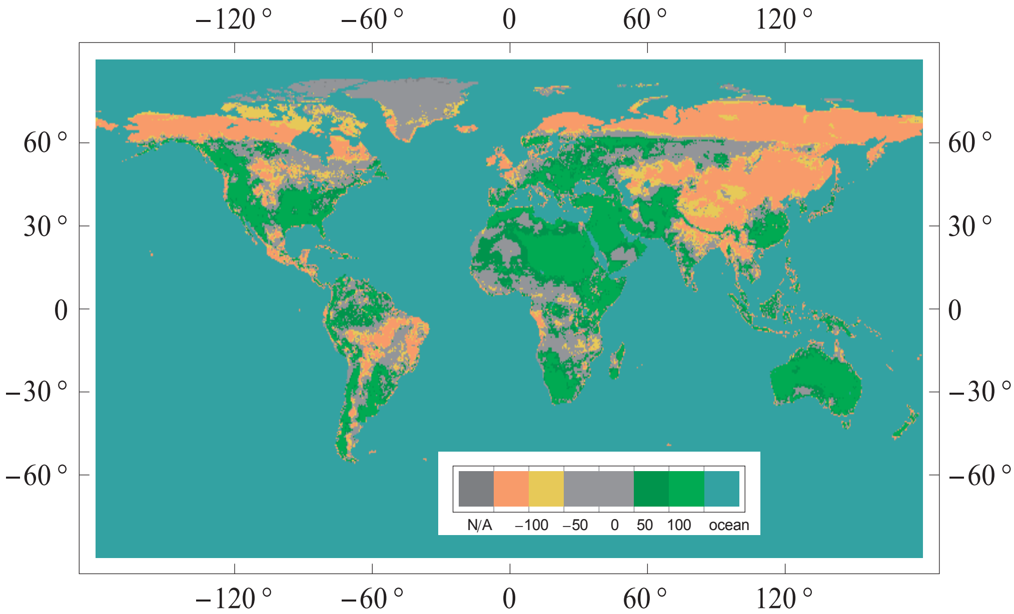

Figure 10.5 - Madison NPP alternative to Normative NPP 1.14.1. Units: gC m^{-2} y^{-1}

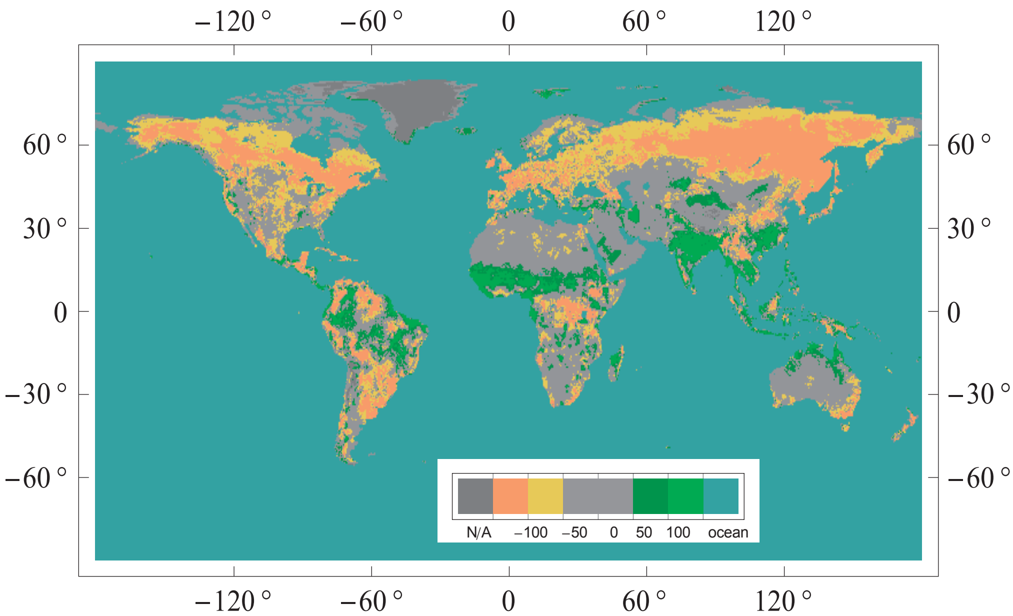

Figure 10.6 - Miami NPP alternative to Normative NPP 1.14.1. Units: gC m^{-2} y^{-1}

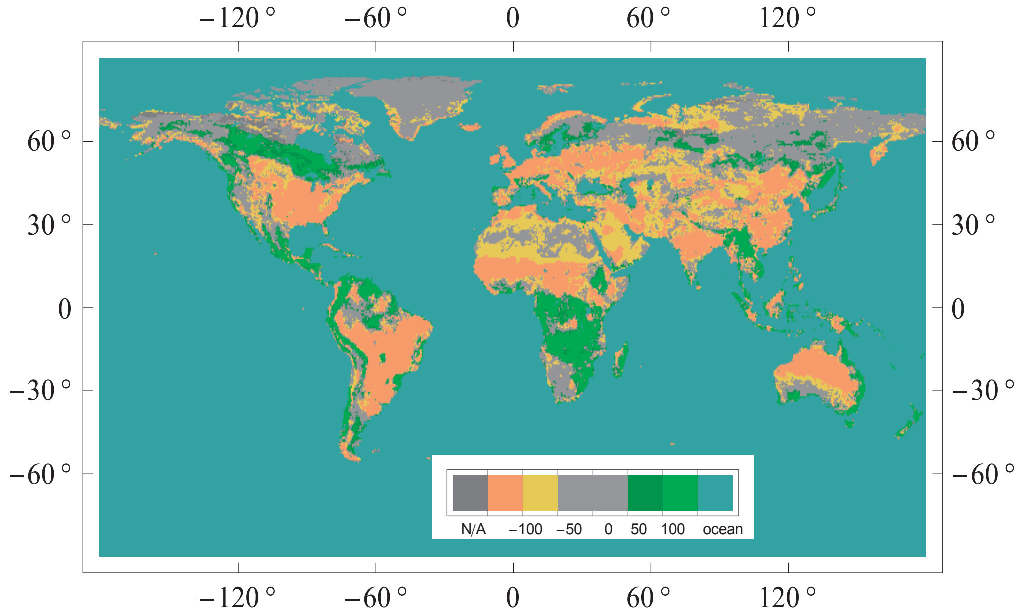

Figure 10.7 - MODIS-NPP alternative to Normative NPP 1.14.1. Units: gC m^{-2} y^{-1}

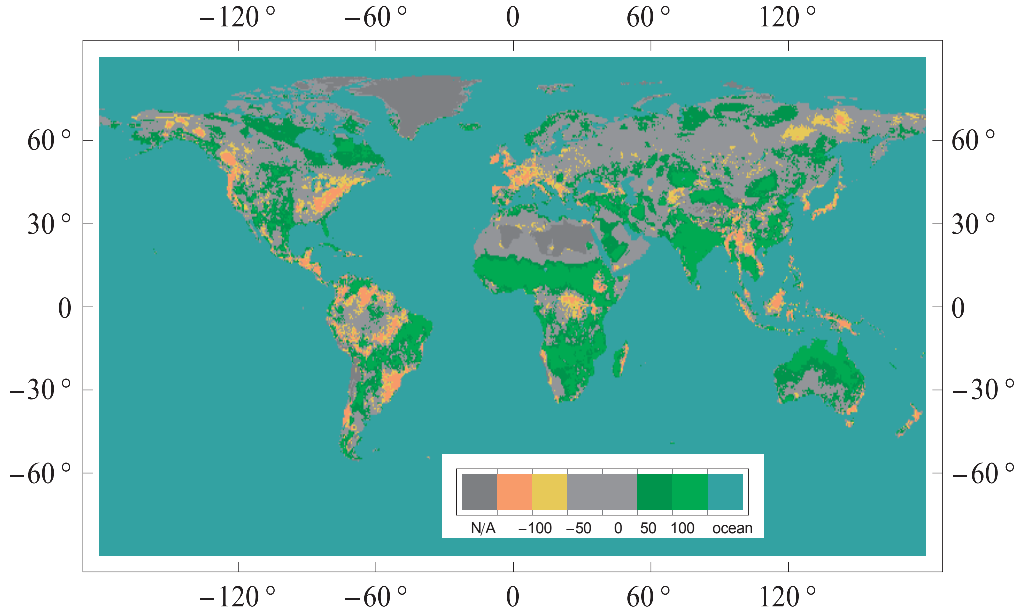

Figure 10.8 - Montreal NPP alternative to Normative NPP 1.14.1. Units: gC m^{-2} y^{-1}

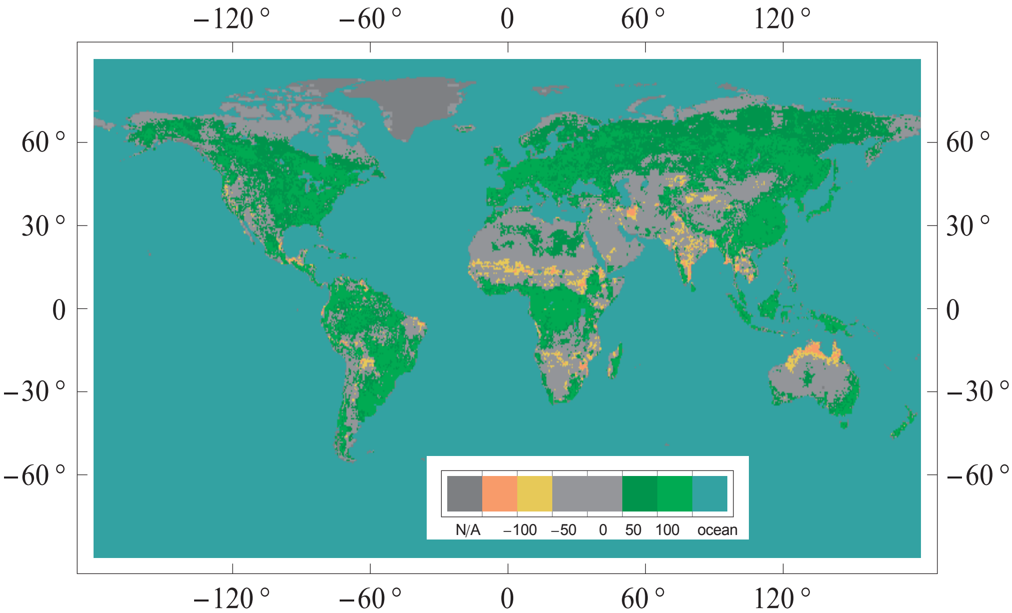

Figure 10.9 - Potsdam NPP (high) alternative to Normative NPP 1.14.1. Units: gC m^{-2} y^{-1}

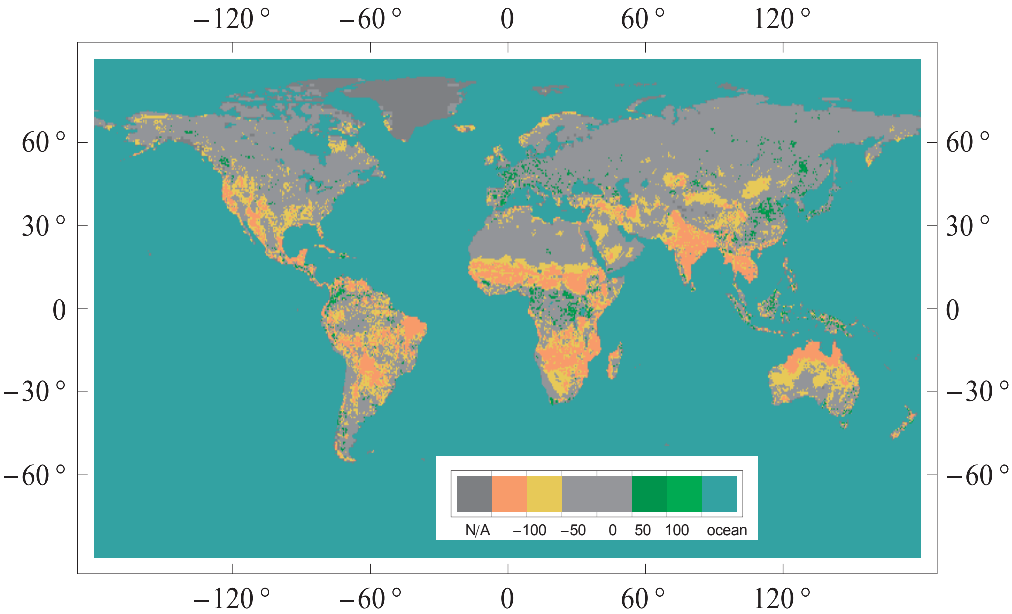

Figure 10.10 - Potsdam NPP (low) alternative to Normative NPP 1.14.1. Units: gC m^{-2} y^{-1}

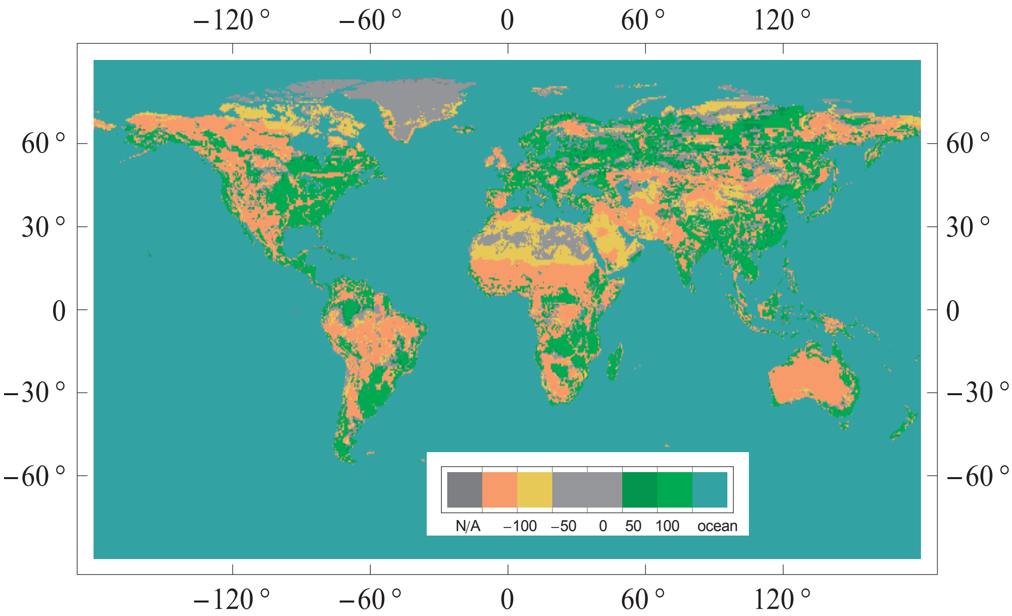

Figure 10.11 - Sim-CYCLE (rev) alternative to Normative NPP 1.14.1. Units: gC m^{-2} y^{-1}

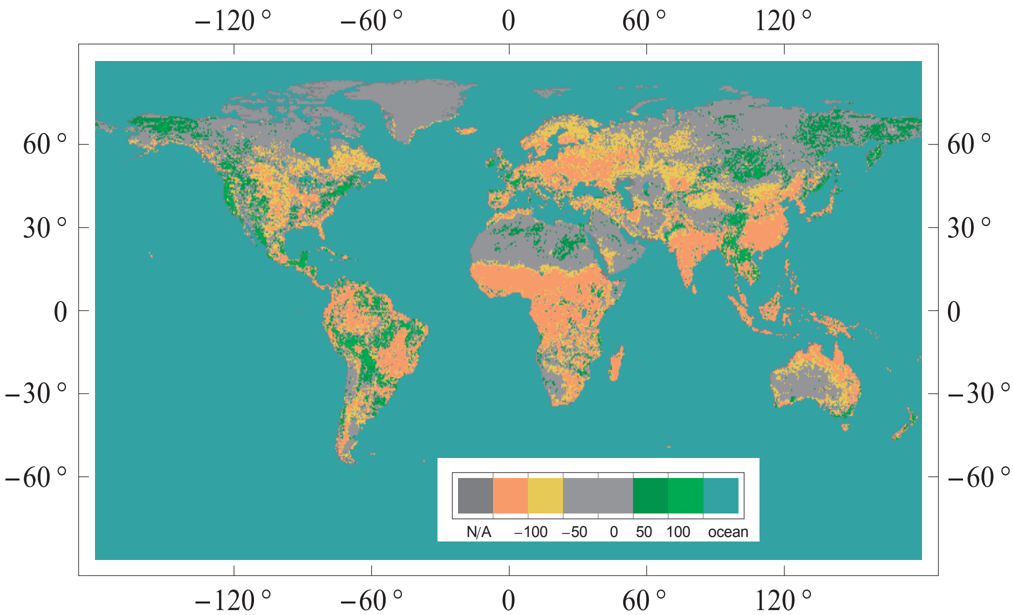

Figure 10.12 - TGER-NPP alternative to Normative NPP 1.14.1. Units: gC m^{-2} y^{-1}

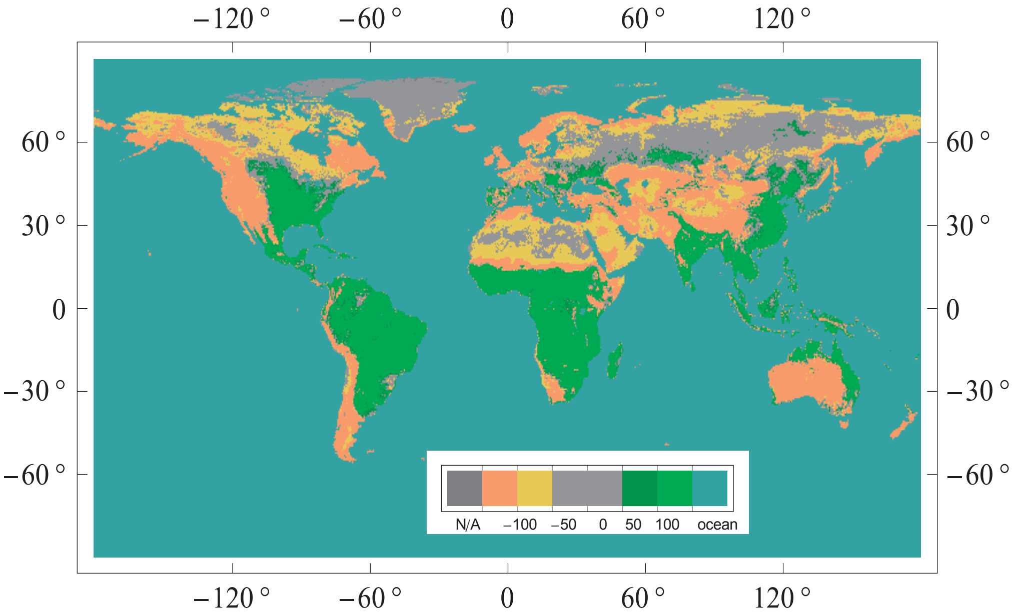

Figure 10.13 - TsuBiMo 1 alternative to Normative NPP 1.14.1. Units: gC m^{-2} y^{-1}

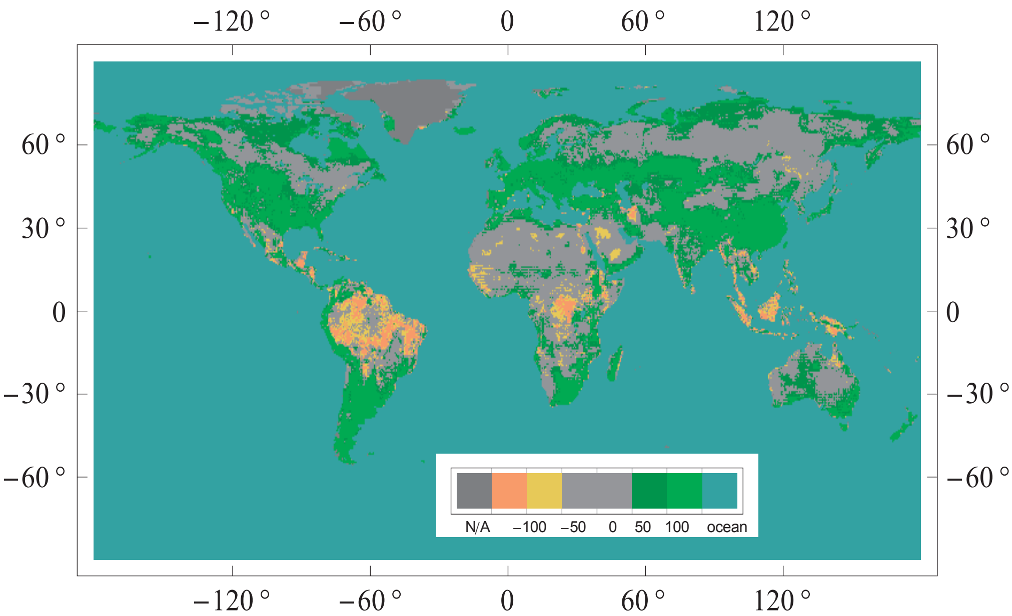

Figure 10.14 - VEGAS alternative to Normative NPP 1.14.1. Units: gC m^{-2} y^{-1}

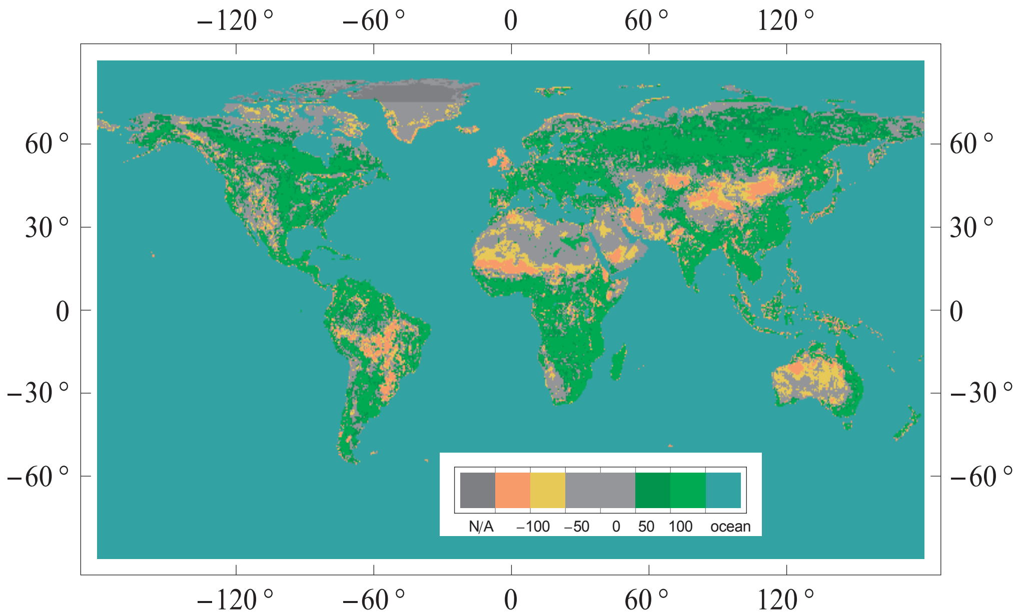

Figure 10.15 - Alternative NPP 1.14.1 vs Normative NPP 1.14.1. Units: gC m^{-2} y^{-1}

5.11 Alternatives to Normative NPP: charts

The plots displaying in which biome a given model implies higher or lower productivity than Normative NPP.

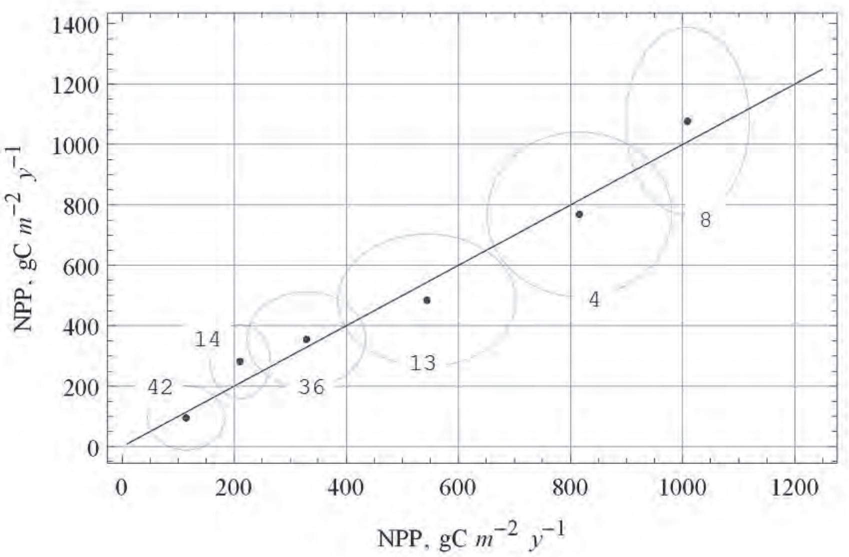

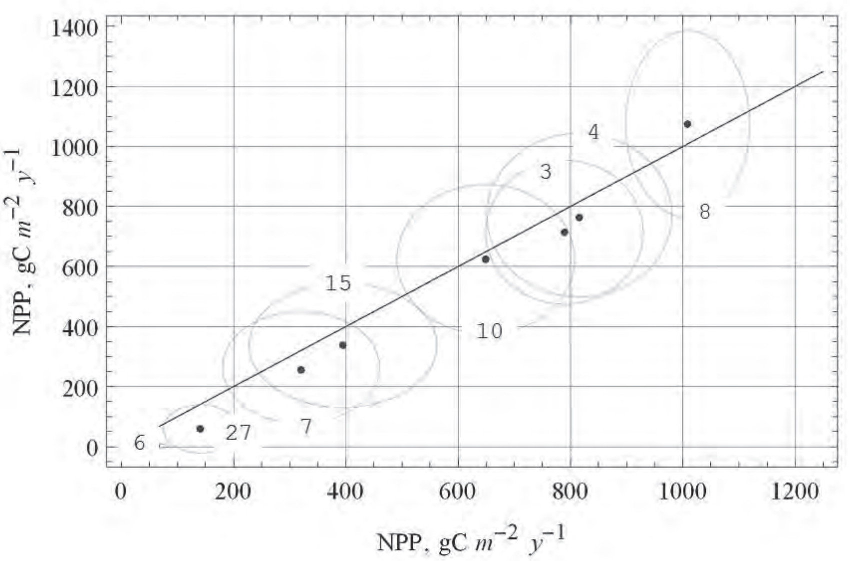

Figure 11.1- BEAMS NPP of major vegetation zones plotted against Normative NPP 1.14.1.

Points mark mean values, ellipses delineate standard deviations from the mean values. See Figure 9.1 for the Legend.

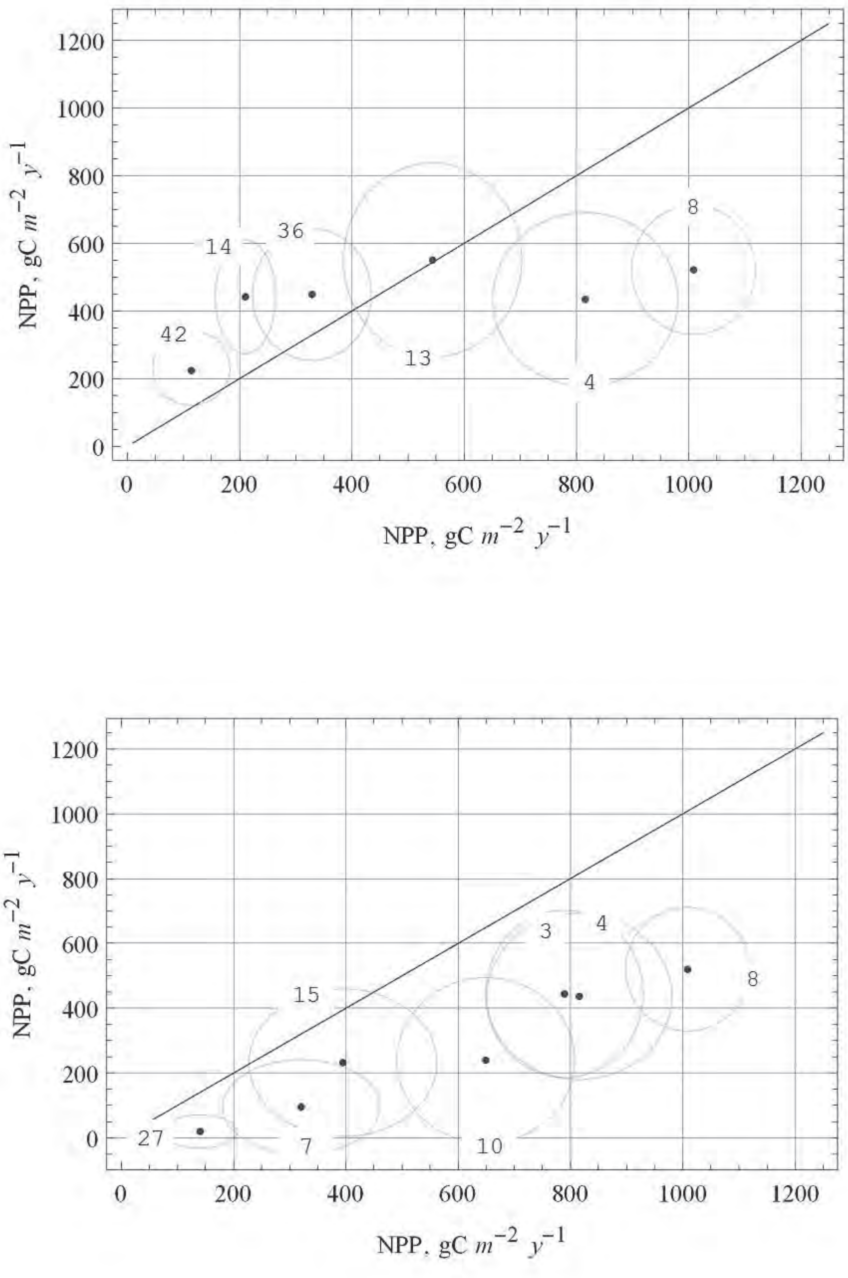

Figure 11.2 - Biome-BGC NPP of major vegetation zones plotted against Normative NPP 1.14.1.

Points mark mean values, ellipses delineate standard deviations from the mean values.

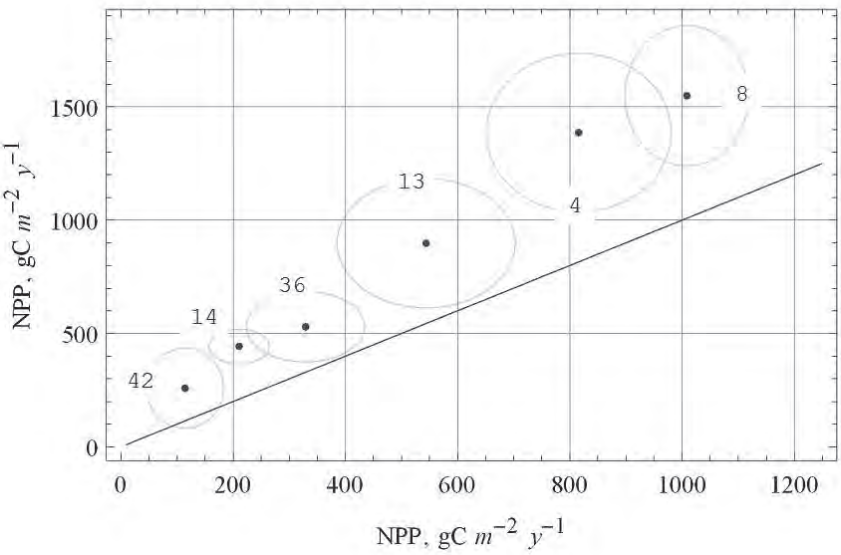

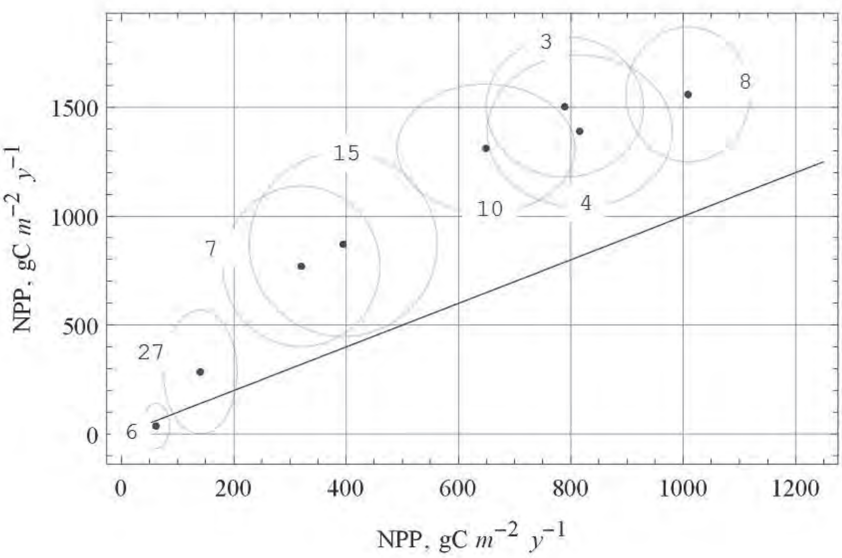

Figure 11.3 - GLO-PEM NPP of major vegetation zones plotted against Normative NPP 1.14.1.

Points mark mean values, ellipses delineate standard deviations from the mean values.

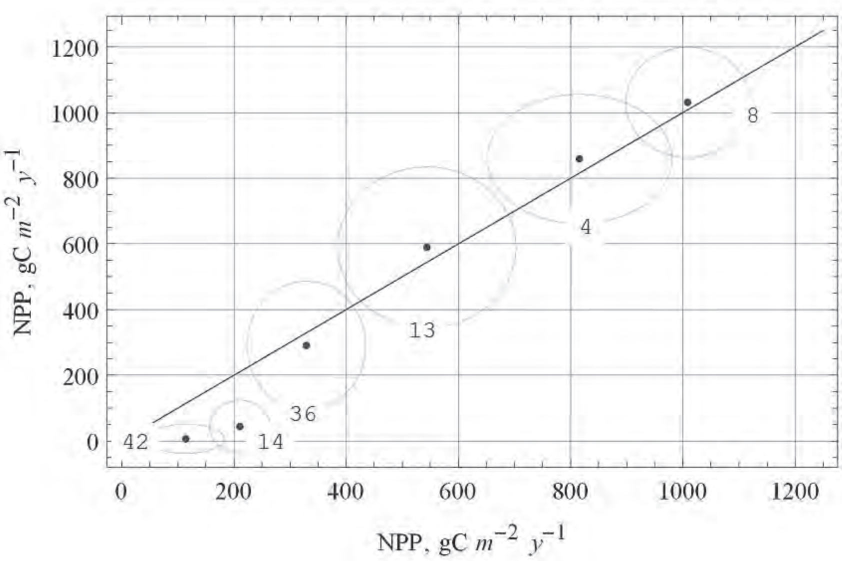

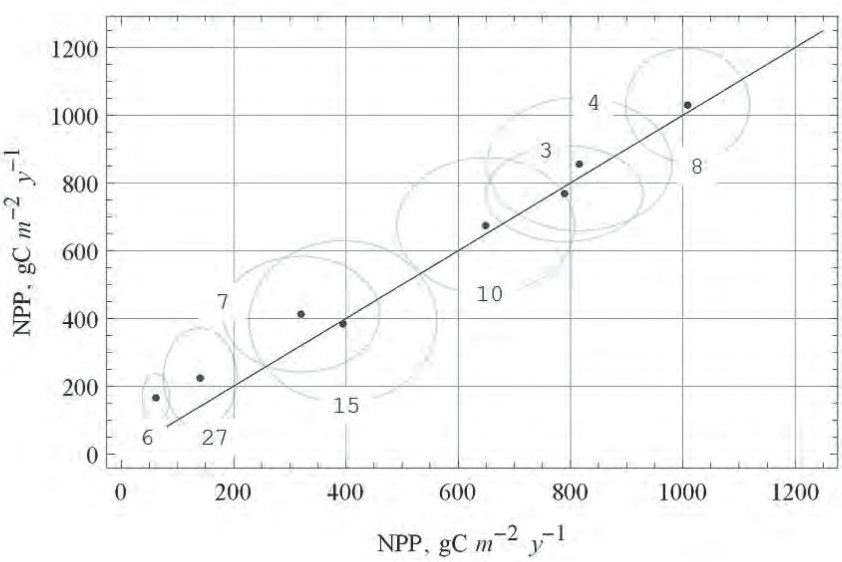

Figure 11.4 - Madison NPP of major vegetation zones plotted against Normative NPP 1.14.1.

Points mark mean values, ellipses delineate standard deviations from the mean values.

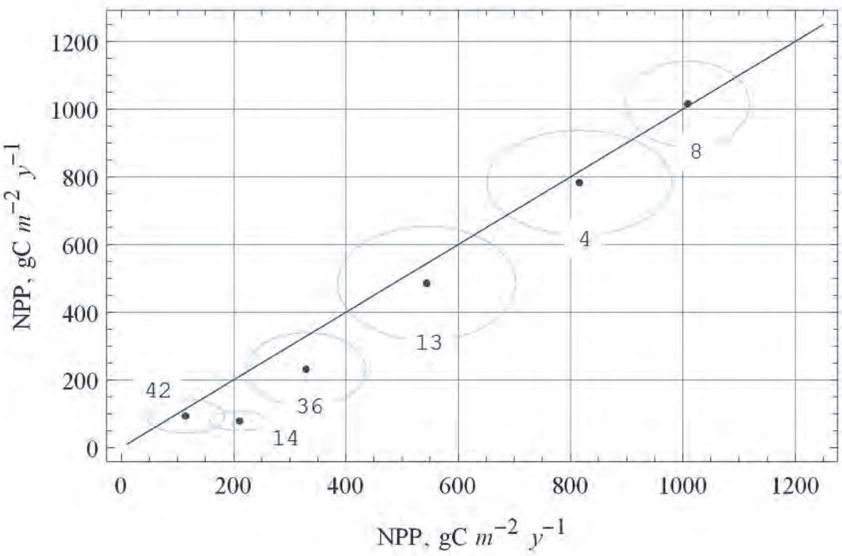

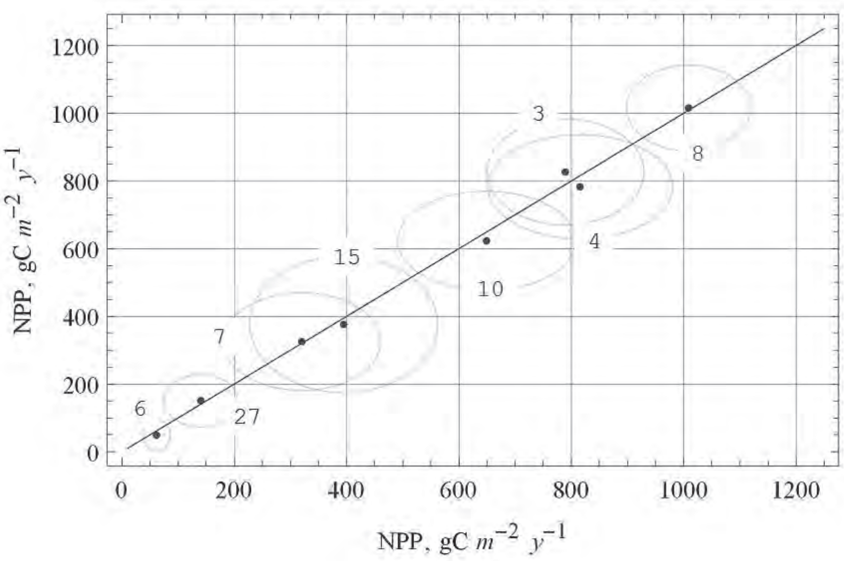

Figure 11.5 - Miami NPP of major vegetation zones plotted against Normative NPP 1.14.1.

Points mark mean values, ellipses delineate standard deviations from the mean values.

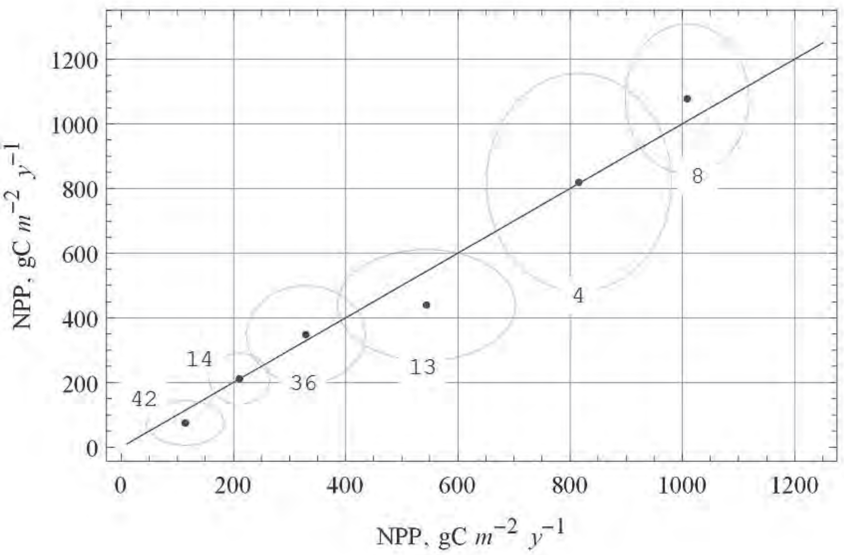

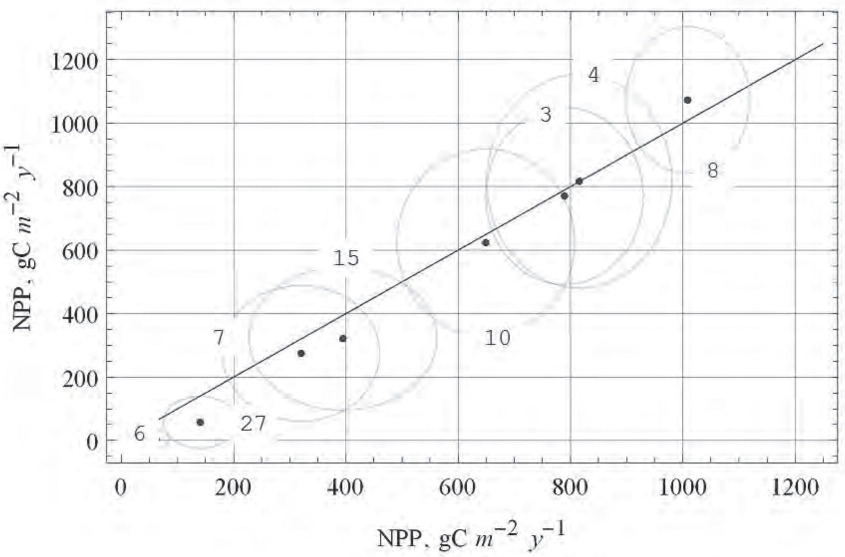

Figure 11.6 - MODIS-NPP of major vegetation zones plotted against Normative NPP 1.14.1.

Points mark mean values, ellipses delineate standard deviations from the mean values.

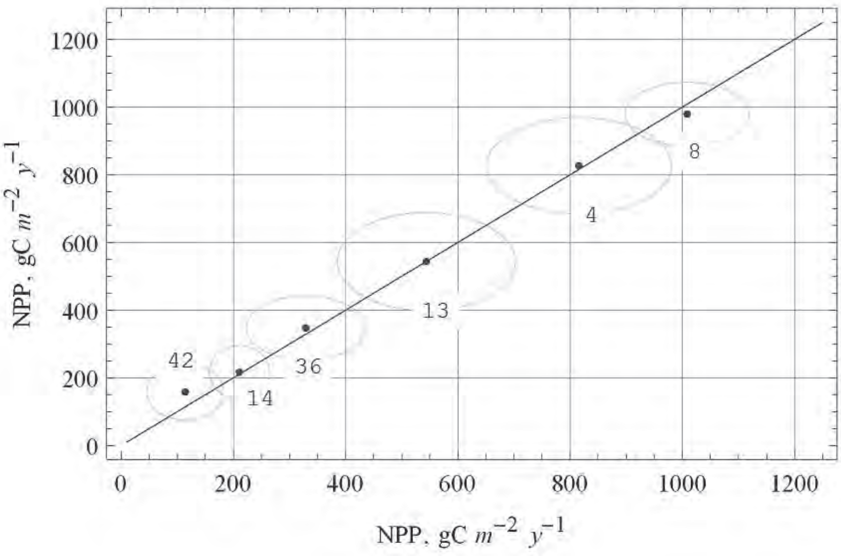

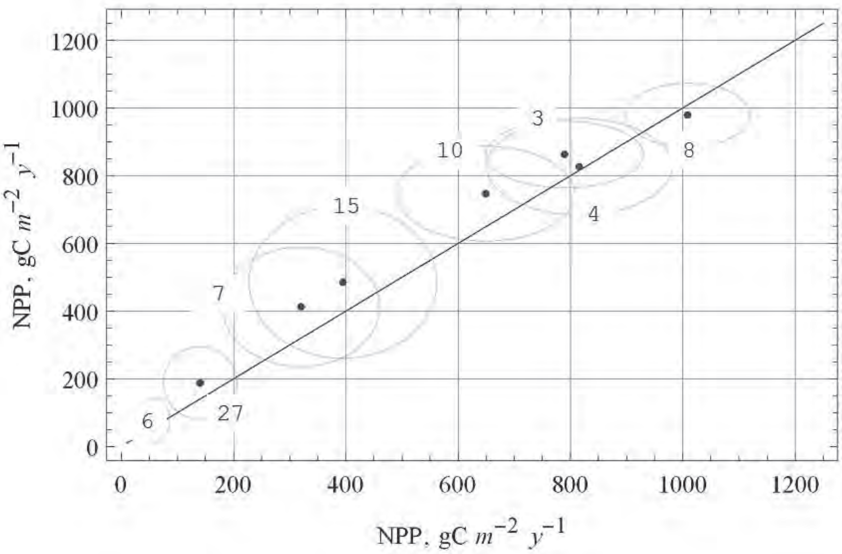

Figure 11.7- Montreal NPP of major vegetation zones plotted against Normative NPP 1.14.1.

Points mark mean values, ellipses delineate standard deviations from the mean values.

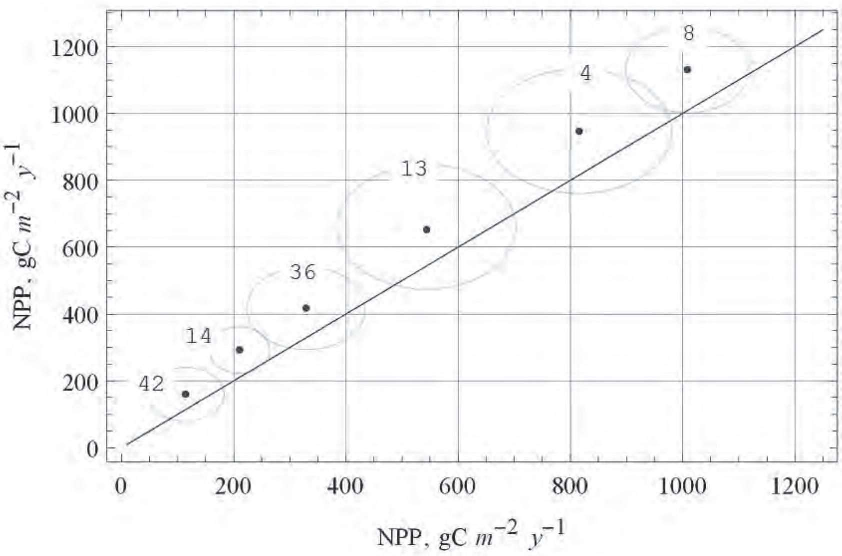

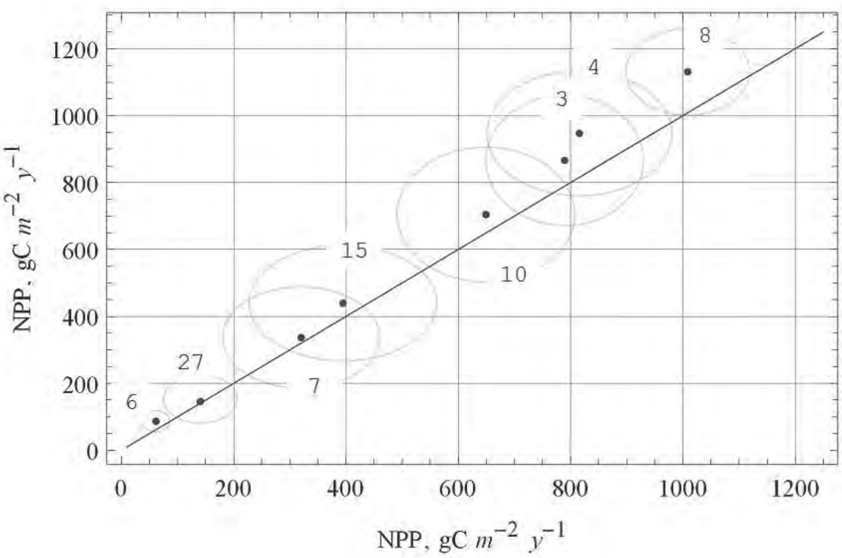

Figure 11.8 - Potsdam NPP (high) of major vegetation zones plotted against Normative NPP 1.14.1.

Points mark mean values, ellipses delineate standard deviations from the mean values.

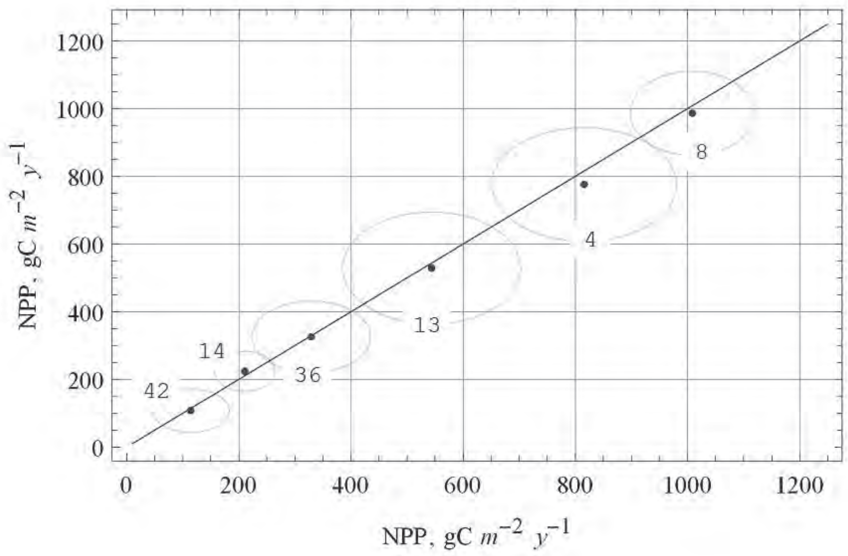

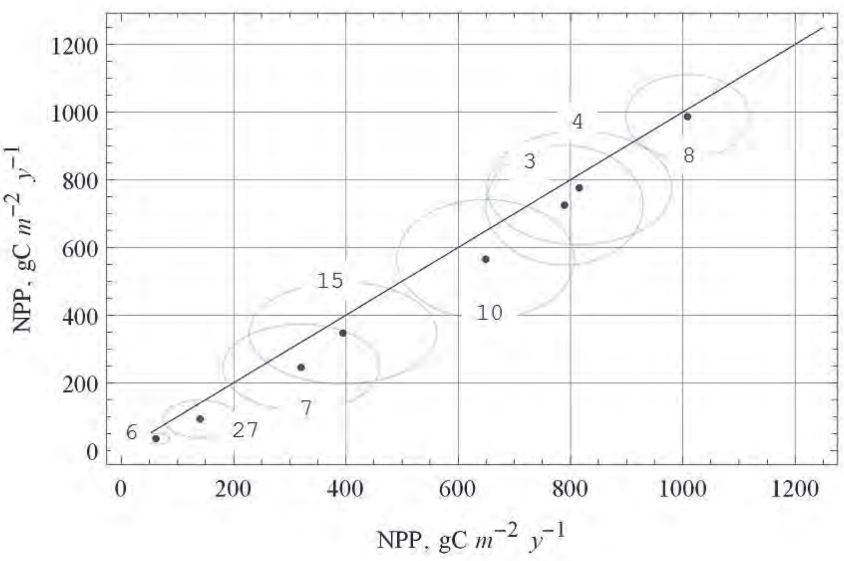

Figure 11.9 - Potsdam NPP (low) of major vegetation zones plotted against Normative NPP 1.14.1.

Points mark mean values, ellipses delineate standard deviations from the mean values.

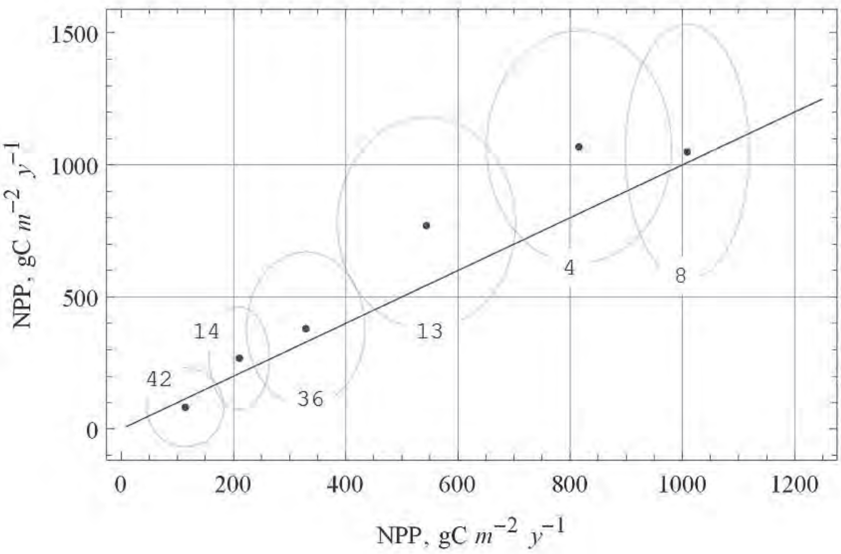

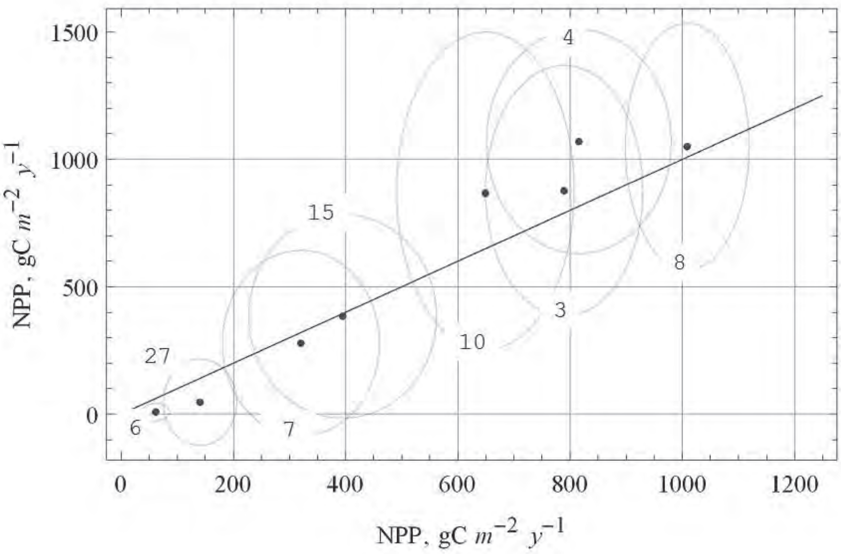

Figure 11.10 - Sim-CYCLE (rev) NPP of major vegetation zones plotted against Normative NPP 1.14.1.

Points mark mean values, ellipses delineate standard deviations from the mean values.

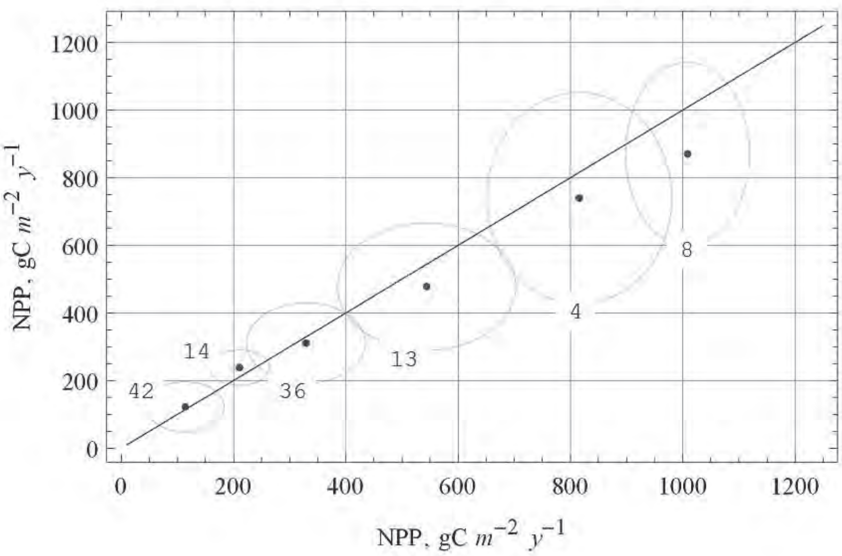

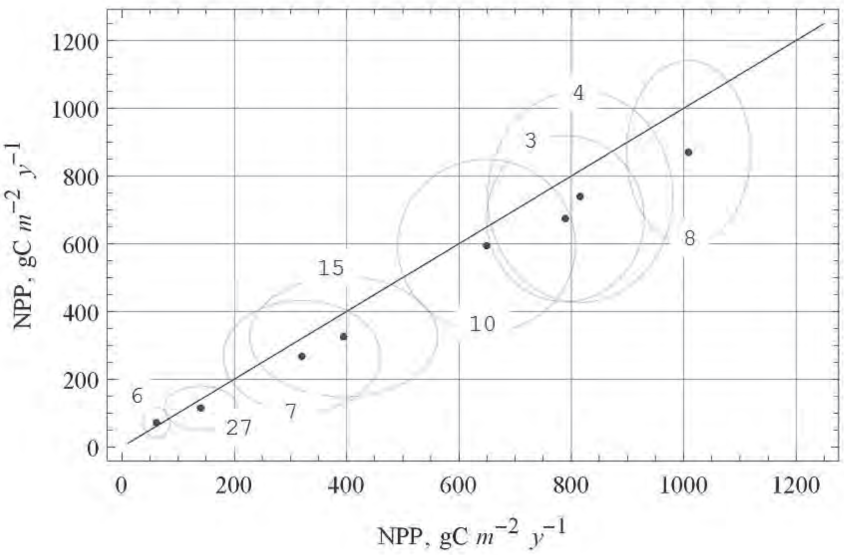

Figure 11.11 - TGER-NPP of major vegetation zones plotted against Normative NPP 1.14.1.

Points mark mean values, ellipses delineate standard deviations from the mean values.

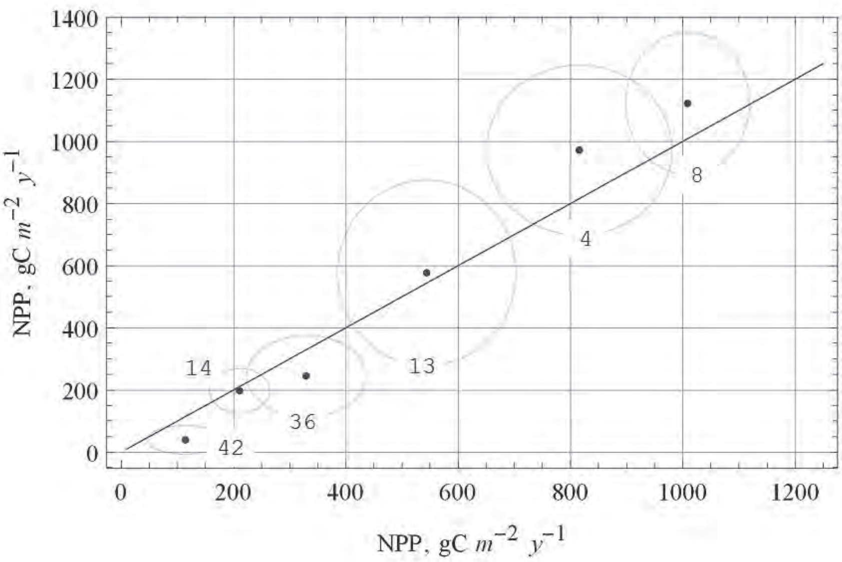

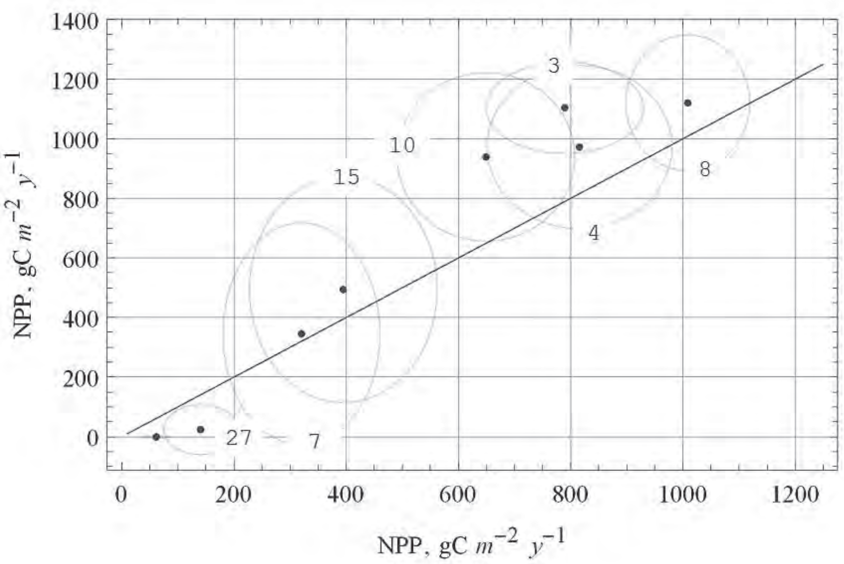

Figure 11.12 - TsuBiMo 1 NPP of major vegetation zones plotted against Normative NPP 1.14.1.

Points mark mean values, ellipses delineate standard deviations from the mean values.

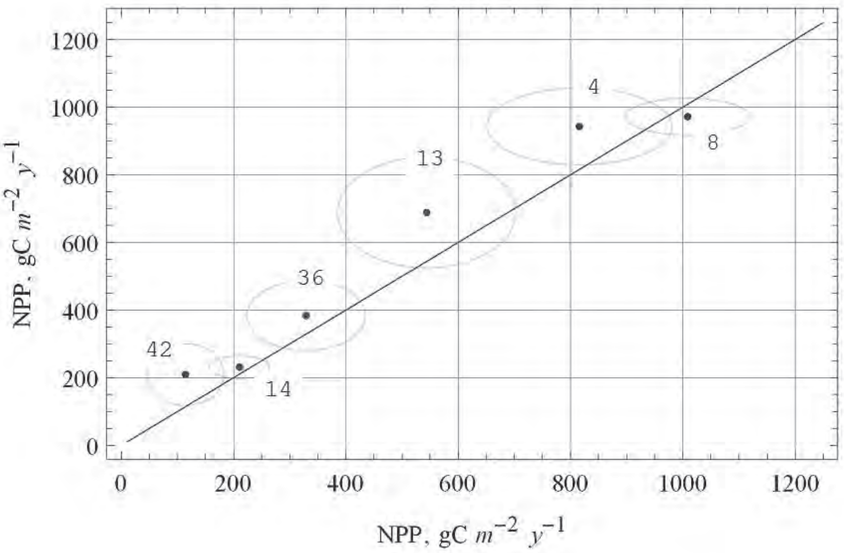

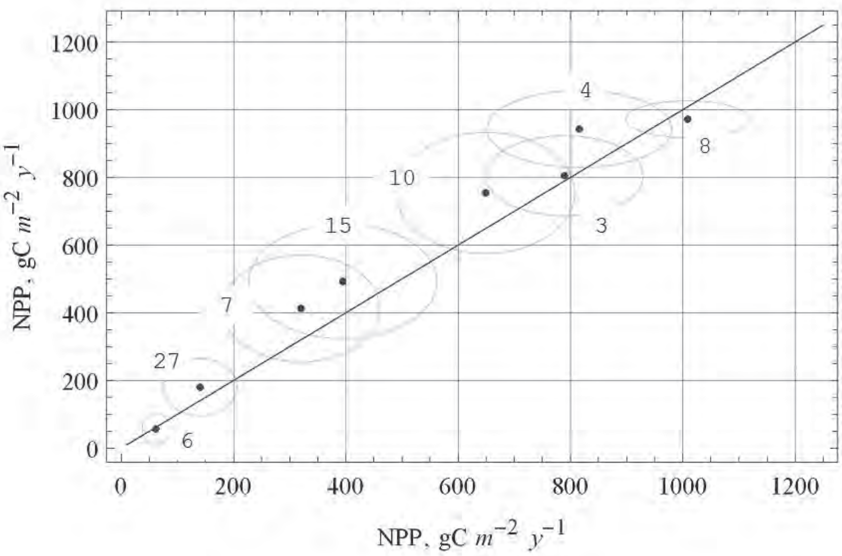

Figure 11.13 - VEGAS NPP of major vegetation zones plotted against Normative NPP 1.14. 1

Points mark mean values, ellipses delineate standard deviations from the mean values.

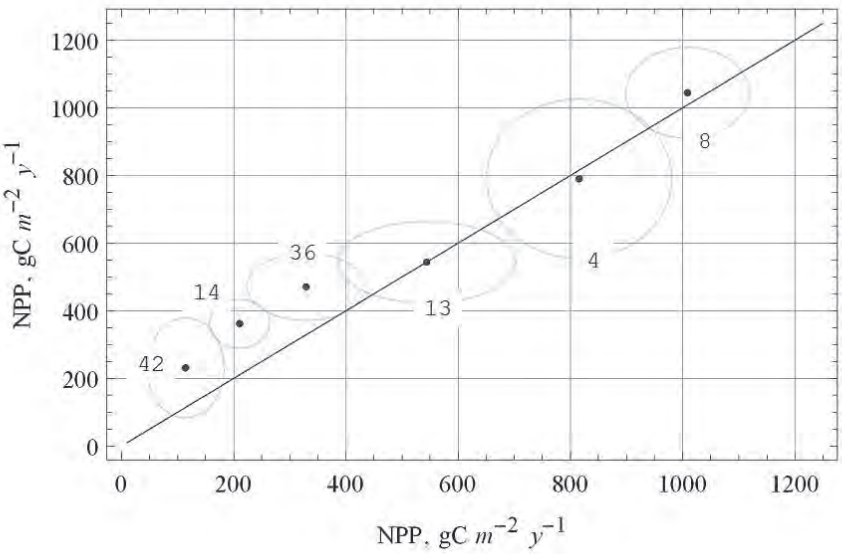

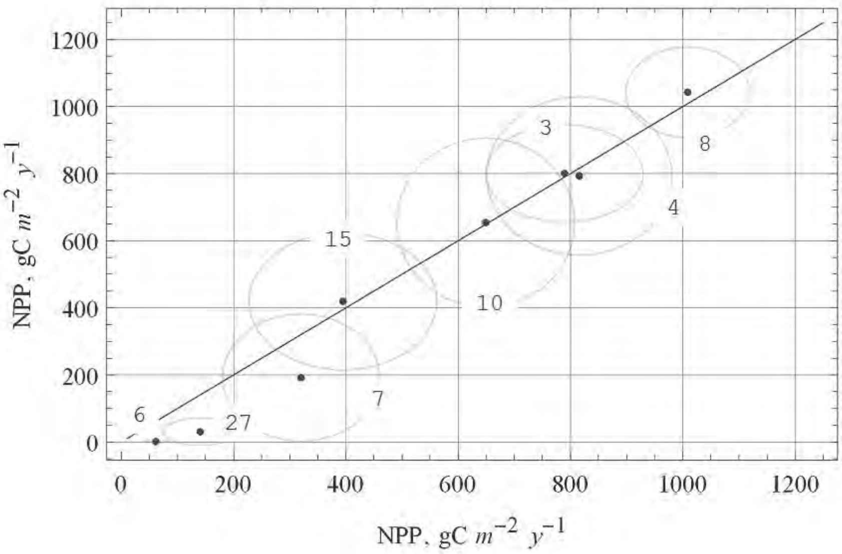

Figure 11.14 - LPJ NPP of major vegetation zones plotted against Normative NPP 1.14. 1

Points mark mean values, ellipses delineate standard deviations from the mean values.

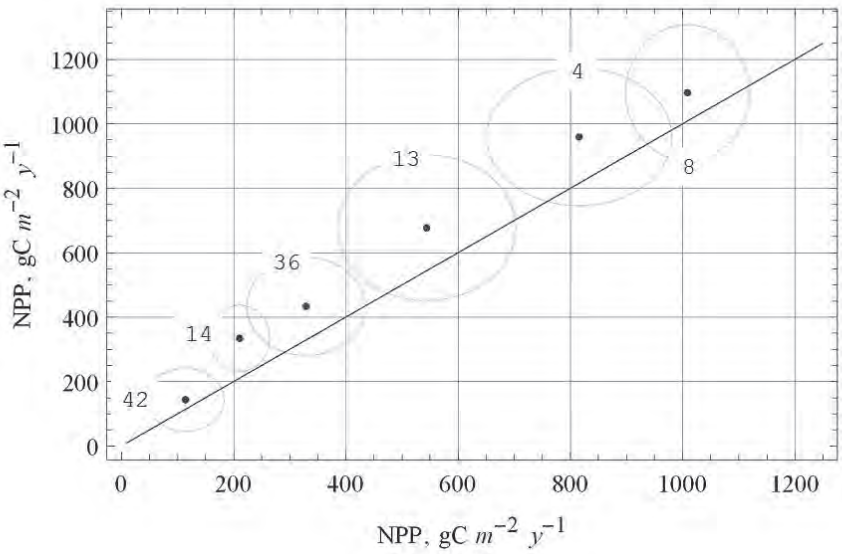

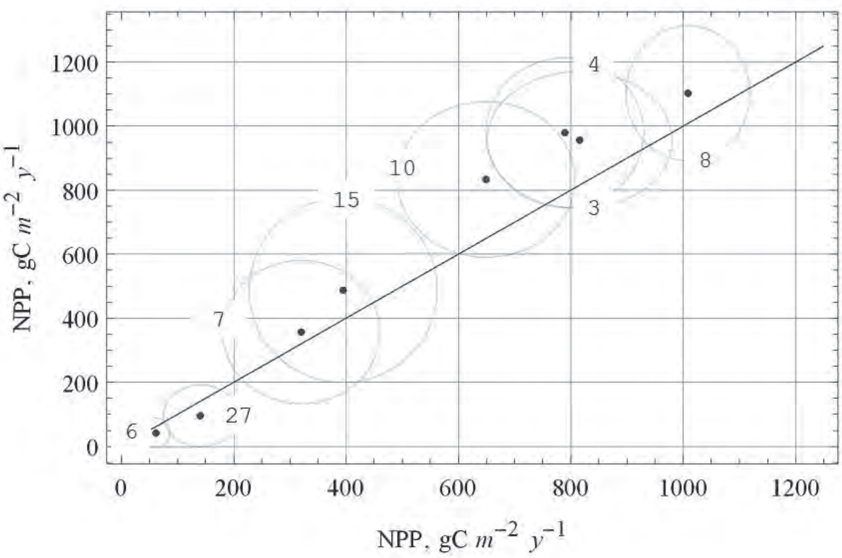

Figure 11.15 - Alternative NPP 1.14.1 of major vegetation zones plotted against Normative NPP 1.14.1

Points mark mean values, ellipses delineate standard deviations from the mean values.

References

1. Pielke RA: **Usable Information for Policy - An Appraisal of the US Global Change Research-Program.** *Policy Sciences* 1995, **28:** 39-77.

2. Kheshgi HS, Jain AK, Wuebbles DJ: **Accounting for the missing carbon-sink with the CO_2-fertilization effect.** *Climatic Change* 1996, **33:** 31-62.

3. Houghton RA: **Balancing the Global Carbon Budget.** *Annual Review of Earth and Planetary Sciences* 2007, **35:** 313-347.

4. Keeling RF, Piper SC, Heimann M: **Global and hemispheric CO_2 sinks deduced from changes in atmospheric O_2 concentration.** *Nature* 1996, **381:** 218-221.

5. Houghton RA, Davidson EA, Woodwell GM: **Missing sinks, feedbacks, and understanding the role of terrestrial ecosystems in the global carbon balance.** *Global Biogeochemical Cycles* 1998, **12:** 25-34.

6. Alexandrov GA, Chan D, Chen M, Gurney K, Higuchi K, Ito A, Jones CD, Komarov A, Mabuchi K, Matross DM, Veroustraete F, Verstraeten WW: **Model-data fusion in studies of the terrestrial carbon sink.** In *Environmental Modelling, software and decision support*. Edited by Jakeman AJ, Voinov AA, Rizzoli AE, Chen SH. Amsterdam: Elsevier; 2009:329-344.

7. Karim A, Veizer J, Barth J: **Net ecosystem production in the great lakes basin and its implications for the North American missing carbon sink: A hydrologic and stable isotope approach.** *Global and Planetary Change* 2008, **61:** 15-27.

8. Friedlingstein P, Fung I, Holland E, John J, Brasseur G, Erickson D, Schimel D: **On the Contribution of CO_2 Fertilization to the Missing Biospheric Sink.** *Global Biogeochemical Cycles* 1995, **9:** 541-556.

9. Adger WN, Brown K: **Policy implications of the missing global carbon sink.** *Area* 1995, **27:** 311-317.

10. House JI, Prentice IC, Ramankutty N, Houghton RA, Heimann M: **Reconciling apparent inconsistencies in estimates of terrestrial CO_2 sources and sinks.** *Tellus, Series B: Chemical and Physical Meteorology* 2003, **55:** 345-363.

11. Gifford RM: **The Global Carbon-Cycle - A Viewpoint on the Missing Sink.** *Australian Journal of Plant Physiology* 1994, **21:** 1-15.

12. Sedjo RA: **The Global Carbon-Cycle - Are Forests the Missing Sink.** *Journal of Forestry* 1990, **88:** 33-34.

13. Churkina G, Trusilova K, Vetter M, Dentener F: **Contributions of nitrogen deposition and forest regrowth to terrestrial carbon uptake.** *Carbon Balance and Management* 2007, **2:** 5.

14. Canadell JG, Le Quere C, Raupach MR, Field CB, Buitenhuis ET, Ciais P, Conway TJ, Gillett NP, Houghton RA, Marland G: **Contributions to accelerating atmospheric CO_2 growth from**

economic activity, carbon intensity, and efficiency of natural sinks. *Proceedings of the National Academy of Sciences of the United States of America* 2007, **104:** 18866-18870.

15. National Institute for Environmental Studies. Outline of the Second Five-Year Plan (2006-2010). http://www.nies.go.jp/gaiyo/pamphlet/e-pam_small.pdf . 2007.
Ref Type: Electronic Citation

16. Declaration on access to public research data from public funding. Annex I to Final Communique of OECDCommittee for Science and Technological Policy at Ministerial Level: Science, Technology, and Innovation for the 21st Century, Paris, 29 to 30 January 2004. OECD Committee for Science and Technological Policy . 2004.
Ref Type: Electronic Citation

17. OECD: *OECD principles and guidelines for access to research data from public funding*. Paris: OECD Publications; 2007.

18. Arzberger P, Schroeder P, Beaulieu A, Bowker G, Casey K, Laaksonen L, Moorman D, Uhlir P, Wouters P: **Promoting Access to Public Research Data for Scientific, Economic, and Social Development.** *Data Science Journal* 2004, **3:** 135-151.

19. CODATA. White paper on the GEOSS data sharing principles. http://www.earthobservations.org/geoss_dsp.shtml . 2009.
Ref Type: Electronic Citation

20. Iwata S: **Scientific "Agenda" of Data Science.** *Data Science Journal* 2008, **7:** 54-56.

21. CDIAC. Carbon Dioxide Information Analysis Center. http://cdiac.ornl.gov/ . 2009.
Ref Type: Electronic Citation

22. ORNL DAAC. The Oak Ridge National Laboratory Distributed Active Archive Center. http://daac.ornl.gov/ . 2009.
Ref Type: Electronic Citation

23. IPCC DDC. The Data Distribution Centre of the Intergovernmental Panel on Climate Change. http://www.ipcc-data.org/ . 2009.
Ref Type: Electronic Citation

24. UNEP. GEO Data Portal. http://geodata.grid.unep.ch/ . 2009.
Ref Type: Electronic Citation

25. Hayashi S: **Information and Communications Technology and Shiso.** *Science & Technology Trends-Quarterly Review* 2007, **23:** 11-22.

26. Imhoff ML, Bounoua L, Ricketts T, Loucks C, Harriss R, Lawrence WT: **Global patterns in human consumption of net primary production.** *Nature* 2004, **429:** 870-873.

27. Heimann M, Reichstein M: **Terrestrial ecosystem carbon dynamics and climate feedbacks.** *Nature* 2008, **451:** 289-292.

28. Zeng N: **Carbon sequestration via wood burial.** *Carbon Balance and Management* 2008, **3:** 1.

29. Gurney K, Raymond L: **Targeting deforestation rates in climate change policy: a 'Preservation Pathway' approach.** *Carbon Balance and Management* 2008, **3:** 2.

30. Kindermann G, Obersteiner M, Rametsteiner E, McCallum I: **Predicting the deforestation-trend under different carbon-prices.** *Carbon Balance and Management* 2006, **1:** 15.

31. van Minnen J, Strengers B, Eickhout B, Swart R, Leemans R: **Quantifying the effectiveness of climate change mitigation through forest plantations and carbon sequestration with an integrated land-use model.** *Carbon Balance and Management* 2008, **3:** 3.

32. Alexandrov G: **Carbon stock growth in a forest stand: the power of age.** *Carbon Balance and Management* 2007, **2:** 4.

33. Steffen W, Noble I, Canadell J, Apps M, Schulze ED, Jarvis PG, Baldocchi D, Ciais P, Cramer W, Ehleringer J, Farquhar G, Field CB, Ghazi A, Gifford R, Heimann M, Houghton R, Kabat P, Korner C, Lambin E, Linder S, Mooney HA, Murdiyarso D, Post WM, Prentice IC, Raupach MR, Schimel DS, Shvidenko A, Valentini R: **The terrestrial carbon cycle: Implications for the Kyoto Protocol.** *Science* 1998, **280:** 1393-1394.

34. Alexandrov GA, Oikawa T, Yamagata Y: **The scheme for globalization of a process-based model explaining gradations in terrestrial NPP and its application.** *Ecological Modelling* 2002, **148:** 293-306.

35. Lieth H: **Modeling the primary productivity of the world.** In *Primary Productivity of the Biosphere*. 1975:237-263.

36. Esser G: **Sensitivity of global carbon pools and fluxes to human and potential climatic impacts.** *Tellus* 1987, **39 B:** 245-260.

37. Box EO: **Estimating the seasonal carbon source-sink geography of a natural, steady-state terrestrial biosphere.** *J Appl Meteorol* 1988, **27:** 1109-1124.

38. Box EO, Holben BN, Kalb V: **Accuracy of the AVHRR vegetation index as a predictor of biomass, primary productivity and net CO_2 flux.** *Vegetatio* 1989, **80:** 71-89.

39. Oikawa T: **Simulation of forest carbon dynamics based on dry-matter production model: 1. Fundamental model structure of a tropical rainforest ecosystem.** *Bot Mag* 1985, **98:** 225-238.

40. Oikawa T: **A simulation study of surplus productivity as influenced by the photosynthesis and respiration rates of a single leaf.** *J Agr Met* 1986, **42:** 207-216.

41. Oikawa T, Saeki T: **Light regime in relation to plant population geometry. I. A Monte Carlo simulation of light microclimates within a random distribution foliage.** *Bot Mag Tokyo* 1977, **90:** 1-10.

42. Smith FW, Sampson DA, Long JN: **Comparison of leaf area index estimates from tree allometrics and measured light interception.** *For Sci* 1991, **37:** 1682-1688.

43. Alexandrov GA, Oikawa T: **Contemporary variations of terrestrial net primary production: The use of satellite data in the light of an extremal principle.** *Ecological Modelling* 1997, **95:** 113-118.

44. Alexandrov GA, Yamagata Y: **A peaked function for modeling temperature dependence of plant productivity.** *Ecological Modelling* 2007, **200:** 189-192.

45. Prince SD, Goward S: **Global net primary production: a remote sensing approach.** *Journal of Biogeography* 1995, **22:** 815-835.

46. Goetz SJ, Prince SD, Goward SN, Thawley MM, Small J: **Satellite remote sensing of primary production: An improved production efficiency modeling approach.** *Ecological Modelling* 1999, **122:** 239-255.

47. Sasai T, Ichii K, Yamaguchi Y, Nemani R: **Simulating terrestrial carbon fluxes using the new biosphere model "biosphere model integrating eco-physiological and mechanistic approaches using satellite data" (BEAMS).** *Journal of Geophysical Research-Biogeosciences* 2005, **110**.

48. Zhao M, Heinsch FA, Nemani RR, Running SW: **Improvements of the MODIS terrestrial gross and net primary production global data set.** *Remote Sensing of Environment* 2005, **95:** 164-176.

49. Running SW, Nemani RR, Heinsch FA, Zhao M, Reeves M, Hashimoto H: **A Continuous Satellite-Derived Measure of Global Terrestrial Primary Production.** *BioScience* 2004, **54:** 547-560.

50. Zaks DPM, Ramankutty N, Barford CC, Foley JA: **From Miami to Madison: Investigating the relationship between climate and terrestrial net primary production.** *Global Biogeochemical Cycles* 2007, **21:** GB3004-doi:10.1029/2006GB002705.

51. Ito A, Oikawa T: **Global Mapping of Terrestrial Primary Productivity and Light-Use Efficiency with a Process-Based Model.** In *Global Environmental Change in the Ocean and on Land*. Edited by Shiyomi M. Tokyo: Terrapub; 2004:343-358.

52. Zeng N: **Glacial-interglacial atmospheric CO_2 change - The glacial burial hypothesis.** *Advances in Atmospheric Sciences* 2003, **20:** 677-693.

53. Zeng N, Mariotti A, Wetzel P: **Terrestrial mechanisms of interannual CO_2 variability.** *Global Biogeochemical Cycles* 2005, **19**.

54. Sitch S, Smith B, Prentice IC, Arneth A, Bondeau A, Cramer W, Kaplan JO, Levis S, Lucht W, Sykes MT, Thonicke K, Venevsky S: **Evaluation of ecosystem dynamics, plant geography and terrestrial carbon cycling in the LPJ dynamic global vegetation model.** *Global Change Biol* 2003, **9:** 161-185.

55. Schneider S, Lane J: **Integrated Assessment Modeling of Global Climate Change: Much Has Been Learned?Still a Long and Bumpy Road Ahead.** *Integrated Assessment* 2005, **5**.

56. Alexandrov G: **Best scientific advice is to read the climate report - Most researchers agree on the need to back Kyoto: let politicians deal with the politics.** *Nature* 2004, **431:** 739.

57. Tebaldi C, Knutti R: **The use of the multi-model ensemble in probabilistic climate projections.** *Philosophical Transactions of the Royal Society A* 2007, **365:** 2053-2075.

58. Hoffman F, Bonan G, Covey C, Fung I, Lee YH, Randerson J, Running S, Thornton P: **The Carbon-Land Model Intercomparison Project (C-LAMP): A Protocol and Evaluation Metrics for Global Terrestrial Biogeochemistry Models.** 2008.

59. Robertson AW, Lall U, Zebiak SE, Goddard L: **Improved combination of multiple atmospheric GCM ensembles for seasonal prediction.** *Mon Weather Rev* 2004, **132:** 2732-2744.

60. Alexandrov GA, Matsunaga T: **Evaluating consistency of biosphere models: software tools for a web-based service.** In: *Proceedings of the iEMSs Fourth Biennial Meeting: International Congress on Environmental Modelling and Software (iEMSs 2008)*; 2008; Barcelona.

61. Alexandrov GA, Matsunaga T: **Normative productivity of the global vegetation.** *Carbon Balance and Management* 2008, **3:** 8.

62. Cramer W, Kicklighter DW, Bondeau A, Moore III B, Churkina G, Nemry B, Ruimy A, Schloss AL: **Comparing global models of terrestrial net primary productivity (NPP): Overview and key results.** *Global Change Biol* 1999, **5:** 1-15.

63. Ajtay GL, Ketner P, Duvigneaud P: **Terrestrial primary production and phytomass.** *The Global Carbon Cycle* 1979, 129-181.

64. Box EO, Dye D, Kajiwara K, Tateishi R, Bai X: *Global Environmental Data Sets from the Toyota Crown Laboratory Global Engineering Research Project (1991-1994) on CD-ROM* 1994.

65. Alexandrov GA, Oikawa T, Esser G: **Estimating terrestrial NPP: what the data say and how they may be interpreted?** *Ecological Modelling* 1999, **117:** 361-369.

66. Healy S: **Epistemological pluralism and the `politics of choice'.** *Futures* 2003, **35:** 689-701.

67. Parker W: **Understanding Pluralism in Climate Modeling.** *Foundations of Science* 2006, **11:** 349-368.

68. van Asselt MBA, Rotmans J: **Uncertainty in integrated assessment modelling: From positivism to pluralism.** *Climatic Change* 2002, **54:** 75-105.

69. Socolow R: **Climate change mitigation under strong carbon constraints.** *Proceedings of 50th Anniversary of the Global Carbon Dioxide Record Symposium: 28-30 November* 2007.

70. Cicerone RJ: **Climate Change: It is not just scientists.** *Proceedings of 50th Anniversary of the Global Carbon Dioxide Record Symposium: 28-30 November* 2007, 28-30.

71. Alexandrov G, Heimann M, Jones C, Tans P: **On 50th Anniversary of the Global Carbon Dioxide Record.** *Carbon Balance and Management* 2007, **2:** 11.

72. Bradie M: **Epistemology from an Evolutionary Point of View.** In *Conceptual Issues in Evolutionary Biology*. Edited by Sober E. MIT Press; 1994:453-476.